

1 **Methane, ethane, and propane production in Greenland ice**
2 **core samples and a first isotopic characterization of excess**
3 **methane**

4 Michaela, Mühl¹, Jochen Schmitt¹, Barbara Seth¹, James E. Lee², Jon S. Edwards³, Edward J.
5 Brook³, Thomas Blunier⁴, Hubertus Fischer¹

6
7 ¹Climate and Environmental Physics and Oeschger Centre for Climate Change Research, University of Bern,
8 Bern, 3012, Switzerland

9 ²Los Alamos National Laboratory, Earth Systems Observation, Los Alamos, NM 87545, USA

10 ³College of Earth, Ocean, and Atmospheric Sciences, Oregon State University, Corvallis, OR 97331, USA

11 ⁴Centre for Ice and Climate, Niels Bohr Institute, University of Copenhagen, Copenhagen, 2200, Denmark
12

13 *Correspondence to:* Michaela Mühl (michaela.muehl@unibe.ch)

14
15
16
17
18
19
20
21
22
23
24
25
26
27
28
29
30
31
32
33
34
35

Formatiert: Links: 2,5 cm, Rechts: 2,5 cm, Oben: 2,5 cm,
Kopfzeilenabstand vom Rand: 1,25 cm, Fußzeilenabstand
vom Rand: 1,25 cm

hat gelöscht: Excess m

37 **Abstract.** Air trapped in polar ice provides unique records of the past atmospheric composition
 38 ranging from key greenhouse gases such as methane (CH₄) to short-lived trace gases like ethane
 39 (C₂H₆) and propane (C₃H₈). Recently, the comparison of CH₄ records obtained using different
 40 extraction methods revealed disagreements in the CH₄ concentration for the last glacial in
 41 Greenland ice. Elevated methane levels were detected in dust-rich ice core sections measured
 42 discretely pointing to a process sensitive to the melt extraction technique. To shed light on the
 43 underlying mechanism, we performed targeted experiments and analyzed samples for methane
 44 and the short-chain alkanes ethane and propane covering the time interval from 12 to 42 kyears.
 45 Here, we report our findings of these elevated alkane concentrations, which scale linearly with
 46 the amount of mineral dust within the ice samples. The alkane production happens during the
 47 melt extraction step of the classic wet extraction technique and reaches 14 to 91 ppb of CH₄
 48 excess in dusty ice samples. We document for the first time a co-production of excess methane,
 49 ethane, and propane with the observed concentrations for ethane and propane exceeding their
 50 past atmospheric background at least by a factor of 10. Independent of the produced amounts,
 51 excess alkanes were produced in a fixed molar ratio of approximately 14:2:1, indicating a
 52 shared origin. The carbon isotopic signature of excess methane is $(-47.0 \pm 2.9) \text{‰}$ and its
 53 deuterium isotopic signature is $(-326 \pm 57) \text{‰}$ in the samples analyzed. With the co-production
 54 ratios of excess alkanes and the isotopic composition of excess methane we established a
 55 fingerprint that allows us to constrain potential formation processes. This fingerprint is not in
 56 line with a microbial origin. Moreover, an adsorption-desorption process of thermogenic gas
 57 on dust particles transported to Greenland appears not very likely. Rather, the alkane pattern
 58 appears to be indicative of abiotic decomposition of organic matter as found in soils and plant
 59 leaves.

60 1. Introduction

61
 62 Atmospheric air entrapped in polar ice represents a unique archive of the past atmospheric
 63 composition including the concentration of greenhouse gases like carbon dioxide (CO₂)
 64 methane (CH₄) and nitrous oxide (N₂O) but also short-lived trace gases such as ethane (C₂H₆)
 65 and propane (C₃H₈). The ongoing anthropogenic increase in the atmospheric concentrations of
 66 these gases makes a detailed understanding of their preindustrial variations and biogeochemical
 67 cycling of paramount importance and only polar ice cores are able to provide this information.
 68 However, to interpret reconstructions of the atmospheric composition from polar ice cores
 69 requires that archived atmospheric trace gases are not altered within the ice itself. Furthermore,
 70 the air must be extracted from the ice sample without altering the original composition. Thus,

hat gelöscht: Provided that the analyzed species concentrations and their isotopic fingerprints accurately reflect the past atmospheric composition, biogeochemical cycles can be reconstructed.

hat formatiert: Schriftart: 12 Pt.

hat formatiert: Schriftart: 12 Pt.

hat gelöscht: other

hat gelöscht: occurring in dust-rich sections of Greenland ice cores.

hat gelöscht: (in extractu)

hat gelöscht: for

hat gelöscht: (excess alkanes)

hat formatiert: Schriftart: 12 Pt.

hat gelöscht: The amount of excess alkanes scales linearly with the amount of mineral dust within the ice samples.

hat gelöscht: isotopic characterization of excess CH₄ reveals a relatively heavy

hat gelöscht: (-46.4 ± 2.4)

hat gelöscht: a light

hat gelöscht: of

hat gelöscht: reconfine

hat gelöscht: a, nd rather unlikely for

hat formatiert: Schriftart: 12 Pt.

hat gelöscht: rather

hat gelöscht: such an

hat gelöscht: is

hat gelöscht: sediments,

hat gelöscht: . This study provides first indications for an abiotic reaction producing excess alkanes during ice core analyses and discusses potential mechanisms. ¶

We see an urgent need to correct the already existing discrete CH₄ records for excess CH₄ contribution (CH_{4(exs)}, δ¹³C-CH_{4(exs)}, δD-CH_{4(exs)}) in dust-rich intervals in Greenland ice. Specifically, excess CH₄ has a significant effect on the assessments of the hemispheric CH₄ source distribution. As we observe that in some intervals excess CH₄ is in the same range as the Inter-Polar Difference, previous interpretations of relative contribution of high latitude northern hemispheric CH₄ sources need to be revised. ¶

hat gelöscht: and the global warming caused by it

107 the comparison of ice core records obtained using different extraction techniques and from
108 different ice cores requires careful consideration and interpretation.

109
110 It is known that not all drill sites or specific time intervals are equally suitable to derive pristine
111 atmospheric trace gas records. For example CO₂ data from Greenland ice are subject to CO₂ in
112 situ production due to impurities in the ice (Anklin et al., 1995; Smith et al., 1997). In situ
113 production is also observed for N₂O, for example in glacial Antarctic ice core samples
114 characterized by higher dust content (Schilt et al., 2010). In contrast, CH₄ in polar ice cores, in
115 the absence of melt layers, was considered to be not affected by such in situ processes.
116 However, more recent results from Greenland showing elevated CH₄ concentrations in glacial
117 dust-rich ice (Lee et al., 2020) and high amplitude CH₄ spikes in Holocene ice (Rhodes et al.,
118 2013, 2016) question this assumption.

119
120 This becomes especially worrisome as atmospheric methane shows a significant North-South
121 gradient, reflecting the predominance of Northern Hemisphere sources. Ice cores from
122 Greenland and Antarctica have been used to quantify this Inter-Polar Difference (IPD) in past
123 CH₄ concentrations (Chappellaz et al., 1997; Baumgartner et al., 2012, Beck et al., 2018) with
124 the goal to derive the relative contribution of Northern and Southern hemispheric sources to the
125 overall CH₄ changes. The Holocene IPD is on the order of several tens of ppb, i.e., one order
126 of magnitude smaller than the past atmospheric CH₄ concentration. Thus, any small CH₄ bias
127 on the order of a few ppb to tens of ppb has a strong impact on the conclusions drawn from this
128 IPD, while the influence on the total radiative forcing by such small biases is negligible. In
129 summary, existing results of CH₄ concentrations from Greenland and Antarctic ice cores have
130 to be carefully scrutinized for such effects.

131
132 A first step in this direction has been made in previous work by Lee et al. (2020), for example
133 by comparing CH₄ records derived using different measurement techniques. Past CH₄
134 concentrations ([CH₄]) are retrieved by measurements of Greenland and Antarctic ice cores
135 using traditional discrete and relatively new continuous melt extraction techniques. While
136 discrete ice measurements deliver one single value for each sample, Continuous Flow Analyses
137 (CFA) gradually melt a thin stick of the ice core providing a continuous record for this section.
138 Although in both techniques the ice sample is melted, the CFA technique separates air from the
139 meltwater stream in about 1-2 min providing only a short time for any reaction in the water
140 while for the discrete technique the contact time is typically 15-30 min. Comparing [CH₄]

hat gelöscht: , f

hat gelöscht: has been traditionally interpreted as "the good guy", which

hat gelöscht: is

hat gelöscht: y

hat gelöscht: also

hat gelöscht: H

hat gelöscht: Bipolar ice core studies

hat gelöscht: n

hat gelöscht: s

hat gelöscht: h

hat gelöscht:

hat gelöscht: error

hat formatiert: Nicht Durchgestrichen

hat gelöscht: prismatic

hat gelöscht:

hat gelöscht: ¶

158 histories from several Greenland ice cores measured discretely (NGRIP, GISP2, GRIP) with
159 the continuous Greenland NEEM and the continuous Antarctic WAIS records over the last
160 glacial period, higher [CH₄] can be found in the discrete Greenland measurements for specific
161 time intervals (Lee et al., 2020; Fig. 1 therein), where dust concentrations are especially high,
162

163 Looking at the NGRIP methane hydrogen isotope ($\delta D-CH_4$) record (Bock et al., 2010b), which
164 was also measured with a discrete melt extraction technique (Bock et al., 2010a), it turns out
165 that in the high dust ice sections, the isotopic values are also affected. Several negative
166 hydrogen isotopic excursions with a maximum depletion of 16 ‰ (permil) prior to the onset of
167 Dansgaard-Oeschger (DO) event 8 were identified (Bock et al., 2010b). At the time of that
168 publication there was no straightforward explanation for these depletions that could lead to
169 “lighter” $\delta D-CH_4$ values during times of a relatively stable climate. Using ice from Antarctica
170 much smaller $\delta D-CH_4$ variations (3-4 ‰) during this interval were found in measurements
171 performed at the University of Bern (unpublished data), again questioning the atmospheric
172 origin of these $\delta D-CH_4$ depletions prior to the DO onset.
173

174 All these variations recorded in Greenland ice give reason to assume that a hitherto unknown
175 process exists that produces or releases additional methane in some time intervals in Greenland
176 ice cores (from here on referred to as “excess methane” or CH_{4(xss)}). This process is related to
177 the extraction technique (only found in records obtained by discrete melt extractions) and has
178 only been observed in glacial Greenland ice with high mineral dust concentrations.
179

180 A first attempt to characterize CH_{4(xss)} was made by Lee et al. (2020) who analyzed [CH₄] in
181 discrete ice samples with different impurity composition and concentration from several ice
182 cores (GISP2, NEEM, WAIS, SPICE) using a multiple melt-refreeze technique. They were able
183 to quantify CH_{4(xss)} contributions of up to 30-40 ppb for Greenland samples. Sequential melt-
184 refreeze extractions showed that the process leading to CH_{4(xss)} is slow and not completed during
185 the first melt-refreeze cycle (i.e., within around 30 min). A special set of samples was analyzed
186 with the admixture of a HgCl₂ solution to suppress microbial activity in the meltwater. No
187 difference in the measured [CH₄] was observed between the poisoned samples and replicates
188 without HgCl₂, excluding a microbial CH₄ production after melting. In addition, Lee et al.,
189 (2020) used the NGRIP [CH₄] (Baumgartner et al., 2014) and $\delta D-CH_4$ records (Bock et al.,
190 2010b) to estimate the deuterium isotopic signature of the CH_{4(xss)}. Assuming a two-component

hat gelöscht:

hat gelöscht: discrepancies in

hat gelöscht: between the existing records

hat gelöscht: in

hat gelöscht: .

hat gelöscht: Greenland

hat gelöscht: These differences are particularly visible ~500 years prior to the onset of Dansgaard-Oeschger (DO) event 8 and 12 at around 39.5–40.0 kyears and 48.0–48.5 kyears, respectively, where the discrete NGRIP [CH₄] record shows elevated values (~30 ppb) while the continuous NEEM and WAIS [CH₄] records stay basically flat. Similar observations were also made on the GISP2 and GRIP record (Lee et al., 2020).

A closer look by Lee et al. (2020) into the existing records revealed further corollaries with other ice core parameters: intervals with elevated [CH₄] in the discrete Greenland CH₄ record correspond to stadial ice with a high abundance of mineral dust (indicated by high Ca²⁺ concentrations), especially visible again prior to DO-8 (and DO-12) when [CH₄] and [Ca²⁺] simultaneously rise. When Ca²⁺ decreases again to low interstadial levels, [CH₄] drops by 10-20 ppb. Note that over the same intervals the corresponding continuous NEEM and WAIS CH₄ records remain stable.

hat gelöscht: – as well

hat gelöscht: -

hat gelöscht: –

hat gelöscht: se

hat gelöscht: anomalous

hat gelöscht: , as explained above

hat gelöscht:

hat gelöscht: DO-

hat gelöscht: (for example by a change in the source types)

hat gelöscht: b

hat gelöscht: Iseli, 2019

hat gelöscht: ¶

hat gelöscht: With their data t

hat gelöscht:

hat formatiert: Tiefgestellt

hat gelöscht: .

hat gelöscht: ,

231 mixture of atmospheric methane and excess methane their model led to a best estimate of (-293
232 ± 31) ‰ for $\delta D-CH_{4(xs)}$.

233
234 A straightforward explanation for $CH_{4(xs)}$ may be that CH_4 is either produced in the meltwater,
235 or it was produced beforehand and only released during the melt extraction. With respect to
236 that, Lee et al. (2020) reviewed several mechanisms that could account for the observed
237 variations in Greenland ice core records. None perfectly matched all their observations but
238 lastly, three of the proposed mechanisms were short-listed by Lee et al. (2020): (1) an
239 adsorption process on dust particles prior to the deposition on the ice sheet; (2) an in situ
240 production in the ice; or (3) an abiotic reaction during melt extraction.

241
242 Here we resume the work by Lee et al. (2020) and shed more light upon the potential formation
243 processes using a targeted and more comprehensive study to quantify $CH_{4(xs)}$. We analyzed
244 specific NGRIP and GRIP ice core samples discretely with two different wet extraction
245 systems. With our $\delta^{13}C-CH_4$ device we are able to measure [methane], [ethane], [propane], and
246 $\delta^{13}C-CH_4$ on a single ice sample in two subsequent extractions. With our second device we add
247 [experimental information](#) on $\delta D-CH_4$. In Sect. 2 we provide information on our sampling
248 strategy and measurement techniques. With our new experimental results, presented in Sect. 3,
249 we provide quantitative data for $CH_{4(xs)}$ in NGRIP and GRIP samples and extend our
250 observations to other “excess alkanes” (ethane and propane), which are revealed to be co-
251 produced during the excess CH_4 production. The observed molar ratios between methane,
252 ethane, and propane are evaluated and their relation to the abundance of mineral dust (Ca^{2+})
253 within the ice samples is quantified. A 2nd extraction of the meltwater enables us to estimate
254 the temporal dynamics of excess alkane production. Using a Keeling-plot approach to our
255 isotopic results, we calculate the carbon and deuterium isotopic signature of excess CH_4 ($\delta^{13}C-$
256 $CH_{4(xs)}$ and $\delta D-CH_{4(xs)}$). Based on our new and improved evidence, we finally come back to the
257 discussion of the hypotheses proposed by Lee et al. (2020) in Sect. 4 and offer potential
258 mechanisms that could explain the excess alkanes in ice core samples. **For readers not interested**
259 **in all the experimental details, we recommend to jump straight to Sect. 4 to see the disussion.**

260

261 2. Ice core samples and measurements

262 2.1 Ice core samples

263

hat gelöscht:

hat gelöscht: a

hat gelöscht: further data

hat gelöscht:

hat gelöscht: s

hat formatiert: Nicht Hervorheben

hat formatiert: Nicht Hervorheben

hat formatiert: Nicht Hervorheben

hat gelöscht: ¶

271 Mixing ratios of alkanes (methane, ethane, and propane) and the stable carbon ($\delta^{13}\text{C}-\text{CH}_4$) and
272 hydrogen ($\delta\text{D}-\text{CH}_4$) isotope ratios of methane were measured on ice core samples from the
273 North Greenland Ice Core Project (NGRIP) ice core. For this study, a total of 19 NGRIP ice
274 core samples were measured for $\delta^{13}\text{C}-\text{CH}_4$ and alkane concentrations and nine NGRIP ice
275 samples for $\delta\text{D}-\text{CH}_4$ covering the depth between 1795.84 m and 1933.25 m. The NGRIP
276 samples are from the late glacial Marine Isotope Stages (MIS) 3 and 2 (22.6 to 30.6 kyears BP).
277 These time intervals are characterized by sharp atmospheric CH_4 increases in parallel to rapid
278 warmings, the so-called Dansgaard-Oeschger events, but we mostly sampled intervals with
279 stable CH_4 concentrations. From the same time period, we also investigate measurements of 41
280 NGRIP and 12 GRIP ice core samples which were carried out in 2011 and 2018, respectively,
281 and which have not previously been published. See Fig. 1 for an overview of all analyzed
282 NGRIP and GRIP ice core samples over time.

283
284 We also included 22 ice core samples from the European Project for Ice Coring in Antarctica
285 (EPICA) ice core from Dome C (MIS 4), which are not affected by a measurable excess CH_4
286 production and which we use as long-term monitoring ice for the system performance and to
287 quantify the blank contribution of the analytical system (see Appendix B).
288 The late glacial time period, which includes the age of most of the measured NGRIP samples,
289 is characterized by an overall high impurity and dust content and low atmospheric methane
290 concentrations. For our analysis, we have selected ice core bags (where for NGRIP and GRIP
291 ice cores, a bag is a 55 cm long ice core section) in which we expect the same atmospheric CH_4
292 concentration but see a high range of mineral dust content (Ca^{2+}). In this way we can compare
293 neighbouring samples that have the same low stadial CH_4 levels due to stable atmospheric
294 concentrations and temporal smoothing by the slow bubble enclosure process, but are expected
295 to vary in measured concentrations due to contributions of excess alkanes. Ca^{2+} content across
296 our NGRIP samples range from 307 ng/g to 1311 ng/g. This sample selection is also critical to
297 quantify the isotopic signature of the $\text{CH}_{4(\text{xs})}$ produced using the Keeling-plot approach
298 (Keeling, 1958). The underlying assumptions of this mass balance approach are that (1) there
299 is only a two-component mixture (atmospheric methane and excess methane) and that (2) the
300 isotopic ratio of the mixture changes only by a varying input of the second source ($\text{CH}_{4(\text{xs})}$).

301
302 To select the samples, we use high-resolution mineral dust records measured using an Abakus
303 laser attenuation device (Klotz, Germany) for particulate dust (Ruth et al., 2003) as well as Ca^{2+}
304 concentrations (Erhardt et al., 2022) as dissolved mineral dust tracer derived from the Bern

hat formatiert: Schriftart: 12 Pt.

Formatiert: Kommentartext, Abstand zwischen asiatischem und westlichem Text anpassen, Abstand zwischen asiatischem Text und Zahlen anpassen

hat formatiert: Schriftart: 12 Pt.

hat gelöscht: stem

hat gelöscht: s

hat gelöscht: .

hat gelöscht: ¶

hat gelöscht:

hat gelöscht: not to be

hat formatiert: Tiefgestellt

hat gelöscht: that

hat gelöscht: Note that Antarctic ice core samples have not shown any signs of $\text{CH}_{4(\text{xs})}$.

hat gelöscht: firm

hat gelöscht: es

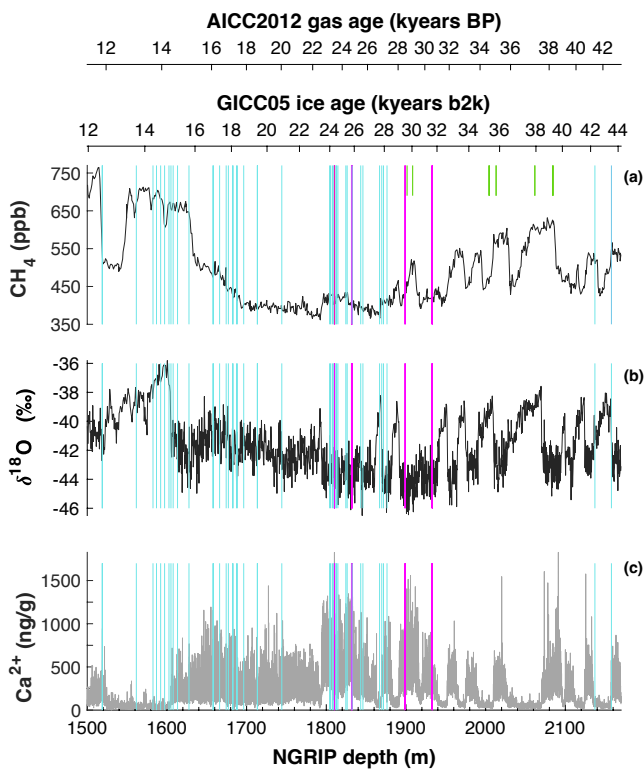
hat gelöscht: Mineral dust

hat formatiert: Hochgestellt

hat gelöscht: ¶

Formatiert: Standard, Leerraum zwischen asiatischem und westlichem Text nicht anpassen, Leerraum zwischen asiatischem Text und Zahlen nicht anpassen

318 Continuous Flow Analysis System (Kaufmann et al., 2008). In principle, particulate dust and
 319 the specific soluble dust tracer Ca^{2+} are strongly correlated. However, depending on acidity of
 320 the ice (mainly due to H_2SO_4 and HNO_3), variable amounts of CaCO_3 are converted into soluble
 321 CaSO_4 and $\text{Ca}(\text{NO}_3)_2$ leading to a variable Ca^{2+} /dust ratio (Legrand and Delmas, 1988). As an
 322 example, Fig. 2 shows the Ca^{2+} and mineral dust concentration of the NGRIP bag 3292 which
 323 we used to select the individual samples, and the relevant parameters measured for each sample
 324 of this bag. The data overview for all other measured NGRIP bags can be found in the Appendix
 325 A.



326 **Figure 1: Overview of the analyzed NGRIP and GRIP samples over time.** All analyzed NGRIP and GRIP ice
 327 core samples are indicated on the NGRIP depth (m) on the bottom axis. To indicate an absolute age for the gas
 328 and ice records both the AICC2012 gas age (kyears BP) and the GICC05 ice age (kyears b2k) scale are provided
 329 on the upper axes. Note that for the purpose of describing the excess CH_4 production in a certain ice sample the
 330 age is irrelevant and we provide all records on depths throughout this manuscript. NGRIP samples measured from
 331 the five main bags (3292, 3331 & 3332, 3453, 3515) for the Keeling-plot approach are indicated with vertical lines
 332 in pink, NGRIP samples measured in 2011 and individual NGRIP ice core samples measured in 2019-2020 (not
 333 included in the Keeling-plot analyses) in turquoise, and GRIP ice core samples in green. (a) $[\text{CH}_4]$ record measured
 334 by wet extraction from NGRIP samples from Baumgartner et al. (2012, 2014). (b) $\delta^{18}\text{O}$ record from North
 335 Greenland Ice Core Project members (2004). (c) Ca^{2+} record from Erhardt et al. (2022).

hat gelöscht: as dissolved mineral dust tracer (Erhardt et al., 2022)

hat gelöscht: ent

hat gelöscht: higher

hat gelöscht: ¶

hat gelöscht: on the NGRIP depth

hat gelöscht: ¶

¶ Note that all regression lines are calculated by following the method of York (1968) and York et al. (2004). ¶ ... [1]

hat formatiert: Schriftfarbe: Text 1

hat formatiert: Schriftart: 10 Pt., Nicht Kursiv, Schriftfarbe: Text 1, Englisch (USA)

hat formatiert: Schriftart: 10 Pt., Nicht Kursiv, Schriftfarbe: Text 1

hat formatiert: Schriftart: Fett

hat gelöscht: and

hat gelöscht: &

hat formatiert: Tiefgestellt

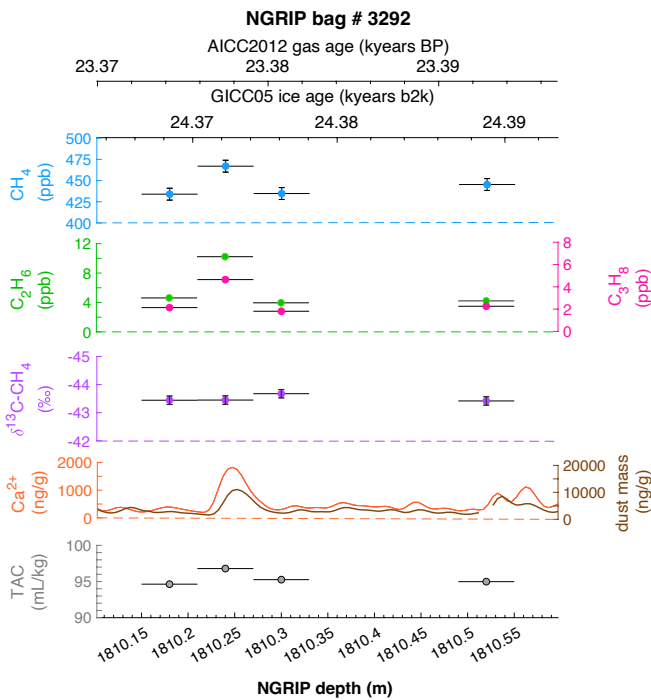
hat formatiert: Schriftart: Fett

hat formatiert: Schriftart: Fett

hat formatiert: Schriftart: Fett

hat formatiert: Schriftart: 9 Pt., Kursiv, Schriftfarbe: Text 2

350



351 **Figure 2: Detailed data overview for NGRIP bag 3292.** Bag-specific overview of several parameters measured
 352 for each sample in this bag at a given depth: methane, ethane, propane, Ca^{2+} , mineral dust mass, TAC (Total Air
 353 Content), $\delta^{13}\text{C}-\text{CH}_4$. At the top the AICC2012 gas age (upper top axis) and the GICC05 ice age (lower top axis) of
 354 the respective depth are indicated. The mineral dust record is taken from Ruth et al. (2003), the Ca^{2+} record from
 355 Erhardt et al. (2022). The data overview for all further measured NGRIP bags can be found in the Appendix A.
 356

351

352

353

354

355

356

357

358

359

360

361

362

363

364

365

366

367

368

369

370

2.2 CH_4 , C_2H_6 , C_3H_8 and $\delta^{13}\text{C}-\text{CH}_4$ Analysis of Ice Core Samples

The short-chain alkanes and $\delta^{13}\text{C}-\text{CH}_4$ were measured at the University of Bern using the discrete wet extraction technique as described in detail in Schmitt et al. (2014). With this method it is possible to measure mixing ratios of methane, ethane, and propane as well as the methane carbon isotopic signature and other trace gases on a single ice core sample of about 150 g.

Briefly, ice core samples are placed in a glass vessel locked by a stainless-steel flange which is attached to the vacuum line to evacuate laboratory air (see Fig. 3, step a). Before melting the ice sample, the leak tightness of the vacuum extraction line is tested with a so-called He blank. The ice sample is then melted under vacuum with the help of infrared radiation for ~35 min to

hat gelöscht: ¶

hat formatiert: Schriftart: 10 Pt., Nicht Kursiv, Schriftfarbe: Text 1, Englisch (USA)

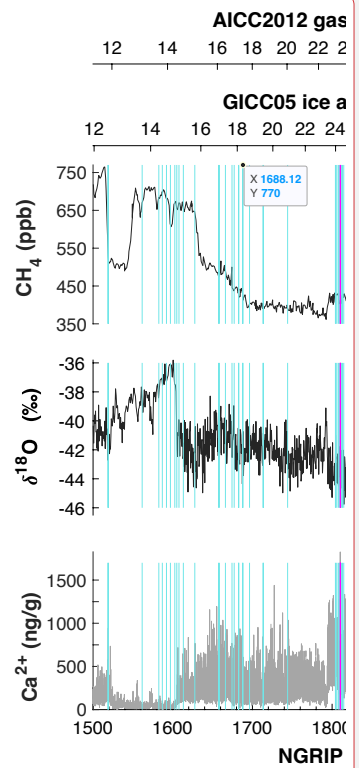
hat formatiert: Schriftart: 10 Pt., Nicht Kursiv, Schriftfarbe: Text 1

hat gelöscht: ,

hat gelöscht: indicated at the NGRIP depth (bottom axis) and the

hat formatiert: Schriftart: 12 Pt., Schriftfarbe: Automatisch

Formatiert: Links, Vom nächsten Absatz trennen



hat gelöscht:

¶
 Figure 1: Overview of the analyzed NGRIP and GRIP samples over time. All analyzed NGRIP and GRIP ice core samples are indicated on the NGRIP depth (m) on the bottom axis and the AICC2012 gas age (kyears BP) & GICC05 ice age (kyears b2k) scale on the upper axes. NGRIP samples measured from the five main bags (3292, 3331 & 3332, 3453, 3515) for the Keeling-plot approach are indicated with vertical lines in pink, NGRIP samples measured in 2011 and individual NGRIP ice core samples measured in 2019-2021 [21]

hat formatiert: Schriftfarbe: Text 1

Formatiert: Abstand zwischen asiatischem und westlichem Text anpassen, Abstand zwischen asiatischem Text und Zahlen anpassen

hat formatiert: Schriftfarbe: Text 1

400 release the enclosed air (step b). The released air is continuously removed from the sample
401 vessel by a pressure gradient towards an adsorbing AirTrap (activated carbon), collecting all
402 relevant air components at -180°C. After melting is completed, the temperature of the meltwater
403 is stabilized close to 0°C, but does not refreeze again. Afterwards, He is sparged with 4 mL/min
404 at standard temperature and pressure (equivalent to 100-400 mL at the varying low pressure in
405 the headspace) through the melt water for ~14 min through a capillary at the bottom of the
406 vessel to transfer any remnant gas species dissolved in the melt water onto the AirTrap (step c).
407 The sample vessel is then sealed by closing inlet and outlet valves (step d). Consecutively, the
408 AirTrap is warmed up in two steps to first remove N₂ and O₂ and in a second step to release the
409 gases of interest which are then sent after a cryofocus step to the gas chromatograph (GC) for
410 separation and quantification using an isotope ratio mass spectrometer (Isoprime 100,
411 Elementar).

413 Precision of this method for CH₄ is about 8 ppb and 0.1 % for $\delta^{13}\text{C-CH}_4$ based on the
414 reproducibility of the 1st extraction of ice core samples where isotopic data are expressed using
415 the δ notation on the international Vienna Pee Dee Belemnite (VPDB) scale. For C₂H₆ the
416 precision is 0.02 ppb or 1 % for C₃H₈ 0.03 ppb or 5 % (whatever is higher) based on the
417 reproducibility of standard air samples which are by definition not subject to excess production
418 (Schmitt et al., 2014). Blank levels for these species based on melted artificial (gas-free) ice
419 samples are 1-2 ppb for CH₄, 0.3 ppb for C₂H₆ and 0.2 ppb for C₃H₈ (Schmitt et al., 2014),
420 which are below the values measured on Antarctic ice, where excess production is minimal
421 compared to glacial Greenland samples (see Appendix B for details).

423 With their experimental investigations, Lee et al. (2020) were already able to demonstrate that
424 production/ release of CH_{4(x)s} is time dependent. We therefore conclude that this process does
425 not have to be completed in the time available for the gas extraction described above. We
426 continued the analyses of excess alkane production with an additional extraction step (here
427 referred to as 2nd extraction, steps d-g in Fig. 3) following the normal ice extraction routine.
428 After all sample air is collected in the 1st extraction, the meltwater is left in the isolated sample
429 vessel (the vessel is closed and not connected to the carbon trap) and held at temperatures close
430 to 0°C for ~100 min (step d). After this “waiting time” of ~100 min, He is purged through the
431 meltwater for ~24 min to extract the gases that have been accumulated during this time interval
432 simulating the extraction time of the 1st extraction, followed by another ~14 min of He purging
433 to mimic the last step of the ice extraction when the sample had completely melted (step f). The

hat formatiert: Schriftart: Nicht Kursiv, Schriftfarbe: Text 1, Englisch (USA)

hat gelöscht: After melting is completed, the temperature of the melt water is stabilized close to 0°C. Afterwards, He is flushed through the melt water for ~14 min through a capillary at the bottom of the vessel to bubble He through the melt water to transfer any remnant gas species dissolved in the melt water onto the AirTrap (step c).

hat formatiert: Schriftfarbe: Text 1

hat gelöscht: 5

hat formatiert: Nicht Hervorheben

hat gelöscht: ,

hat gelöscht: 5

hat formatiert: Hochgestellt

hat gelöscht: , and

hat gelöscht: f

hat gelöscht: both

hat gelöscht: and C₃H₈

hat gelöscht: 0.2

hat gelöscht: b

hat gelöscht: 5

hat formatiert: Tiefgestellt

hat formatiert: Tiefgestellt

hat formatiert: Nicht Hervorheben

hat gelöscht: for the typical NGRIP samples used in our study, where isotopic data are expressed using the δ notation on the international Vienna Pee Dee Belemnite (VPDB) scale

hat gelöscht: using this device

hat gelöscht: at

hat gelöscht: 4

hat gelöscht: 4

hat gelöscht: 3

hat gelöscht: .

hat gelöscht:

Formatiert: Standard

hat formatiert: Schriftfarbe: Text 1

hat gelöscht:

hat formatiert: Schriftart: (Standard) Times New Roman, Nicht Fett, Schriftfarbe: Text 1, Englisch (USA)

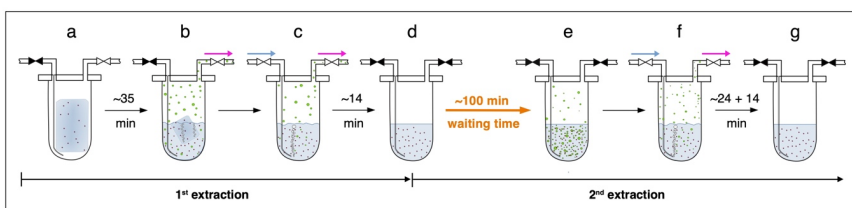
hat formatiert: Schriftart: (Standard) Times New Roman, Nicht Fett, Schriftfarbe: Text 1

hat gelöscht:

hat gelöscht: (step f)

463 gases from this 2nd extraction are collected and measured following the same trapping and
 464 separation steps as in the 1st extraction. Note that the procedure of the 2nd extraction can be
 465 repeated any number of times (e.g. 3rd extraction).
 466

467 The amount of gases that we obtain from the 1st extraction comprises the atmospheric amount,
 468 a possible contribution by in situ production, and a potential time-dependent production/release
 469 in the meltwater (*in extractu*). The 2nd extraction, however, targets only the *in extractu* fraction.
 470 The system blank for the 2nd extraction was estimated using the 2nd extraction of Antarctic ice
 471 (Talos Dome, EDC) and were 2 ppb, 0.3 ppb and 0.3 ppb for CH₄, C₂H₆ and C₃H₈, respectively,
 472 assuming an ice core sample air volume of 14 mL at standard temperature and pressure, which
 473 is the typical ice sample size of 150 g with a total air content of 0.09 mL/g. For CH₄, this is <
 474 1% of the amount of extracted species in the 1st extraction of glacial Greenland ice. Due to the
 475 small amount of CH₄ analyzed in this 2nd extraction (about a factor of 20 to 50 less than for an
 476 ice core sample) the precision for the $\delta^{13}\text{C}$ analysis is much lower than for the 1st (ice sample)
 477 extraction and we estimate the precision for the $\delta^{13}\text{C}$ -CH₄ to 2 % and for [CH₄] to be 2 ppb or 10
 478 % (based on the reproducibility of 2nd extractions of Antarctic EDC samples). For C₂H₆ and
 479 C₃H₈, the precision is comparable to the 1st extraction. Note that throughout the manuscript we
 480 do not perform blank corrections (neither for the measured alkane concentrations nor for the
 481 isotopic values). The only exception is for the calculation of the temporal dynamics of excess
 482 ethane production (see Appendix C) as the blank contribution would otherwise bias the samples
 483 with low Ca²⁺ content.
 484
 485



486
 487 **Figure 3. Sequential steps (a-g) happening in the ice core sample vessel during the 1st and the 2nd extraction**
 488 **in the $\delta^{13}\text{C}$ -CH₄ extraction line.** Scheme illustrates the subsequent steps as described in detail in the text.
 489 **Brownish spots indicate dust particles in the ice/ meltwater. Green circles indicate gas species (methane, ethane,**
 490 **and propane) in the meltwater or in the headspace of the vessel. Closed valves are indicated in black, open valves**
 491 **in white. Blue arrows indicate the He flow through the inlet capillary into the sample vessel, pink arrows indicate**
 492 **the flow direction from the sample vessel towards the AirTrap.**

- hat gelöscht: ¶
- Formatiert: Zeilenabstand: 1,5 Zeilen
- hat gelöscht:
- hat gelöscht: quantified
- hat gelöscht: very clean
- hat formatiert: Nicht Hervorheben
- hat formatiert: Nicht Hervorheben
- hat formatiert: Nicht Hervorheben
- hat formatiert: Hochgestellt, Nicht Hervorheben
- hat formatiert: Schriftfarbe: Text 1
- hat formatiert: Schriftfarbe: Text 1
- hat formatiert: Schriftfarbe: Text 1, Tiefgestellt
- hat formatiert: Schriftfarbe: Text 1
- hat gelöscht: and
- hat gelöscht: ice
- hat formatiert: Nicht Hervorheben
- hat formatiert: Hochgestellt
- hat formatiert: Nicht Hervorheben
- hat gelöscht: and lower than the measurement uncertainty
- hat formatiert: Schriftfarbe: Text 1
- hat gelöscht: ¶
- hat formatiert: Schriftart: Nicht Kursiv
- hat formatiert: Schriftfarbe: Text 1
- hat gelöscht: core
- hat formatiert: Schriftfarbe: Text 1, Nicht Hervorheben
- hat formatiert: Schriftfarbe: Text 1
- hat formatiert: Schriftart: Nicht Kursiv
- hat formatiert: Schriftfarbe: Text 1
- hat formatiert: Schriftfarbe: Text 1
- hat gelöscht: ,
- hat formatiert: Schriftfarbe: Text 1, Hochgestellt
- hat formatiert: Schriftfarbe: Text 1
- hat formatiert: Schriftfarbe: Text 1, Nicht Hervorheben
- hat formatiert: Schriftfarbe: Text 1
- hat formatiert: ... [3]
- hat formatiert: ... [4]
- hat formatiert: ... [5]
- hat gelöscht: The blank values analyzed were 2 ppb, 0 ... [6]
- Formatiert: ... [7]
- hat formatiert: ... [8]
- Formatiert: ... [9]
- hat formatiert: Schriftart: 10 Pt., Schriftfarbe: Text 1
- hat gelöscht: ¶ ... [10]
- hat formatiert: Schriftart: 10 Pt., Schriftfarbe: Text 1
- hat gelöscht: ¶ ... [11]
- hat gelöscht: ¶

531 **2.3 δ D-CH₄ Analysis of Ice Core Samples**

532 All δ D-CH₄ data presented here were measured at the University of Bern using the discrete wet
533 extraction technique as described in detail in Bock et al. (2010a, 2014). This δ D-CH₄ device
534 allows to measure the concentration of methane and its deuterium isotopic signature (δ D-CH₄)
535 on a single ice core sample of about 300 g.

537 Briefly, ice core samples are melted after evacuation of the headspace using a warm water bath
538 at 40°C for 25-30 min to release the enclosed air into the sample vessel headspace. Once all the
539 ice is melted, the warm water bath is replaced by an ice-water bath to keep the meltwater
540 temperature and water vapor pressure low but without refreezing. Note, in contrast to the δ^{13} C-
541 CH₄ method, the inlet and outlet valves are closed during the melting process. The released air
542 leads to an increased pressure in the sample vessel headspace enhancing the solubility of gases
543 in water. After the melting is complete, the inlet and outlet valves are opened and He is purged
544 for ~40 min with a flow of 360 mL/min to transfer the accumulated air in the headspace and
545 bubble He through the meltwater to strip dissolved gases. Just like for the δ^{13} C-CH₄ method,
546 the air is collected on an activated carbon trap followed by further purification steps including
547 GC separation. Note that compared to the δ^{13} C-CH₄ device, we performed only one extraction
548 with the δ D-CH₄ device.

550 For both methods, we assume that the time for an *in extractu* production during the ice
551 extraction procedure starts with the first presence of meltwater until He purging is stopped.
552 Note that this time is considerably longer for the δ D-CH₄ analysis (~60 min) compared to the
553 time of the 1st extraction in the δ^{13} C-CH₄ analysis (~35 min).

554 Using this method we can measure [CH₄] and δ D-CH₄ with a precision of about 15 ppb and 3
555 ‰ (based on standard ice sample measurements), where isotopic data are expressed using the
556 δ notation on the international Standard Mean Ocean Water (SMOW) scale.

559 **3. Characterization of excess alkanes in ice cores**
560 **3.1 Methane, ethane, propane concentrations**

561 As described in detail in Sect. 2.2 a full ice sample measurement includes the regular ice sample
562 extraction (1st extraction) and, after the waiting time of ~100 min, a 2nd gas extraction in the

hat gelöscht: ¶

hat gelöscht: .

hat gelöscht: ¶

hat gelöscht:

hat gelöscht: Consecutively

hat gelöscht:

hat gelöscht: As

hat gelöscht:

hat gelöscht: 9

hat gelöscht: ¶

577 meltwater. Gas from the 1st extraction is comprised of atmospheric air, a possible contribution
578 from in situ production, a potential time-dependent contribution by an *in extractu* process, and
579 any contribution from the device itself (blank). For the gas species discussed here (methane,
580 ethane, propane), these individual fractions are very different in magnitude. For polar ice core
581 samples, the atmospheric air is the major fraction of methane even in dust-rich, glacial ice from
582 Greenland prone to CH_{4(xS)} production (see below). The opposite is expected for ethane and
583 propane, which are dominated by the *in extractu* component in dust-rich Greenland ice. To
584 establish a better knowledge of alkanes in Greenland ice, we evaluated the measured
585 concentrations of methane, ethane, and propane, their ratios to each other and the relation to the
586 content of mineral dust in the ice for both the 1st and the 2nd extraction.

hat gelöscht:

hat gelöscht: y

hat gelöscht: We expect that

hat gelöscht: t

hat gelöscht: T

hat gelöscht: true

hat gelöscht: with respect to

587
588 Note that different units to indicate concentrations of the trace gases of interest are used
589 throughout this study. By using mixing ratios in units of [ppb], as typically used for atmospheric
590 concentrations, the concentration of trace gases is related to the amount of air included in the
591 ice. Ice core samples with a low air content cause higher mixing ratio values for any additional
592 molecules produced in situ or *in extractu* compared to ice core samples with a high air content
593 and the interpretation might be biased. Alternatively, for any additional molecules produced in
594 situ or *in extractu*, [mol absolute per sample] denotes the absolute amount of trace gases and is
595 independent of the ice core air content. In the following, both units are used and great care has
596 to be taken to avoid misinterpretation of the results with respect to the different units.

598 3.1.1 Excess alkanes in the 1st extraction

hat gelöscht: ¶

599
600 Figure 4 and 5 show results from the 1st extraction of our NGRIP and GRIP ice core samples.
601 For dust-rich samples, ethane ranges between 2 ppb and 12 ppb, and propane concentrations
602 between 1 ppb and 5 ppb. In contrast, low-dust samples from both GRIP and NGRIP have much
603 lower concentration (ca. 0.5 ppb for ethane, and 0.3 ppb for propane) consistent with estimates
604 of past atmospheric ethane and propane concentrations from the 15th to 19th century of the
605 common era being about 0.4 ppb in Greenland ice (Nicewonger et al., 2016) and lower for
606 propane (Helmig et al., 2013). Emissions of ethane and propane were likely reduced during the
607 glacial (Bock et al., 2017; Nicewonger et al., 2016; Dyonisius et al., 2020) thus, 0.5 ppb appears
608 to be an upper limit of past atmospheric concentrations of ethane and propane. This estimate of
609 past atmospheric ethane concentrations is an order of magnitude smaller than the values we
610 obtained from our dust-rich ice core samples from the 1st extraction, pointing to a strong,

Formatiert: Leerraum zwischen asiatischem und westlichem Text nicht anpassen, Leerraum zwischen asiatischem Text und Zahlen nicht anpassen

hat gelöscht: over

hat gelöscht: a

hat gelöscht: not drastically larger

hat gelöscht: n

623 additional source of these alkanes for dust-rich samples. Thus, the unusually high mixing ratios
624 indicates that ethane and propane in glacial ice extracted using our melt technique on discrete
625 samples do not represent atmospheric levels.

hat formatiert: Schriftart: (Standard) Times New Roman

hat gelöscht: leads us to believe

hat formatiert: Schriftart: (Standard) Times New Roman

hat formatiert: Schriftart: (Standard) Times New Roman

hat formatiert: Schriftfarbe: Automatisch

626
627 As illustrated in Fig. 4 (left panel), the ethane and propane concentrations are highly correlated,
628 pointing to a common production of excess ethane and excess propane. The weighted mean
629 ratio and its weighted standard deviation (both weighted according to the number of samples
630 measured per bag) is (2.25 ± 0.09) ppb ethane/ ppb propane. Note that all regression lines are
631 calculated by following the method of York (1968) and York et al. (2004). York's analytical
632 solution to the best-fit line accounting for normally distributed errors both in x and y is widely
633 used to determine an isotopic mixing line and has been proven as the least biased method (Wehr
634 and Saleska, 2017; Hoheisel et al., 2019). Throughout the manuscript we use the 1 sigma (1σ)
635 standard deviation to express uncertainties. In Fig. 4, where the individual bags studied are

hat gelöscht: 5

hat gelöscht: and its weighted standard deviation (calculated by Gaussian error propagation of the weighted mean)

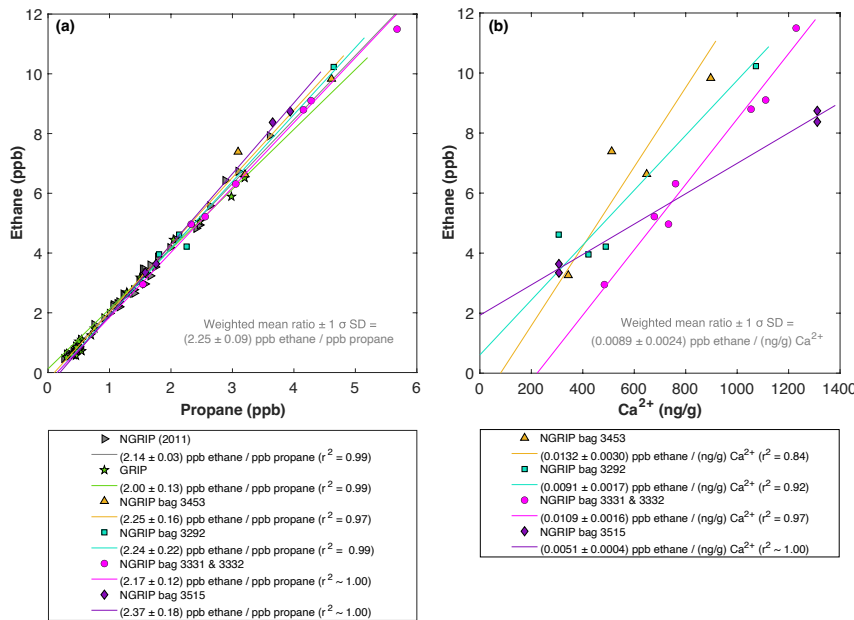
hat formatiert: Englisch (USA)

hat gelöscht: 5

636 color-coded, we can clearly see that the ratio is essentially the same between the individual bags
637 and that the correlation is also very high within each bag (although we have to consider for the
638 significance of this correlation that the number of samples per bag is very low). This indicates
639 that for NGRIP ice ethane and propane are found in a fixed ratio. Accordingly, excess ethane
640 and propane production can be well represented by the weighted mean ratio and ethane and
641 propane are produced in a ratio of approximately 2:1. Very similar results were also observed
642 in NGRIP samples measured in 2011 and in GRIP samples revealing an ethane to propane ratio
643 of 2.14 ± 0.03 ($r^2 = 0.99$) and 2.00 ± 0.13 ($r^2 = 0.99$), respectively (see Fig. 4, left panel).

hat gelöscht: 5

hat gelöscht: ¶



651
652 **Figure 4:** NGRIP and GRIP results of ethane and propane from the 1st extraction. (a) Concentrations of ethane
653 and propane and their ratios to each other for NGRIP and GRIP samples measured in the 1st extraction of the $\delta^{13}C$ -
654 CH_4 device. Colors and symbols indicate the different NGRIP bags or cores used. (b) Bag-specific production
655 ratios of ethane in relation to the Ca^{2+} concentration for NGRIP samples. Note that for bag 3515 there is a data gap
656 in the Ca^{2+} record and an anomaly of the Ca^{2+} to dust mass ratio for the replicate sample at 1932.7 m. Thus, the
657 Ca^{2+} concentration for these two data points is likely overestimated (see Fig. A3).

658
659
660 Methane concentrations range from 407 ppb to 476 ppb and are predominantly of atmospheric
661 origin (see Fig. 5). The amount of $CH_{4(xS)}$ is the difference between the measured methane
662 concentration and the atmospheric background concentration. To quantify $CH_{4(xS)}$ we use the
663 fact that due to the low-pass filtering of the bubble enclosure process all samples within one
664 bag should have the same atmospheric CH_4 concentration. This also ensures that any physical
665 processes that potentially influence the atmospheric alkanes in our samples (gravitational
666 enrichment, thermodiffusion, disequilibrium effects on CH_4 isotopes) are the same for all
667 samples within one bag. The only difference between these samples is, thus, the degree of
668 $CH_{4(xS)}$ production which can be estimated from the linear fit between the measured CH_4
669 concentration and the concentration of another species (e.g. ethane, propane, mineral dust, or
670 Ca^{2+}), which serves as a proxy for $CH_{4(xS)}$ production. The closest relationship was found for
671 [C_2H_6] and quantifying $CH_{4(xS)}$ was done by extrapolating the linear regression between ethane

Formatiert: Nicht vom nächsten Absatz trennen

hat formatiert: Schriftart: 10 Pt., Nicht Kursiv

hat gelöscht: Note that for a coherent presentation throughout the paper and a better comparison, ethane is always plotted on the y-axis while we partly discuss ratios the other way round.

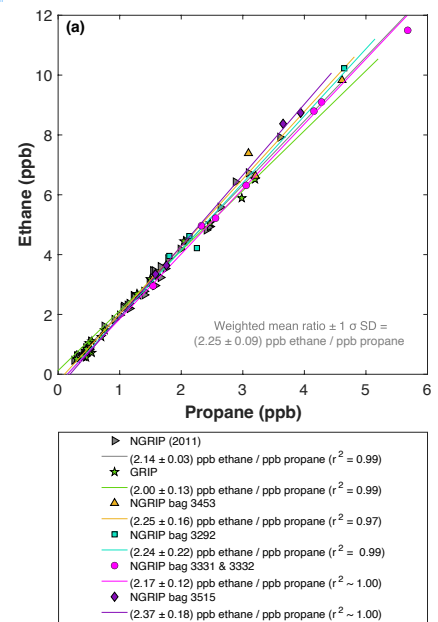


Figure 4:

hat formatiert: Schriftart: 10 Pt., Nicht Kursiv, Schriftfarbe: Text 1

hat formatiert: Schriftart: 10 Pt., Nicht Kursiv, Schriftfarbe: Text 1

hat formatiert: Schriftfarbe: Text 1

hat gelöscht: 4

hat gelöscht: is calculated from the

hat gelöscht: most precise

682 and methane to an ethane concentration of 0.39 ppb, the assumed atmospheric [C₂H₆]. This
683 leads to an estimate of the true atmospheric [CH₄] value within the respective bag, a value that
684 can then be subtracted from the measured CH₄ concentration to obtain the CH_{4(xS)} in each
685 sample. The uncertainty of the calculated CH_{4(xS)} is typically 8 ppb.

687 Using the relation of ethane to methane this approach translates into CH_{4(xS)} in the range of 14
688 ppb to 91 ppb for these five NGRIP bags with a mean excess of 39 ppb. Equivalent calculations
689 can be made using propane, dust, or Ca²⁺ as proxy for CH_{4(xS)} production, however, the
690 relationship between dust parameters and CH_{4(xS)} is more variable and does not lead to equally
691 precise values for CH_{4(xS)}. Nevertheless, the obtained mean CH_{4(xS)} using the relation of mineral
692 dust or Ca²⁺ to methane is similar [in size](#) to the one obtained by ethane.

694 We find that there [exists](#) a constant production ratio between [all three excess alkanes for all](#)
695 [bags investigated](#). The weighted mean [production ratio](#) and its weighted standard deviation was
696 calculated to be (6.42 ± 1.57) ppb methane / ppb ethane and (14.3 ± 3.7) ppb methane/ ppb
697 propane for the samples of the five main NGRIP bags, and (2.25 ± 0.09) ppb ethane/ ppb
698 propane (also including NGRIP2011 and GRIP here). [Note that there is a flagged sample for](#)
699 [CH₄ in bag 3453 \(yellow asterisk in Fig. 5\), where one vent \(V6\) was unintentionally open](#)
700 [during the measurement, which may have compromised the result. We therefore excluded the](#)
701 [production ratio determined from bag 3453.](#)

703 [In summary, we can characterize the excess alkane production in our measured NGRIP samples](#)
704 [by an overall methane/ethane/propane ratio of approximately 14:2:1.](#) This constant relationship
705 between different alkanes suggests that excess alkanes are produced in a fixed ratio by a
706 common production process.

708 Another important observation is the close relation between excess alkanes and the content of
709 mineral dust within the ice core samples. Using measurements on GISP2 and NEEM ice core
710 samples, Lee et al. (2020) reported for the first time the close relation of CH_{4(xS)} to chemical
711 impurities with the highest correlation with Ca²⁺. This is supported by our measurements on
712 NGRIP and GRIP samples revealing [an overall increase of CH_{4\(xS\)}, ethane, and propane with](#)
713 [increasing Ca²⁺ \(see for example the ethane/Ca²⁺ relationship in Fig. 4, right panel\).](#) Although
714 the connection between ethane and Ca²⁺ is more variable than for ethane and propane between
715 the different bags, the slopes of the linear regressions in Fig. 4 (right panel) are still the same

hat gelöscht: Note, this mean value is not representative for this time interval as values are biased towards higher values as we intentionally selected samples with high Ca²⁺ content for our study.

hat gelöscht: is

hat gelöscht: the measured

hat gelöscht: . Production ratios are the average of single-bag ratios weighted by the numbers of samples measured per bag.

hat gelöscht: Alkane concentrations were highly correlated within single bags.

hat gelöscht: (weighted by the number of samples in each bag)

hat formatiert: Schriftart: 12 Pt.

hat formatiert: Schriftart: 12 Pt., Nicht Kursiv

hat formatiert: Schriftart: 12 Pt.

hat gelöscht: x

hat formatiert: Schriftart: 12 Pt.

hat gelöscht: as

hat gelöscht: ent

hat formatiert: Schriftart: 12 Pt.

hat formatiert: Schriftart: 12 Pt.

hat formatiert: Schriftart: 12 Pt.

hat gelöscht: have

hat formatiert: Schriftart: 12 Pt.

hat gelöscht: sample from the ratio of

hat formatiert: Schriftart: 12 Pt.

hat gelöscht: We therefore

hat gelöscht: with

hat gelöscht: o

hat gelöscht: as well as

hat gelöscht:

hat formatiert: Hochgestellt

hat gelöscht: 5

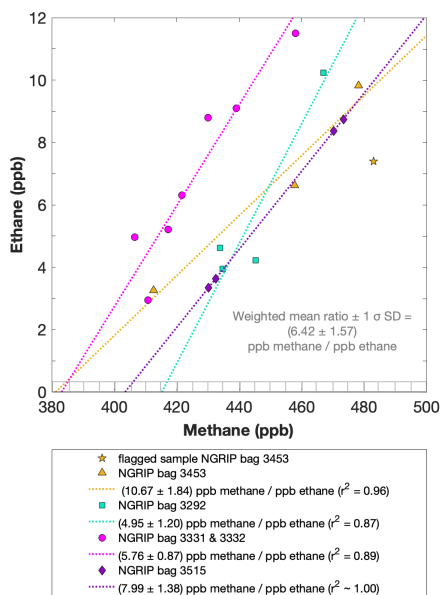
hat gelöscht: 5

740 within the 2 σ uncertainty and the weighted mean ratio of all NGRIP samples amounts to
 741 (0.0089 ± 0.0024) ppb ethane/ (ng/g) Ca^{2+} . However, this weighted mean value is likely biased
 742 low due to the relatively low ethane/ Ca^{2+} slope of bag 3515. Due to a data gap at 1932.7 m in
 743 the Ca^{2+} record, the corresponding Ca^{2+} concentration for two of the samples of this bag is
 744 subject to a large interpolation error and overestimated Ca^{2+} (see Fig. A3).

745
 746 The results agree with results from GRIP and older NGRIP (2011) samples, revealing an ethane/
 747 Ca^{2+} ratio of 0.0105 ± 0.0029 ($r^2 = 0.76$) and 0.0090 ± 0.0006 ($r^2 = 0.91$), respectively.

748 Based on the fixed ratio of excess CH_4 and ethane described above this translates into a
 749 weighted mean excess $\text{CH}_4/\text{Ca}^{2+}$ ratio of (0.0529 ± 0.0111) ppb methane per (ng/g) Ca^{2+} .

750



751

752 **Figure 5: NGRIP results of methane and ethane from the 1st extraction.** Concentrations of methane (ppb) and
 753 ethane (ppb) and their ratios to each other for NGRIP samples measured in the 1st extraction of the $\delta^{13}\text{C}\text{-CH}_4$
 754 device. Different colors and symbols indicate the different NGRIP bags used for our analysis. Note that there is a
 755 flagged sample for CH_4 in bag 3453 as indicated with a yellow asterisk, which is not included in the ratio of bag
 756 3453. The grey hatched area indicates past atmospheric ethane concentrations of maximum 0.39 ppb as estimated
 757 by Nicewonger et al. (2016).

758

759

760

hat gelöscht: ¶

hat gelöscht: Note also the mismatch in the peak shape of the Ca^{2+} and that of the dust mass suggesting an anomalous aerosol chemistry for this peak.

hat formatiert: Durchgestrichen

hat gelöscht: se

hat gelöscht: ¶

hat gelöscht: +. Note that due to the larger variability in the excess CH_4 /ethane variation and the substantial variability in the ethane/ Ca^{2+} relationship the relative uncertainty of this excess $\text{CH}_4/\text{Ca}^{2+}$ relationship is relatively large and dust and Ca^{2+} are less suitable proxies to estimate $\text{CH}_4(\text{xs})$ compared to ethane or propane.

hat gelöscht:

Formatiert: Vom nächsten Absatz trennen

hat formatiert: Schriftfarbe: Text 1, Englisch (USA)

hat formatiert: Schriftart: 10 Pt., Nicht Kursiv, Schriftfarbe: Text 1, Englisch (USA)

hat formatiert: Schriftart: 10 Pt., Nicht Kursiv, Schriftfarbe: Text 1

hat gelöscht: 5

hat formatiert: Schriftart: Nicht Kursiv

hat gelöscht: x

hat gelöscht: ¶

hat formatiert: Englisch (USA)

hat gelöscht: ¶
 Taken these findings together, we see a constant relationship between excess methane, ethane, and propane, but also a close relation to the content of mineral dust within the ice core sample, which, however, is not as tight as for the alkanes and suggests that dust parameters are only an indirect proxy of the alkane excess. ¶

hat gelöscht: ¶

hat formatiert: Schriftart: Nicht Fett, Schriftfarbe: Automatisch

Formatiert: Standard, Zeilenabstand: einfach

823 3.1.2 Excess alkanes in the 2nd extraction

824

825 With the 2nd extraction of the $\delta^{13}\text{C}$ -CH₄ analyses we can evaluate the temporal dynamics of
826 excess alkane production, assuming that all alkanes extracted in the 2nd extraction were
827 produced in the time after the 1st extraction was completed.

828 For our Greenland samples we measured a range of about 0.2 to 2.4 pmol for ethane and a range
829 of 0.1 to 1.2 pmol for propane in the 2nd extraction (Fig. 6, right panel). These values in pmol
830 are equivalent to 0.2 to 4.8 ppb of ethane and 0.2 to 2 ppb of propane assuming that the amount
831 of excess alkanes was added to 14 mL of ice core air (which is the typical ice sample size of
832 150 g with a total air content of 0.09 mL/g). The measured amount of methane ranges between
833 3 pmol and 20 pmol (Fig. 6, left panel).

834

835 The ratio of the measured amount for the individual species between the 1st and the 2nd
836 extraction amounts to 3.6 ± 0.85 ($r^2 = 0.78$) for ethane (Fig. 7, right panel), 3.3 ± 0.33 ($r^2 =$
837 0.78) for propane (combined data of NGRIP and GRIP) and 3.8 ± 1.62 ($r^2 = 0.33$) for methane
838 (only NGRIP data), where the uncertainty for CH₄ is again much larger. Thus, we can conclude
839 that the amount of alkanes produced during the waiting time after the 1st extraction until the 2nd
840 extraction was finished, was approximately 30% of the amount produced during the 1st
841 extraction. Results from the 2nd extraction also demonstrate that this process is slow and not
842 completed during the time of the 1st extraction. We can thereby confirm the results of Lee et al.
843 (2020) but we are able to show for the first time that this process leads also to production of
844 excess ethane and propane.

845

846 For a better estimate of the temporal reaction kinetics of the underlying process, we can relate
847 the measured amount of the individual species to the time available for a potential reaction in
848 the meltwater during each extraction. For the five GRIP samples that were measured with a 2nd
849 and 3rd extraction (see Sec. 2.2 for details) we take the cumulative production amount (where
850 the first data point is the produced amount in the 1st extraction, the second data point is the sum
851 of the 1st and 2nd extraction, and the third data point is the sum of the 1st, 2nd, and 3rd extraction).

852 In the example shown for ethane (Fig. C1, Appendix C) we can see the assumed first-order
853 reaction kinetics with a saturation of ethane accumulation over time providing a good model
854 for our measurements (details on the calculation can be found in the Appendix C). With that,
855 we can estimate the half-life time (τ) of the production to be approximately 30 min. Note that
856 this long half life has also an implication for a potential excess production of CH₄ in continuous

hat gelöscht: in

hat gelöscht: gas extraction during the 1st extraction was quantitative and

hat gelöscht: (Fig. 6, right panel)

Formatiert: Abstand zwischen asiatischem und westlichem Text anpassen, Abstand zwischen asiatischem Text und Zahlen anpassen

hat gelöscht: ¶

hat gelöscht: ¶
We can therefore safely conclude that excess alkanes are also produced/ released during the 2nd extraction.

hat gelöscht: and here

hat gelöscht:

hat gelöscht: 2.1 and

hat gelöscht: Exemplarily

hat gelöscht: B

hat gelöscht: B

hat formatiert: Nicht Hervorheben

hat gelöscht: an exponential accumulation of ethane

hat gelöscht: (accompanied by an exponential decay of organic precursor substances)

hat gelöscht: .

hat formatiert: Tiefgestellt

hat gelöscht: Compared to

876 flow techniques, where the reaction time before the air is separated from the liquid water stream,
877 is only 1-2 min. Thus, only 5-10 % of the *in extractu* production found in our 1st extraction can
878 be expected [in such continuous flow measurements, which are difficult to detect](#).

879

880 The goodness of fit of the ratios of the measured concentrations between the 1st and the 2nd
881 extraction is $r^2 = 0.78$ for both ethane and propane, indicating that the production/release in the
882 1st extraction in relation to the 2nd extraction is well correlated for both species (see Fig. 7b for
883 ethane). Thus, samples that produced higher excess alkanes during the 1st extraction also
884 produced more excess alkanes in the 2nd extraction, suggesting that the production is dependent
885 on the amount of some reactant present in the samples from which excess alkanes are produced.
886 Again, for CH₄ this relationship is more variable which is likely related to the higher uncertainty
887 in measuring CH₄ for the 2nd extraction.

888

889 The ratio of ethane to propane of all measured Greenland samples in the 2nd extraction is 1.98
890 ± 0.07 ($r^2 = 0.99$). The ratio of methane to ethane is 8.17 ± 1.14 ($r^2 = 0.86$). Accordingly, the
891 overall relationship between methane, ethane, and propane in the 2nd extraction can be
892 characterized by a ratio of approximately 16:2:1. However, comparing the ratios of
893 ethane/propane and methane/ethane between the 1st and the 2nd extraction, there is no significant
894 difference within the 2σ uncertainties from 2.25 ± 0.09 to 1.98 ± 0.07 , and from 6.42 ± 1.57 to
895 8.17 ± 1.14 . We can conclude that within the error limits, the production ratios stayed the same,
896 suggesting that the same *in extractu* process is at play during both extractions.

897

898 In the 2nd extraction, we can again observe the relation between excess alkanes and the amount
899 of mineral dust. Figure 7a shows the correlation of ethane (fmol/g meltwater) to Ca²⁺ (ng/g) in
900 all measured NGRIP and GRIP samples in the 2nd extraction revealing a production of $(0.0085$
901 $\pm 0.0011)$ fmol/(g meltwater) ethane per (ng/g) Ca²⁺ with $r^2 = 0.70$. For methane, we observe a
902 production ratio of (0.0556 ± 0.01513) fmol/(g meltwater) methane per (ng/g) Ca²⁺ with a
903 correlation of $r^2 = 0.47$ (data not shown).

904

905 Overall, excess alkane concentrations are increasing with increasing Ca²⁺ concentrations, in
906 both the 1st and the 2nd extraction. The total alkane production/release, however, decreased in
907 the 2nd extraction, suggesting the progressive exhaustion over time of some reactant necessary
908 for the *in extractu* process. We propose that this reactant co-varies with Ca²⁺ and particulate

hat gelöscht: ,

hat gelöscht: 2.00

hat gelöscht: 34

hat gelöscht: 07

hat gelöscht: 93

hat gelöscht: C

hat gelöscht:

hat gelöscht:

hat gelöscht: 2

hat gelöscht: 2.00

hat gelöscht: 34

hat gelöscht: 1.07

hat gelöscht: (left panel)

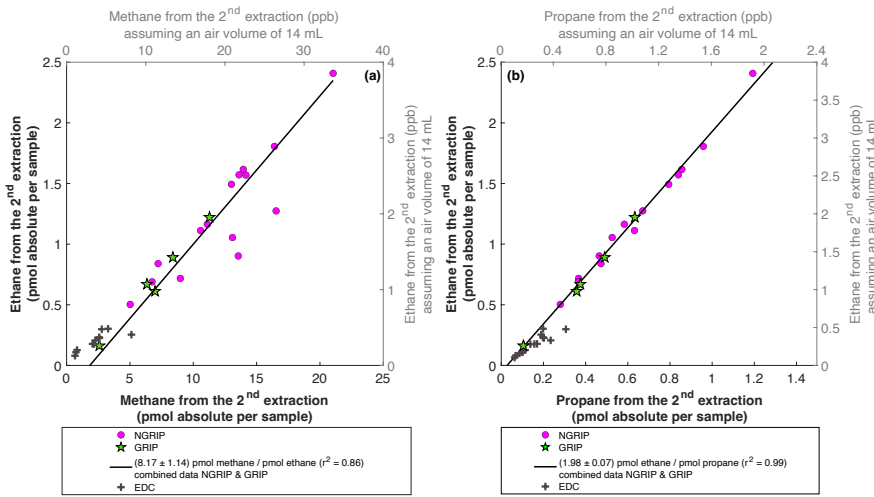
hat gelöscht:

hat gelöscht:

hat gelöscht:

925 dust, where Ca^{2+} is of course not a reactant itself and represents only a proxy for higher in
 926 extractu production.

927



928

929 **Figure 6. NGRIP and GRIP results of excess methane, ethane, and propane from the 2nd extraction. (a)**
 930 **Concentrations of methane and ethane and their ratios to each other. (b) Concentrations of propane and ethane and**
 931 **their ratios to each other. Units are given as pmol absolute per sample on the primary axis in black and in ppb**
 932 **assuming an air volume of 14 mL of the ice core sample on the secondary axis in grey. Grey crosses indicate the**
 933 **blank level of the system estimated from 2nd extractions of EDC ice core samples.**

934

935

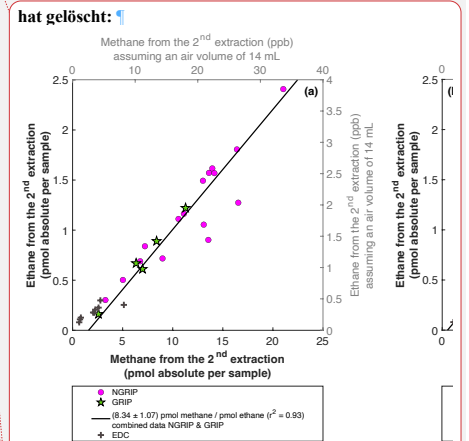
936

- hat gelöscht: and that
- hat formatiert: Schriftart: 12 Pt.
- hat gelöscht: n
- hat formatiert: Schriftart: 12 Pt.
- hat formatiert: Schriftart: 12 Pt.
- hat formatiert: Schriftart: 12 Pt.
- hat gelöscht: concentrations are

hat formatiert: Schriftart: 10 Pt., Nicht Kursiv, Schriftfarbe: Text 1

hat formatiert: Schriftart: 10 Pt., Nicht Kursiv, Schriftfarbe: Text 1

hat formatiert: Schriftart: 10 Pt., Nicht Kursiv, Schriftfarbe: Text 1

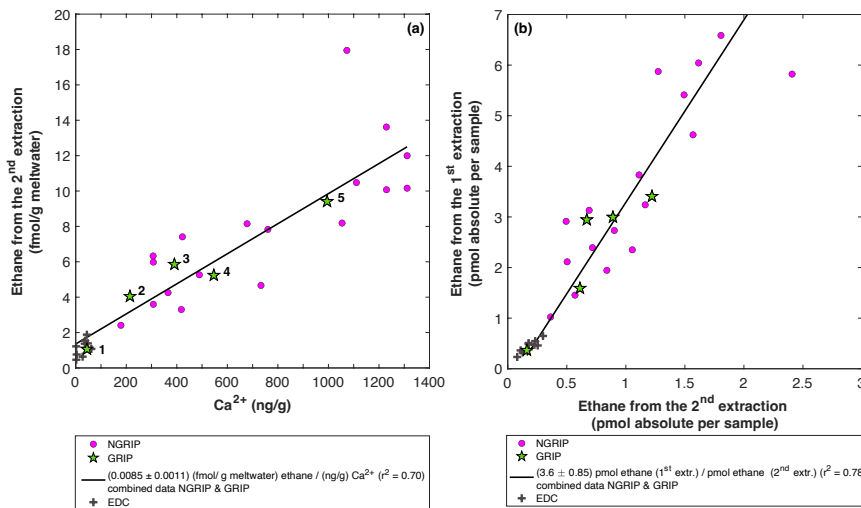


61

Figure 6:

hat formatiert: Schriftart: Nicht Kursiv, Hochgestellt

hat gelöscht: e measurements



945
946
947 **Figure 7. GRIP and GRIP results of ethane from the 2nd extraction in relation to the Ca²⁺ concentration**
948 **and to the 1st extraction. (a)** Produced amount of ethane in the meltwater (fmol/g meltwater) in relation to the
949 Ca²⁺ concentration in the ice core samples. **The numbered GRIP samples are used in Figure C1 to evaluate the**
950 **temporal dynamics. Grey crosses indicate the blank level of the system estimated from 2nd extractions of EDC**
951 **ice core samples. (b)** Relation of the amount of ethane (pmol) measured in the 1st and 2nd extraction.

952 3.2 Isotopic composition of excess methane

953
954
955 In this section we characterize the isotopic signature of excess methane and explore how we
956 can use this parameter to better identify its source or production pathway. The evaluation of the
957 carbon and deuterium isotopic signature of excess methane ($\delta^{13}\text{C-CH}_{4(\text{xs})}$ and $\delta\text{D-CH}_{4(\text{xs})}$) is
958 based on the Keeling-plot approach (Keeling, 1958, 1961; Köhler et al., 2006).

960 3.2.1 $\delta^{13}\text{C-CH}_4$ isotopic signature of excess methane

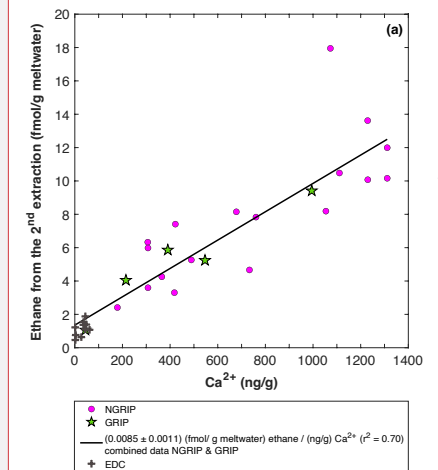
961
962 Figure 8 (left panel) shows the $\delta^{13}\text{C-CH}_4$ results of the 1st extraction. The carbon isotopic
963 signature of excess CH₄ from the 1st extraction of the ice core sample measurements within one
964 NGRIP bag are obtained from the y-intercept of the Keeling-plot, representing the excess $\delta^{13}\text{C-}$
965 CH₄ value for this bag. **Note that the two NGRIP bags 3331 and 3332 are neighbouring bags**
966 **and were therefore combined into one Keeling y-intercept. As the individual samples in these**
967 **two bags span less than 10 years between each other, they are the same within the age**
968 **distribution, and the assumptions for the Keeling-plot approach (see Sec. 2.1) are met.** All bags
969 show agreement in $\delta^{13}\text{C-CH}_4$ signature (y-intercepts) within 2σ uncertainties. The weighted

Formatiert: Nicht vom nächsten Absatz trennen

hat formatiert: Schriftart: 10 Pt., Schriftfarbe: Text 1

hat formatiert: Schriftart: 10 Pt., Schriftfarbe: Text 1

hat gelöscht:



7
Figure 7: N

hat gelöscht:

hat gelöscht: with

hat gelöscht:

hat gelöscht: Grey crosses indicate the blank level of the system estimated from EDC ice core sample measurements.

hat formatiert: Englisch (USA)

hat gelöscht:

hat nach unten verschoben [1]: The evaluation of the carbon and deuterium isotopic signature of excess methane ($\delta^{13}\text{C-CH}_{4(\text{xs})}$ and $\delta\text{D-CH}_{4(\text{xs})}$) is based on the Keeling-plot approach (Keeling, 1958, 1961; Köhler et al., 2006).

hat gelöscht: Here

hat gelöscht: ,

hat gelöscht: want to

hat verschoben (Einfügung) [1]

hat gelöscht: the 12

989 mean isotopic signature is $(-47.0 \pm 2.9)\%$, with weights assigned by the number of samples
990 that constrained each individual Keeling plot regression line.

hat gelöscht: (-46.4 ± 2.4)

992 Figure 8 (right panel) shows the isotopic results in relation to the amount of CH_4 produced
993 during the 2nd extraction. No atmospheric CH_4 is present during the 2nd extraction and the
994 individual isotopic values in Fig. 8 (right panel) are the directly measured values of excess CH_4
995 without applying the Keeling-plot approach. For a better comparison, the produced CH_4 is
996 shown both in pmol (lower axis in Fig. 8, right panel) and in a mixing ratio CH_4 scale (ppb).
997 The Keeling y-intercept values of the 1st extraction are added in the right panel of Fig. 8.

hat gelöscht:

hat gelöscht: , where we assume that the excess CH_4 produced during the 2nd extraction is diluted into an air volume of 14 mL at standard temperature and pressure, which is a typical value for the amount of air extracted from our samples in the 1st extraction.

999 The $\delta^{13}\text{C}-\text{CH}_4$ values of the 2nd extraction range between -34% and -48% with the mean being
1000 $(-41.2 \pm 2.2)\%$. This value appears isotopically somewhat heavier compared to the weighted
1001 mean of $(-47.0 \pm 2.9)\%$ inferred from the Keeling analysis, however, is still the same within
1002 the 2σ error limits. We note that the measured peak areas for the 2nd extractions are very small
1003 and lie outside of the typical range of our gas chromatography mass spectrometry analysis for
1004 $\delta^{13}\text{C}-\text{CH}_4$ and we cannot exclude some bias in these results. However, we mimicked these small
1005 peak areas with injections of small amounts of standard air and observed no significant bias in
1006 the measured $\delta^{13}\text{C}-\text{CH}_4$ values given that the precision of such small peaks is around 2% .

hat gelöscht: ¶

hat formatiert: Schriftfarbe: Text 1

hat gelöscht: is

hat gelöscht: (-46.4 ± 2.4)

hat gelöscht: 1

hat gelöscht: 2

hat gelöscht: □ □

1008 Another caveat is the considerable blank contribution for CH_4 that we observe for the 2nd
1009 extraction. Since Antarctic ice cores do not show a sizable *in extractu* production (Fig. 7, grey
1010 crosses for EDC) we measured EDC samples with the same protocol of a 2nd extraction as for
1011 our Greenland samples to provide an upper boundary of this blank. Hence the 2nd extraction of
1012 the EDC samples are a conservative blank estimate while the true system blank is lower. As
1013 can be seen in Fig. 8 (right panel) the amount of CH_4 measured for these EDC samples (grey
1014 crosses) is on average about 2 pmol (equivalent to about 3 ppb). For comparison, our ice
1015 samples from Greenland show a range of about 5 to 20 pmol, indicating a considerable blank
1016 contribution in the 2nd extraction.

hat gelöscht:

hat formatiert: Schriftart: Nicht Kursiv, Schriftfarbe: Text 1, English (USA)

1017
1018 To estimate the influence of the blank on the isotopic signature that occurs during the 2nd
1019 extraction we used the values from our EDC measurements and applied an isotope mass balance
1020 approach. The $\delta^{13}\text{C}-\text{CH}_4$ blank signature obtained from these EDC samples is -39.0% , hence
1021 a few % heavier than the mean $\delta^{13}\text{C}-\text{CH}_4$ signature of the excess CH_4 from this 2nd extraction
1022 for the Greenland samples. On average, the correction would shift our NGRIP values towards

hat formatiert: Schriftart: Nicht Kursiv, Schriftfarbe: Text 1

Formatiert: Zeilenabstand: 1,5 Zeilen

lighter (more negative) values by 0.31 ‰. This systematic correction is thus small compared to the typical measurement precision obtained both from the Keeling-plot approach and the direct measurement of the $\text{CH}_{4(\text{xs})}$ with the 2nd extraction. As the $\delta^{13}\text{C}-\text{CH}_4$ signature of the blank is close to the NGRIP values, performing a blank correction has only little leverage. Considering these analytical limitations of our 2nd extraction for $\delta^{13}\text{C}-\text{CH}_4$, these findings suggest that $\text{CH}_{4(\text{xs})}$ produced during the 1st and 2nd extraction has the same $\delta^{13}\text{C}-\text{CH}_4$ isotopic signature within the 2σ error limits and is likely produced/released by the same process in both extractions.

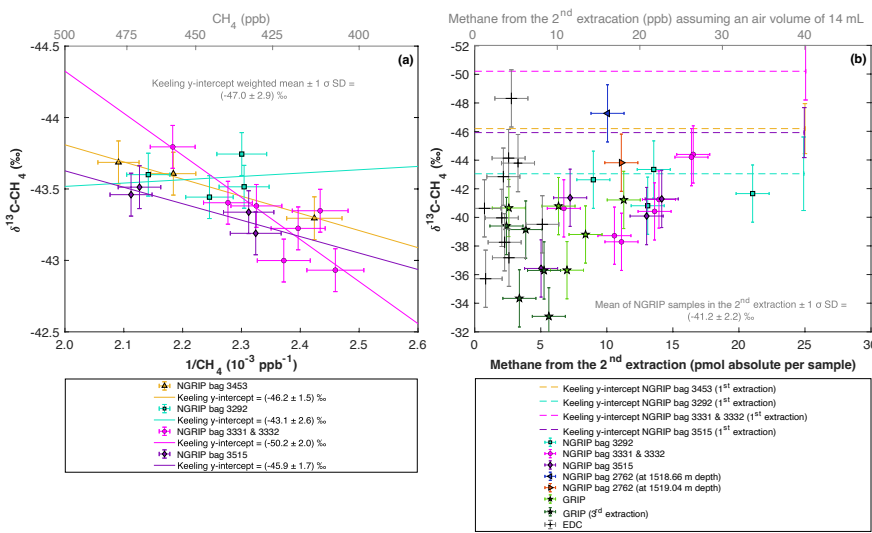


Figure 8; NGRIP (and GRIP) $\delta^{13}\text{C}-\text{CH}_4$ results of the 1st and 2nd extraction measured with the $\delta^{13}\text{C}-\text{CH}_4$ device. (a) Keeling-plot of $\delta^{13}\text{C}-\text{CH}_4$ for NGRIP samples from the five main bags (3292, 3331 & 3332, 3453, 3515) measured in the 1st extraction. Colors and symbols indicate individual measurements of the respective bags. Colored lines indicate the corresponding Keeling regression line of each individual bag. (b) $\delta^{13}\text{C}-\text{CH}_4$ (‰) values in relation to the amount of methane measured for the 2nd extraction. Units for CH_4 are given as pmol absolute per sample on the primary axis in black, and in ppb assuming an air volume of 14mL of an ice core sample on the secondary axis in grey. Colors and symbols indicate individual measurements of the respective bags. Color-coded lines indicate the corresponding Keeling y-intercept of each individual bag as measured in the 1st extraction. Grey crosses indicate the blank level of the system estimated from 2nd extractions of EDC ice core samples.

3.2.2 $\delta\text{D}-\text{CH}_4$ isotopic signature of excess methane

Figure 9 shows the isotopic results of the $\delta\text{D}-\text{CH}_4$ analyses. Due to the larger sample size required for the $\delta\text{D}-\text{CH}_4$ analyses and the sample availability restrictions only two bags could be studied for $\delta\text{D}-\text{CH}_4$. The individual isotopic results obtained from the ice core sample

hat formatiert: Nicht Hervorheben

hat formatiert: Nicht Hervorheben

hat formatiert: Schriftart: Nicht Kursiv, Schriftfarbe: Text 1, Englisch (USA)

hat gelöscht: Another caveat is the considerable blank contribution for CH_4 that we observe for the 2nd extraction. Since Antarctic ice cores do not show a sizable in extractu production (Fig. 7, grey crosses for EDC) we measured EDC samples with the same protocol as for our Greenland samples to provide an upper boundary of this blank. As can be seen in Fig. 8 (right panel) the amount of CH_4 measured for these EDC samples (grey crosses) is on average about 2 pmol (equivalent to about 2 ppb). For comparison, our ice samples from Greenland show a range of about 5 to 20 pmol, thus we have a considerable blank contribution. However, the $\delta^{13}\text{C}-\text{CH}_4$ blank signature obtained from these EDC samples is comparable to or - if at all - only a few ‰ heavier than the $\delta^{13}\text{C}-\text{CH}_4$ signature of the excess CH_4 from this 2nd extraction for the Greenland samples. (more negative) Considering these analytical limitations of our 2nd extraction for $\delta^{13}\text{C}-\text{CH}_4$, these findings suggest that excess CH_4 produced during the 1st and 2nd extraction has a similar the same $\delta^{13}\text{C}-\text{CH}_4$ isotopic signature within the 2σ error limits and is likely produced/released by the same process in both extractions.

Formatiert: Nicht vom nächsten Absatz trennen

hat formatiert: Schriftart: 10 Pt., Nicht Kursiv, Schriftfarbe: Text 1, Englisch (USA)

hat formatiert: Schriftart: 10 Pt., Nicht Kursiv, Englisch (USA)

hat formatiert: Schriftart: 10 Pt., Englisch (USA)

Formatiert: Block

hat gelöscht: 8for [14]

hat formatiert: Englisch (USA)

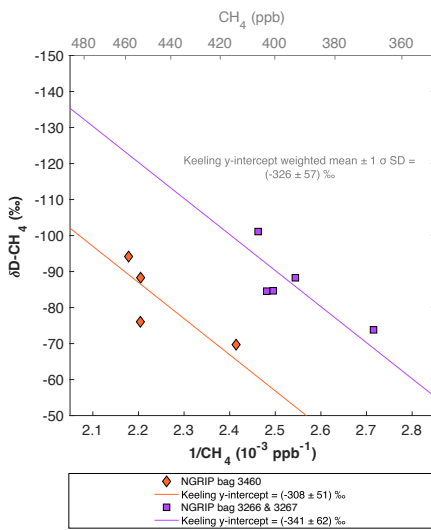
hat gelöscht: Figure 8; NGRIP (and GRIP) $\delta^{13}\text{C}-\text{CH}_4$ results of the 1st and 2nd extraction measured with the $\delta^{13}\text{C}-\text{CH}_4$ device. (a) Keeling-plot of $\delta^{13}\text{C}-\text{CH}_4$ for NGRIP samples from th [15]

hat formatiert: Englisch (USA)

hat gelöscht: were

1110 measurements within one NGRIP bag are again combined into one Keeling y-intercept,
 1111 representing the $\delta D-CH_4$ value for this bag. NGRIP bag 3460 (orange) reveals a Keeling y-
 1112 intercept $\delta D-CH_4$ value of $(-308 \pm 51) \text{ ‰}$. The two NGRIP bags 3266 and 3267 (purple)
 1113 are neighbouring bags and were therefore combined into one Keeling y-intercept revealing a $\delta D-$
 1114 CH_4 value of $(-341 \pm 62) \text{ ‰}$. The difference between the two Keeling y-intercepts of the
 1115 individual bags is within the error limits. Accordingly, we combine the two values to a weighted
 1116 mean and weighted uncertainty of $(-326 \pm 57) \text{ ‰}$.
 1117 Our results are consistent with the findings of Lee et al. (2020), who used the NGRIP $\delta D-CH_4$
 1118 record of Bock et al. (2010b) and the NGRIP $[CH_4]$ record of Baumgartner et al. (2014) to
 1119 estimate the $\delta D-CH_{4(xS)}$ signature in these samples. Assuming a two-component mixture of
 1120 atmospheric methane and excess methane in their model led to a best estimate of (-293 ± 31)
 1121 ‰ for $\delta D-CH_{4(xS)}$ which is within the error limits of our Keeling-plot results.

1122



1123

1124 **Figure 9: NGRIP $\delta D-CH_4$ results.** Keeling-plot of $\delta D-CH_4$ of NGRIP samples measured with the $\delta D-CH_4$ device.
 1125 Colors and symbols indicate individual measurements of the respective bags and colored lines indicate the
 1126 corresponding regression of each individual bag.

1127

1128 4. Testing the hypotheses explaining excess alkanes

1129

1130 In Sect. 3 several pieces of evidence for the production/release of excess alkanes in Greenland
 1131 ice core samples were collected:

hat gelöscht: and thus do not show significant differences

hat gelöscht: ¶

hat gelöscht: a

Formatiert: Nicht vom nächsten Absatz trennen

hat formatiert: Schriftart: 10 Pt.

hat gelöscht: 9

hat gelöscht: ¶

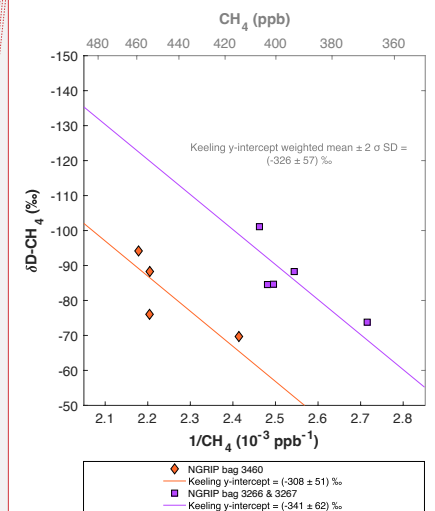


Figure 9:

hat formatiert: Schriftart: 10 Pt., Nicht Kursiv, Schriftfarbe: Text 1

hat formatiert: Schriftart: 10 Pt., Nicht Kursiv, Schriftfarbe: Text 1

hat formatiert: Schriftart: 10 Pt., Nicht Kursiv

hat gelöscht:

Formatiert: Standard, Links

- 1141
- 1142 - We can confirm the observations of Lee et al. (2020) on excess methane in different
- 1143 Greenland ice cores and its covariance with the amount of mineral dust in the ice.
- 1144 Despite the different extraction techniques applied (multiple melt-refreeze method in
- 1145 Lee et al. (2020) versus two subsequent wet extractions in our study), we can further
- 1146 corroborate that the temporal dynamics of the production/release is on the order of hours
- 1147 and production/ release occurs when liquid water is present during extraction.
- 1148 - We document for the first time a co-production/release of excess methane, ethane, and
- 1149 propane, with the observed values for ethane and propane exceeding by far their
- 1150 estimated past atmospheric background concentrations.
- 1151 - Excess alkanes (methane, ethane, propane) are produced/ released in a fixed molar ratio
- 1152 of approximately 14:2:1, indicating a common origin.
- 1153 - We further characterize the isotopic composition of excess CH₄ of $\delta^{13}\text{C}-\text{CH}_{4(\text{xs})}$ and $\delta\text{D}-$
- 1154 $\text{CH}_{4(\text{xs})}$ to be $(-47.0 \pm 2.9) \text{‰}$ and $(-326 \pm 57) \text{‰}$ in NGRIP ice core samples,
- 1155 respectively. Within the error limits, our $\delta\text{D}-\text{CH}_{4(\text{xs})}$ results are consistent with the
- 1156 calculated best estimate of $(-293 \pm 31) \text{‰}$ by Lee et al. (2020).

1158 In the introduction we presented the hypotheses proposed by Lee et al. (2020) explaining their

1159 observations on CH_{4(xs)}. Here we resume the discussion of the original hypotheses and refine

1160 them in light of our new data from NGRIP and GRIP ice sample measurements. An overview

1161 of the different possible sources explaining excess alkanes is illustrated in Fig. 10 and Table 1.

1162 We discuss in the following three options for the origin of the observed excess alkanes;

1164 1.) Excess alkanes could be adsorbed on mineral dust particles prior to their deposition on the

1165 Greenland ice sheet and released in the laboratory during the prolonged melting process. The

1166 adsorption step could happen in the mineral dust source region (East Asian deserts) thereby

1167 adsorbing the alkanes from natural gas seeps within the sediment (process marked as A1, see

1168 Fig. 10). Alternatively, adsorption of atmospheric alkanes on dust particles can happen anytime

1169 starting from the soil surface in the dust source region, during atmospheric transport to the

1170 Greenland ice sheet after deflation, or within the firm layer before pores are closed-off (A2).

1171 The desorption of the adsorbed alkanes happens during the melting process for both cases.

1173 2.) Excess alkanes could be produced microbially. The production happens either in the ice

1174 itself (in situ), the alkanes are adsorbed on dust particles in the ice, and then slowly released

hat gelöscht:

hat gelöscht:

hat gelöscht: 46.4

hat gelöscht: 4

hat formatiert: Schriftart: 12 Pt.

hat gelöscht: .

hat gelöscht: believe that the

hat gelöscht: falls in one of the three categories

hat formatiert: Schriftfarbe: Text 1

hat formatiert: Schriftart: (Standard) Times New Roman, 12 Pt., Schriftfarbe: Text 1, Englisch (USA)

hat formatiert: Schriftart: (Standard) Times New Roman, 12 Pt., Schriftfarbe: Text 1

hat formatiert: Schriftart: (Standard) Times New Roman, 12 Pt., Schriftfarbe: Text 1, Englisch (USA)

hat formatiert: Nicht Hervorheben

hat gelöscht: and

hat gelöscht: there is adsorption of atmospheric alkanes on dust particles either at the soil surface in the dust source region or during atmospheric transport to the Greenland ice sheet after deflation

hat formatiert: Schriftart: (Standard) Times New Roman, 12 Pt., Schriftfarbe: Text 1

hat gelöscht: i

hat gelöscht:

hat gelöscht: the alkanes are

hat gelöscht: subsequently

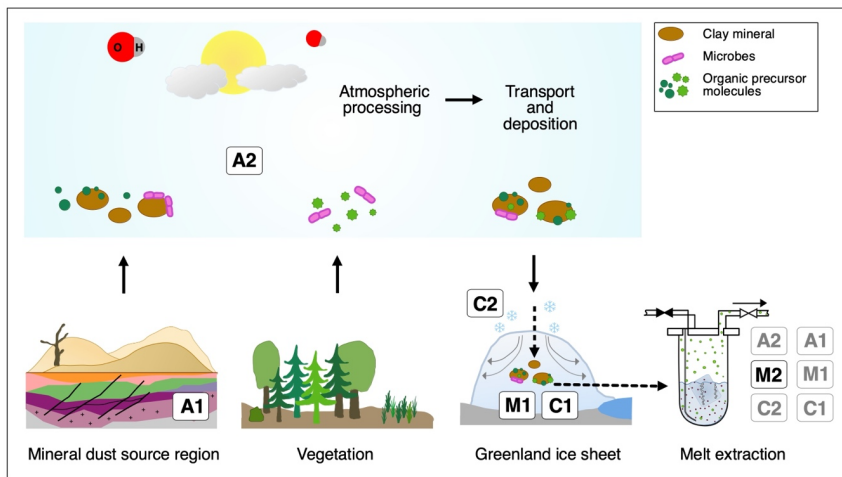
1191 during the melting phase in the laboratory (M1). Alternatively, the microbial production
 1192 happens in the meltwater during the melting process (*in extractu*) (M2). A microbial in situ
 1193 production in the ice without an adsorption-desorption process was already **deemed unlikely** by
 1194 Lee et al. (2020) since it is not compatible with **the lack of excess CH₄ in the CFA CH₄**
 1195 concentration records.

1196 3.) Excess alkanes are produced abiotically, e.g. by the decomposition of labile organic
 1197 compounds. This chemical reaction can happen either in the ice itself (in situ), **where excess**
 1198 **alkanes** are then adsorbed on dust particles and subsequently released during the melting
 1199 process (C1), or in the meltwater during extraction (*in extractu*) (C2). An abiotic in situ
 1200 production in the ice without an adsorption-desorption process can also be ruled out with the
 1201 CFA evidence.

1202

1203 We now discuss these mechanisms in detail and evaluate the viability of the different
 1204 hypotheses in the light of our new experimental observations.

1205



1206

1207 **Figure 10. Overview of the different possibilities explaining excess alkanes in dust-rich Greenland ice.** A
 1208 depicts an adsorption process of alkanes on mineral particles, either from natural gas seeps within the sediment
 1209 (A1) or from the atmosphere (A2) prior to their deposition on the Greenland ice sheet. **This gas is then desorbed**
 1210 **during the melting process in the laboratory.** M depicts a microbial production of excess alkanes, either in the ice
 1211 itself (in situ), **followed by** adsorption on dust particles in the ice and a subsequent **slow** desorption process during
 1212 the melting process (M1), or **a microbial production** in the meltwater (*in extractu*) (M2). C depicts the abiotic/
 1213 chemical production of excess alkanes, either in the ice itself (in situ) **followed by** adsorption on dust particles
 1214 after production in the ice and a subsequent **slow** desorption during the melting process (C1), or **abiotic production**
 1215 in the meltwater (*in extractu*) (C2).

1216

- hat gelöscht:
- hat gelöscht: ruled out
- hat gelöscht: evidence from the
- hat formatiert: Tiefgestellt
- hat gelöscht: Excess CH₄ is not observed in CFA records implying that the extraction/production of excess alkanes is slow relative to the short extraction time of CFA. This was used as evidence for desorption of alkanes from mineral dust particles in the ice which would be released slowly at the presence of liquid water and effect techniques using longer extractions.
- hat gelöscht:
- hat gelöscht: which
- hat gelöscht:

- Formatiert: Nicht vom nächsten Absatz trennen
- hat formatiert: Schriftart: 10 Pt., Nicht Kursiv, Schriftfarbe: Text 1
- Formatiert: Zeilenabstand: einfach
- hat formatiert: Schriftart: 10 Pt., Nicht Kursiv, Schriftfarbe: Text 1
- hat formatiert: Schriftart: Nicht Kursiv
- hat gelöscht: ¶
- hat gelöscht: y
- hat gelöscht: and in relation to a subsequent desorpti (... [16])
- hat formatiert: Schriftart: Nicht Kursiv
- hat gelöscht: and in relation to
- hat gelöscht: an
- hat gelöscht: process
- hat gelöscht: after production
- hat gelöscht:
- hat formatiert: Schriftart: Nicht Kursiv
- hat gelöscht: , and in relation to an
- hat gelöscht: process
- hat gelöscht:
- hat formatiert: Schriftart: Nicht Kursiv
- hat gelöscht: ¶

1250
1251
1252
1253
1254
1255
1256
1257
1258
1259
1260
1261
1262
1263
1264
1265
1266
1267
1268
1269
1270
1271
1272
1273
1274
1275
1276
1277
1278
1279
1280
1281
1282
1283
1284

(1) Adsorption/desorption of alkanes on mineral dust particles

Depending on where the adsorption takes place, the mineral particles might adsorb alkanes of different origin and composition. One possibility is that the adsorption already takes place within the sediment or soil of the dust source region, thus before mineral dust deflation, (erosion of loose material by winds from flat and dry areas; A1). As proposed by Lee et al. (2020), the major source region of mineral dust arriving in Greenland during the glacial (Taklamakan, Tarim Basin) are also regions where natural gas seeps reach the surface (Etiopie and Klusman, 2002; Etiopie et al., 2008). In this case the methane should reflect the isotopic composition and alkane composition of the seep. Alternatively, adsorption of atmospheric alkanes on the particles can happen anytime starting from the soil surface, during transport en route to the Greenland ice sheet after deflation and within the firm layer before pores are closed-off (A2). For the scenario A2 the fingerprint (isotopic composition and ratio of alkanes) of the adsorbed alkanes depends on the past atmospheric composition but could be modulated by selective fractionation processes during adsorption and desorption.

To be a viable mechanism for our problem, it requires that the adsorbed alkanes stay strongly bound at the mineral dust particles while desorption is minor both during the atmospheric transport and during the several hundred years the dust particle spends in the porous firm (age of the firm at bubble close-off). During the melting procedure the adsorbed alkanes would then be released from their mineral dust carrier, which in case of Greenland ice from glacial times is predominately consisting of clay minerals from the Taklamakan (and partly also Gobi) desert (Biscaye et al., 1997; Svensson et al., 2000; Ruth et al., 2003). However, other additional dust sources exist with their relative contribution varying with climate conditions (Han et al., 2018; Lupker et al., 2010).

Several experimental studies showed that clay minerals have a high adsorption capacity and retention potential for alkanes (Sugimoto et al., 2003; Cheng and Huang, 2004; Dan et al., 2004; Pires et al., 2008; Ross and Bustin, 2009; Ji et al., 2012; Liu et al., 2013; Tian et al., 2017). Influencing parameters for an adsorption-desorption process are mainly pressure, temperature, clay mineral type, micropore size, surface area, organic carbon content, and water/ moisture content (Sugimoto et al., 2003; Cheng and Huang, 2004; Dan et al., 2004; Pires et al., 2008; Ross and Bustin, 2009; Ji et al., 2012; Liu et al., 2013; Tian et al., 2017). Most interestingly for us, studies by Sugimoto et al. (2003) and Dan et al. (2004) on the adsorption of CH₄ in micropores on the surface of clay minerals in dried and fresh lake sediment showed that dried

hat gelöscht:

hat gelöscht: release

hat gelöscht: In the following section we discuss the mechanism to explain our observations which are based on the adsorption of excess alkanes onto mineral dust particles.

hat formatiert: Durchgestrichen

hat gelöscht: (erosion of loose material by winds from flat and dry areas)

hat gelöscht: (

hat gelöscht: , the dust particles adsorb alkanes that are present in the atmosphere and the adsorption can

hat formatiert: Schriftart: (Standard) Times New Roman, 12 Pt., Englisch (USA)

hat formatiert: Schriftart: (Standard) Times New Roman, 12 Pt., Englisch (USA)

hat formatiert: Nicht Durchgestrichen

hat gelöscht: either happen at the soil surface in the dust source region or en route to the Greenland ice sheet after deflation (

hat gelöscht: At first order,

hat gelöscht: f

hat gelöscht: .

hat gelöscht: insufficient

hat gelöscht:

hat gelöscht: during

hat gelöscht: Bory, et al., 2003

hat gelöscht: ,

hat gelöscht: ; Rhodes et al., 2013

hat gelöscht: Evidence on the adsorptive capacity of alkanes on clay minerals and its strong retention was accumulating from several experimental studies

hat gelöscht: While all clay minerals are expected to be CH₄ adsorbents (Sugimoto et al., 2003), this was predominantly demonstrated for kaolinite, chlorite, illite, and montmorillonite (Sugimoto et al., 2003; Cheng and Huang, 2004; Ross and Bustin, 2009; Ji et al., 2012; Liu et al., 2013; Tian et al., 2017).

1316 sediment still retains CH₄ and that dried and degassed sediment re-adsorbs ambient CH₄ at
1317 standard pressure and room temperature. The amount of CH₄ adsorbed in their samples is
1318 strongly dependent on pressure and temperature while increasing temperatures and decreasing
1319 pressure lead to a stronger desorption. The addition of water/ moisture leads to a rapid
1320 desorption of already adsorbed gases (Sugimoto et al., 2003; Dan et al., 2004; Pires et al., 2008;
1321 Ji et al., 2012; Liu et al., 2013).

1322
1323 These results in principle support the possibility of an adsorption-desorption process for our
1324 glacial NGRIP and GRIP ice core samples, where alkanes (from fossil seeps or atmosphere)
1325 would be adsorbed on dust particles and desorbed during the measurement procedure when
1326 liquid water is present. Independent of the origin of the alkanes (A1 or A2) the amount of
1327 alkanes deposited onto the Greenland ice sheet by this process would be diminished if mineral
1328 dust particles were already in contact with liquid water during the long-range transport which
1329 may lead to a loss of previously adsorbed alkanes already in the atmosphere. This water contact
1330 could occur for example already at the dust source, as it is known that the deserts in the Tarim
1331 basin receive regular input from water from the surrounding mountain regions also providing
1332 the minerals to the basin that are blown out of the desert afterwards (Ruth et al., 2007).

1333
1334 To explain the constant ratio of methane, ethane, and propane of 14:2:1 in our samples with an
1335 adsorption mechanism, we need to discuss the potential origins of the adsorbed alkanes. First,
1336 we find very high relative excess contributions of ethane and propane in our samples, while we
1337 see a small excess contribution for methane compared to the atmospheric background. If we
1338 assume a comparable adsorption for all three alkanes, this would imply a strong relative
1339 enrichment of ethane and propane over methane in the concentration of these gases during
1340 adsorption. This is not in line with the past atmospheric CH₄/(C₂H₆+C₃H₈) ratio where past
1341 atmospheric ethane concentrations by Nicewonger et al. (2016) are an order of magnitude
1342 smaller (and propane concentrations even less) than the measured concentrations in our NGRIP
1343 and GRIP ice core samples.

1344 In contrast, the ratio of methane, ethane, and propane for our samples of approximately 14:2:1,
1345 translates into a CH₄/(C₂H₆+C₃H₈) ratio of ~5, which is most consistent with a thermogenic
1346 origin (see Fig. 11, left panel). However, due to the different adsorption capacity of mineral
1347 dust particles, also a fractionation of the three alkanes is to be expected during the adsorption
1348 process, which could alter the thermogenic signature.

1349

hat formatiert: Nicht Hochgestellt/ Tiefgestellt

hat gelöscht: of CH₄ a

hat gelöscht: our hypothesis of

hat gelöscht: Yet,

hat formatiert: Nicht Hervorheben

hat gelöscht: ref

hat gelöscht: ¶

hat gelöscht: ¶
Regarding our experimental results, the high correlation between mineral dust (Ca²⁺) and excess alkanes observed in many Greenland ice cores would be generally in line with the theory of adsorption on mineral dust. In our data we see that the amount of released excess alkanes per Ca²⁺ is variable (especially in the 2nd extraction), which can be explained by a varying adsorption capacity of the mineral dust particles or a close relation between the adsorption capacity and the type of clay mineral (Sugimoto et al., 2003; Ji et al., 2012). ¶

hat gelöscht: However,

hat gelöscht: t

hat gelöscht: ¶

hat gelöscht: If we assume instead that excess alkanes have a thermogenic origin, we see that t

hat gelöscht: d

hat gelöscht: , albeit more at the lower limit

hat gelöscht: we

hat gelöscht: also have to question a selective adsorption capacity of mineral dust particles

hat gelöscht: -If ethane and propane are preferentially adsorbed over methane, this would misrepresent the actual ratio between the three alkanes and falsify our interpretation of the origin.

Formatiert: Leerraum zwischen asiatischem und westlichem Text nicht anpassen, Leerraum zwischen asiatischem Text und Zahlen nicht anpassen

1381 To further evaluate the adsorption theory in the light of our experimental evidence, we now
 1382 include the carbon and deuterium isotopic signature of CH_{4(x)s} in our samples. Our NGRIP
 1383 samples reveal a δ¹³C-CH_{4(x)s} value (Keeling y-intercept weighted mean) of (-47.0 ± 2.9) ‰
 1384 which is within the error consistent with contemporaneous atmospheric values or with
 1385 emissions from seeping reservoirs of natural gas. In contrast, our hydrogen isotopic
 1386 measurements on NGRIP samples reveal a very light δD-CH_{4(x)s} value (Keeling y-intercept
 1387 weighted mean) of (-326 ± 57) ‰ and slightly outside of the field of a thermogenic origin (see
 1388 Fig. 11). The value is similar to the estimate by Lee et al. (2020), which, however, lies inside
 1389 the field of a thermogenic origin (see Fig. 11). While both the low CH₄/(C₂H₆+C₃H₈) ratio and
 1390 the δ¹³C-CH_{4(x)s} could be indicative of a thermogenic source (A1), the light δD-CH_{4(x)s} signature
 1391 is far away from the atmospheric δD-CH₄ value and is borderline in line with typical δD-CH₄
 1392 values of a thermogenic origin. Hence, our δD-CH_{4(x)s} values exclude the atmospheric
 1393 adsorption scenario, A2 and put a question mark after the seep adsorption scenario A1.
 1394
 1395 For the seep adsorption scenario A1 to work the dust particles on which the thermogenic gas
 1396 adsorbed are not allowed to experience any contact with liquid water prior to the analysis in the
 1397 lab. In other words, if the particles get in contact with liquid water after the adsorption step, the
 1398 adsorbed alkanes would desorb from the particles as they do it in the laboratory during melting.
 1399 Given the occurrence of wet/dry cycles in the source area (Ruth et al., 2007), we question the
 1400 plausibility of scenario A1. Moreover, we expect the characteristic desorption time to differ
 1401 between the three alkanes, which would be in contradiction to the observation that the alkane
 1402 ratios in the 1st and 2nd extraction are the same within the error limits.
 1403

- Formatiert (... [18])
- hat gelöscht: . In our NGRIP data we document a rela (... [19])
- hat gelöscht: ¶ (... [20])
- hat gelöscht: (
- hat gelöscht: -46.4 ± 2.4
- hat gelöscht: s
- hat gelöscht: a
- hat gelöscht: and outside
- hat gelöscht: of
- hat formatiert (... [21])
- hat formatiert (... [22])
- hat gelöscht: also not strictly
- hat formatiert (... [23])
- hat formatiert (... [24])
- hat formatiert (... [26])
- hat gelöscht: render
- hat formatiert (... [25])
- hat formatiert (... [27])
- hat gelöscht: s
- hat gelöscht: l
- hat formatiert (... [28])
- hat formatiert (... [29])
- hat gelöscht: 2 unrealistic candidates to explain our (... [30])
- hat gelöscht:
- Formatiert (... [31])
- hat gelöscht: ¶ (... [32])
- hat gelöscht: n
- hat gelöscht: now
- hat gelöscht: . In case of the A1 mechanism we have (... [33])
- hat formatiert (... [34])
- hat gelöscht: is
- hat formatiert (... [35])
- hat gelöscht: thus
- hat gelöscht: a
- hat gelöscht: rendering
- hat gelöscht: implausible even if all our isotopic and (... [36])
- hat formatiert (... [37])
- hat formatiert (... [38])
- hat formatiert (... [39])
- hat formatiert (... [40])
- hat formatiert (... [41])
- hat gelöscht: st
- hat formatiert (... [42])
- hat formatiert (... [43])
- hat gelöscht: nd
- hat gelöscht:
- hat formatiert (... [44])

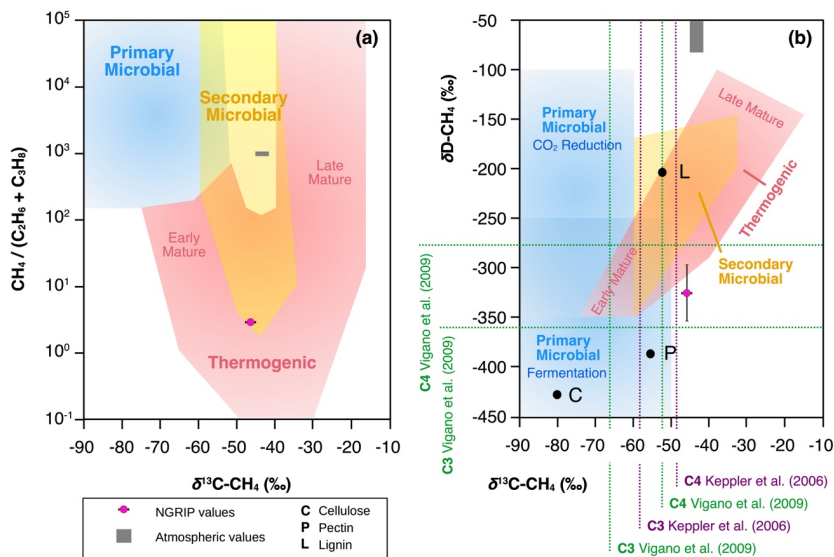


Figure 11: Diagrams of genetic fields for natural gas adopted from Milkov and Etiope (2018). (a) Genetic diagram of $\delta^{13}\text{C}-\text{CH}_4$ versus $\text{CH}_4/(\text{C}_2\text{H}_6 + \text{C}_3\text{H}_8)$. Typical atmospheric values are indicated by a grey star, NGRIP values obtained from this study with a pink dot. (b) Methane genetic diagram of $\delta^{13}\text{C}-\text{CH}_4$ versus $\delta\text{D}-\text{CH}_4$. Values for cellulose (C), lignin (L) and pectin (P) from Vigano et al. (2009) and mean values for C3 and C4 plants, respectively, from studies by Keppler et al. (2006) and Vigano et al. (2009) are added.

(2) Microbial production

The second process that we take into consideration is the microbial production of excess alkanes through methanogenic microbes. Here we must again differentiate between two scenarios: a microbial production can either take place in the ice sheet itself (in situ) by extremophile microbes. This process requires that in situ produced excess alkanes are then adsorbed onto dust particles in the ice and subsequently slowly desorbed during extraction when in contact with liquid water (M1). Or the production takes place during the melt extraction when methanogenic microbes can metabolize in liquid water (*in extractu*; M2). Lee et al. (2020) already excluded a “simple” in situ production of excess CH_4 (microbial in situ production in the ice without an adsorption-desorption process; M0) and this option will therefore not be further discussed here.

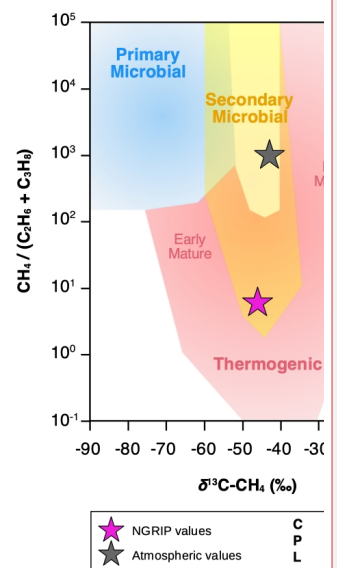
hat formatiert: Schriftart: 10 Pt., Nicht Kursiv, Schriftfarbe: Text 1

hat gelöscht: 11

Formatiert: Beschriftung, Zeilenabstand: einfach

hat gelöscht: with

hat formatiert: Schriftart: 10 Pt., Schriftfarbe: Text 1



hat gelöscht:

Figure 11: Diagrams of genetic fields for natural gas adopted from Milkov and Etiope (2018). (a) Genetic diagram of $\delta^{13}\text{C}-\text{CH}_4$ versus $\text{CH}_4/(\text{C}_2\text{H}_6 + \text{C}_3\text{H}_8)$. Typical atmospheric values are indicated with a grey star, NGRIP values obtained from this study with a pink star. (b) Methane genetic diagram of $\delta^{13}\text{C}-\text{CH}_4$ versus $\delta\text{D}-\text{CH}_4$. Values for cellulose (C), lignin (L) and pectin (P) from Vigano et al. (2009) and mean values for C3 and C4 plants, respectively, from studies by Keppler et al. (2006) and Vigano et al. (2009) are added.

hat gelöscht:

hat gelöscht: regards

1530 The second part of a potential M1 process, the adsorption of the microbially produced excess
 1531 alkanes onto dust particles in the ice and the subsequent desorption during extraction, remains
 1532 difficult to assess. A selective adsorption of the in situ produced alkanes on mineral dust in the
 1533 ice requires that the in situ production is taking place on the dust particles themselves, which
 1534 can be questioned but cannot be ruled out. However, our ratios of excess
 1535 methane/ethane/propane in NGRIP and GRIP samples add another piece of corroborating
 1536 evidence that excess alkanes are not produced microbially. The main microbial production
 1537 process of methane, the decomposition of organic precursors in an anaerobic environment by
 1538 archaea, also co-produces ethane and propane, however only in marginal amounts. The typical
 1539 methanogenesis yields >200 times more methane than ethane and propane (Bernard et al., 1977;
 1540 Milkov and Etiope, 2018) while we find a molar ratio of methane to ethane to propane of 14:2:1
 1541 in our samples. This renders a microbial production pathway (in situ and *in extractu*, i.e. M1
 1542 and M2) unlikely. Moreover, a microbial production of CH₄ is unlikely in view of the δ¹³C-
 1543 CH_{4(xS)} signature which is too heavy for microbial CH₄.

1544 Similar to our argument made for the pure desorption hypothesis, the constant excess alkane
 1545 ratio in the second and first extraction is difficult to reconcile with an expected different
 1546 desorption lifetime for the three alkanes.

1547
 1548 Apart from these quantitative limitations of microbial CH₄ in situ production in ice, there is
 1549 contradicting evidence from the “microbial inhibition experiment” by Lee et al. (2020) also for
 1550 microbial production of alkanes during extraction. Lee et al. (2020) tested whether biological
 1551 CH_{4(xS)} production in the meltwater was inhibited when the ice core samples were treated with
 1552 HgCl₂. As CH_{4(xS)} was still observed in the poisoned samples and as it seems quite unlikely that
 1553 microbes are resistant to HgCl₂, this experiment questions the hypothesis of microbially
 1554 produced CH_{4(xS)} also during extraction (*in extractu*).
 1555

1556 We conclude that regardless of the production pathway, in situ or *in extractu*, the fingerprint of
 1557 the produced excess alkanes in our samples (heavy δ¹³C-CH_{4(xS)} signature and low
 1558 CH₄/(C₂H₆+C₃H₈) ratio) essentially rules out a microbial source and another (abiotic?) process
 1559 for excess alkane production is likely to exist.

1561 (3) Abiotic/ chemical production

1562 In this last section we consider an abiotic or chemical process to be responsible for the observed
 1563 excess alkanes, where excess alkanes would be produced through the abiotic decomposition of

hat gelöscht: ¶

The viability of microbial in situ activity in the ice was substantially discussed in Lee et al. (2020) and references therein. While there is evidence for high cell counts in association with high concentrations of dust in Greenland ice cores, there is no direct evidence of active methanogens capable of producing CH₄ in ice (Tung et al., 2005, 2006; Rohde et al., 2008; Miteva et al., 2009). Calculations on the production of biogenic CH₄ in ice by Price and Sowers (2004), Tung et al. (2005), and Rohde et al. (2008) lead to a best estimate of ~5·10⁻⁵ pmol CH₄/g ice in 35 kyears. In comparison to our observations (for instance when taking the CH_{4(xS)} mean of ~32 ppb in the four samples measured in the NGRIP bag 3515 with a mean ice sample weight of ~139 g) this translates into ~0.13 pmol CH₄/g ice in 32 kyears, which is several magnitudes higher. Moreover, we assume that in situ produced excess alkanes would increase with time (depth) in relation to the amount of mineral dust within the ice until conditions no longer support this process (i.e. nutrient limitation). This was tested by analyzing dust-rich GISP2 samples ranging from 42-75 kyears, however, no time-dependent process was observed (Lee et al., 2020). On the other hand, there are CH₄ anomalies in Greenland ice cores that might be caused by microbial activity. Rhodes et al. (2013) report CH₄ spikes in the NEM S1 core that are not associated with melt events but are characterized by anomalously high concentration of NH₄⁺ and other biomass burning-derived nutrients. Since these CH₄ spikes have been observed both with the classic wet extraction and with the CFA technique that allows minimal reaction time in liquid water during the melt phase, these CH₄ anomalies were likely produced already in the ice, thus qualify as in situ. These narrow CH₄ spikes occur in Holocene ice with typically low dust and Ca²⁺ content, thus having a different impurity composition compared to our high-dust samples where we observe *in extractu* alkanes. Similar CH₄ spikes without an association to melt layers were reported in the GISP2 ice core by Mitchell et al. (2013).
 Moreover, ice samples from different Greenland ice cores that are affected by melt events show CH₄ anomalies (... [45])

hat gelöscht: evaluate

hat gelöscht: ,

hat gelöscht: In particular why should in situ produced alkanes be adsorbed onto mineral dust particles but not (... [46])

hat verschoben (Einfügung) [2]

hat gelöscht:

hat gelöscht:

hat gelöscht: for excess alkanes

hat gelöscht: ¶

hat formatiert: Nicht Hervorheben

hat gelöscht: ¶

hat gelöscht:

hat gelöscht: ¶

hat gelöscht: ¶ (... [47])

hat nach oben verschoben [2]: However, our ratios of excess methane/ ethane/ propane in NGRIP and GRIP samples add another piece of corroborating evidence that

hat gelöscht: t (see Fig. 10

hat gelöscht: ¶

hat gelöscht: ¶

1708 labile organic compounds in the meltwater (C2). **Based on the same arguments presented in the**
 1709 **previous section for a microbial in situ production, we also question an** abiotic in situ production
 1710 in the ice (C1) **as it would require the quantitative adsorption of the in situ produced alkanes**
 1711 onto mineral dust particles but not the atmospheric CH₄ that is available in the ice otherwise.
 1712 **However, as the location of an in situ excess CH₄ production in the ice is not the same as the**
 1713 **location of the bubble or clathrates in the ice, this argument is not able to exclude this**
 1714 **hypothesis. However, given the age of the ice that allows for permeation of gases on the grain**
 1715 **scale and the recrystallization of the ice during that time, which both could bring the**
 1716 **atmospheric CH₄ in contact with the dust particles, we feel this process is less plausible than a**
 1717 **potential C2 mechanism. Moreover (as mentioned before), in view of the expected different**
 1718 **desorption characteristics of the three alkanes we would expect different alkane ratios in the**
 1719 **1st and 2nd extraction, which is not the case. Accordingly, a direct abiotic production during the**
 1720 **melt process appears to be more likely than a desorption process.**

1721
 1722 Organic precursors for this abiotic production during extraction could be any organic matter
 1723 (either microbial or plant-derived). As the amount of excess alkanes is tightly coupled to the
 1724 amount of dust, we assume that these organic compounds are attached to dust particles. This
 1725 “docking” of the organic precursor onto the mineral dust could happen already in the dust
 1726 source region involving organic material available at the surface. **Or it could happen by**
 1727 **adhering of volatile organic molecules or secondary organic aerosols from the atmosphere to**
 1728 **the mineral dust aerosol, either before deflation at the source region or during transport to**
 1729 **Greenland.**

1730
 1731 We consider this pathway **plausible**, as in recent years the prevailing paradigm that methane is
 1732 only produced by methanogenic archaea under strictly anaerobic conditions has been
 1733 challenged. Several experimental studies demonstrated that methane can also be released from
 1734 dried soils (Hurkuck et al., 2012; Jugold et al., 2012; Wang et al., 2013; Gu et al., 2016), fresh
 1735 plant matter and dry leaf litter (Keppler et al., 2006; Vigano et al., 2008, 2009, 2010; Bruhn et
 1736 al., 2009; Derendorp et al., 2010, 2011), different kinds of living eukaryotes (plants, animals
 1737 and fungi) (Liu et al., 2015), single organic structural components (McLeod et al., 2008;
 1738 Messenger et al., 2009; Althoff et al., 2014) and in fact under aerobic conditions. Most of these
 1739 studies focused on methane, however, there is also evidence for simultaneous formation of other
 1740 short-chain hydrocarbons like ethane and propane (McLeod et al., 2008; Derendorp et al., 2010,
 1741 2011). At least three mechanisms have been identified to be relevant: i) photo-degradation, ii)

- hat gelöscht:
- hat gelöscht: Again, we disregard an
- hat gelöscht: based on the same arguments presented in the previous section for a microbial in situ production
- hat gelöscht: ,
- hat gelöscht: This mechanism can also not be ruled out
- hat formatiert: Tiefgestellt
- hat formatiert: Tiefgestellt
- hat formatiert: Nicht Hervorheben
- hat formatiert: Nicht Hervorheben
- hat formatiert: Hochgestellt, Nicht Hervorheben
- hat formatiert: Nicht Hervorheben
- hat gelöscht: st
- hat formatiert: Hochgestellt, Nicht Hervorheben
- hat formatiert: Nicht Hervorheben
- hat gelöscht: nd
- hat gelöscht: p
- hat gelöscht: (East Asian deserts)
- hat gelöscht: to
- hat gelöscht: n
- hat gelöscht: ,
- hat gelöscht: Note that organic substances might potentially experience abiotic preconditioning (ageing) during aerosol transport and only the final step of alkane production may occur during the wet extraction.¶

1759 thermal degradation, or iii) degradation by the reaction with a reactive oxygen species (ROS)
1760 (Schade et al., 1999; Wang et al., 2017). Common to all three pathways is a functional group
1761 (for example a methyl or ethyl group) that is cleaved from the organic precursor molecule. Key
1762 parameters that control the production of abiotic methane are mainly temperature, UV radiation,
1763 water/ moisture, and the type of organic precursor material (Vigano et al., 2008; Derendorp et
1764 al., 2010, 2011; Hurkuck et al., 2012; Jugold et al., 2012; Wang et al., 2013, 2017). ▽

1766 Recent findings demonstrated the large variety of potential organic precursors for abiotic trace
1767 gas formation. For the formation of methane, the plant structural components pectin and lignin
1768 have been identified in many studies as a precursor in different plant materials. Pectin and lignin
1769 contain methoxyl-groups in two different chemical types, ester methoxyl (present in pectin) and
1770 ether methoxyl (present in lignin) (Keppler et al., 2006, 2008; McLeod et al., 2008; Messenger
1771 et al., 2009; Bruhn et al., 2009; Vigano et al., 2008; Hurkuck et al., 2012; Liu et al., 2015; Wang
1772 et al., 2017). Ester methyl groups of pectin were also discovered as precursor for ethane
1773 formation (McLeod et al., 2008). Overall, pectin makes up a large fraction of the primary cell
1774 wall mass of many plants, thus, representing a large reservoir available as organic precursor for
1775 abiotic alkane formation (Keppler et al., 2006; Mohnen et al., 2008; Vigano et al., 2008, 2010;
1776 McLeod et al., 2008), and may be present in sufficient quantities in our ice core samples
1777 attached to mineral dust particles. CH₄ production was also detected from cellulose even though
1778 it does not contain methoxyl groups suggesting that other carbon moieties of polysaccharides
1779 might allow abiotic CH₄ formation (Keppler et al., 2006; Vigano et al., 2008). In addition, poly-
1780 unsaturated fatty acids in plant membranes are suggested to play a key role not only in the
1781 formation of methane but also for ethane and propane (John and Curtis, 1977; Dumelin and
1782 Tappel, 1977; Derendorp et al., 2010, 2011). Further, sulfur-bound methyl groups of
1783 methionine are an important precursor for abiotic CH₄ formation in fungi (Althoff et al., 2014).

1784
1785 Considerably different emission rates were found for the same amount but different type of
1786 organic substances leading to the conclusion that abiotic emissions are strongly dependent on
1787 the type of organic precursor material or single structural components (Keppler et al., 2006;
1788 McLeod et al., 2008; Vigano et al., 2008; Messenger et al., 2009; Hurkuck et al., 2012). Other
1789 factors such as leaf and cell wall structure (McLeod and Newsham, 2007; Watanabe et al.,
1790 2012; Liu et al., 2015) and the organic carbon content (Hurkuck et al., 2012) are suggested to
1791 have an important influence on this process, too.

1792

hat gelöscht: This "new" abiotic pathway of methane formation has not been discussed yet to be active during ice core analyses, however, we believe that this process could be active during our melt extraction. In the following section we discuss the key parameters that generally influence abiotic production with respect to our measurement conditions and review the viability of this process for ice core samples and in the light of our experimental observations. ...

hat gelöscht: -In general, the functional group cleaved from the precursor molecule defines the species to be produced, thus methyl- (or ethyl-) group containing substances for the production of methane (or ethane): ...

hat gelöscht:

1806 To explain the observed excess alkanes in dust-rich Greenland ice core samples by an abiotic
1807 production through the decomposition of labile organic compounds requires adequate quantities
1808 of organic precursors to be present within the ice core samples. Certainly, such material is
1809 present in Greenland ice, but currently, there is no record on the amount and type of organic
1810 substances in NGRIP and GRIP ice available. We have some limited information from
1811 occasional Greenland ice core samples in which different types of organic substances were
1812 detected (Giorio et al., 2018, and references therein), but it does not allow for an overarching
1813 interpretation for our ice samples. A NGRIP record on formaldehyde and a GRIP record on
1814 acetate and formate exists (Fuhrer et al., 1997), which suggest lower levels during the glacial,
1815 but as we do not know which organic precursors lead to the excess CH₄ productions this
1816 observation is only of limited value.
1817
1818 We may also question whether a perfect record of eligible precursor molecules could exist at
1819 all. As we observe that precursor substances are labile and quickly decompose when in contact
1820 with liquid water, a direct measurement of these substances might not be possible but only for
1821 similar, non-reactive substances, which are then not qualified as precursors for the reaction
1822 observed. The problems of sampling, analysis and interpretation of organic material in polar
1823 ice are well summarized and expounded in Giorio et al. (2018).

1824
1825 In any case, it appears likely that the mineral dust carries along soil organic matter or plant
1826 residues or accumulates organic aerosols as a result of organic aerosol aging during transport.
1827 In our data we see a relationship between the amount of mineral dust within the ice core samples
1828 and the amount of excess alkanes. As the amount of excess alkanes per Ca²⁺ (or mass of dust)
1829 is variable, this suggests that mineral dust is just a carrier for (a variable amount of) organic
1830 substances but does not account for the production of excess alkanes itself. The dust content
1831 within the ice core sample can therefore only serve as a rough estimate of organic precursor
1832 availability and whether an abiotic production from organic precursor substances is likely to
1833 occur during extraction.

1834
1835 Again, our experiments can shed some light on the viability of this pathway for excess alkane
1836 production. If we assume that the dust-related organic matter in the ice represents a reservoir
1837 available for an abiotic production, then the decomposition continues until all functional groups
1838 are cleaved from their organic precursor molecules and released as excess alkanes. Once the
1839 reservoir is emptied excess alkane production ceases (Derendorp et al., 2010, 2011). In line, we

hat gelöscht: show

hat formatiert: Tiefgestellt

hat gelöscht: as these substances are only representative for the respective dissolved organic compounds in the ice and not for any organic molecules attached onto the dust particles, they show lower levels during the glacial...

hat gelöscht: However,

hat gelöscht: w

hat gelöscht: also have to

hat gelöscht: at all

hat gelöscht: ,

hat gelöscht: primarily coming from the Taklamakan and Gobi deserts (Biscaye et al., 1997; Bory et al., 2003), ...

1852 interpret that the decrease in the amount of measured excess alkanes from the 1st to the 2nd
1853 extraction may result from an exhaustion of the precursor reservoir. The reaction time is slow
1854 enough to allow for the continuing production during the second extraction but too slow for a
1855 detectable production during continuous flow analysis of CH₄, where the water phase is present
1856 only for less than two minutes before gas extraction. The significantly reduced production
1857 during the 2nd extraction in our samples shows that the time scale for this process is hours (see
1858 Fig. C1) until the reservoir of functional groups is depleted. We note that this implies that the
1859 amount of excess alkanes is strongly dependent on the time span when liquid water is in contact
1860 with the dust, which varies among the methods used for CH₄ analyses. Thus, any excess CH₄
1861 in measurements from different labs performed under different conditions may differ.

1862

1863 To explain an abiotic alkane production, certain conducive boundary conditions must be met.
1864 The most important parameters that control non-microbial trace gas formation are temperature
1865 and UV radiation. This was demonstrated in many field and laboratory experiments (Keppler
1866 et al., 2006; McLeod et al., 2008; Vigano et al., 2008, 2009; Messenger et al., 2009; Bruhn et al.,
1867 2009; Derendorp et al., 2010, 2011; Hurkuck et al., 2012; Jugold et al., 2012; Wang et al.,
1868 2017). Generally, increasing temperatures lead to exponentially increasing CH₄ emissions
1869 (Vigano et al., 2008; Bruhn et al., 2009; Wang et al., 2013; Liu et al., 2015). The same behaviour
1870 was observed for ethane and propane with very low emissions at ambient temperatures (20-
1871 30°C) and a maximum at 70°C (McLeod et al., 2008; Derendorp et al., 2010, 2011). At constant
1872 temperatures emission rates decreased over time, which is at high temperatures on the timescale
1873 of hours and at ambient temperatures of months. Even after months, some production was
1874 observed, pointing to a slowly depleting reservoir of organic precursors (Derendorp et al., 2010,
1875 2011). Increasing emissions observed at temperatures >40°C were also used as indicator to
1876 exclude the possibility of enzymatic activity, as the denaturation of enzymes would lead to
1877 rapidly declining emissions at higher temperatures (Keppler et al., 2006; Derendorp et al., 2011;
1878 Liu et al., 2015). We note that our sample extraction takes place at 0°C or a few °C above,
1879 hence, temperature conditions during the extraction are not conducive of the type of abiotic
1880 alkane production as observed in the studies listed above. Whether the cool temperature of the
1881 meltwater during extraction inhibits abiotic reaction is difficult to say. Derendorp et al. (2010,
1882 2011) observed a much lower temperature dependency of C2-C5 hydrocarbon emissions from
1883 ground leaves than whole leaves, which might also apply to our samples with very fine
1884 fragments of organic substances attached to dust particles.

1885

hat gelöscht: a

hat gelöscht: B

hat gelöscht:

hat gelöscht: conclude

1890 Besides the strong relationship to temperature also UV irradiation seems to have a substantial
1891 effect on an abiotic production. Studies on irradiated samples (dry and fresh plant matter, plant
1892 structural components) showed a linear increase in methane emissions, while UV-B irradiation
1893 seems to have a much stronger effect on the release compared to UV-A (Vigano et al., 2008;
1894 McLeod et al., 2008; Bruhn et al., 2009; Jugold et al., 2012). The influence of visible light (400-
1895 700 nm), however, seems controversial (Keppler et al., 2006; Bruhn et al., 2009; Austin et al.,
1896 2016). Further, samples that were heated and irradiated show a different emission curve than
1897 just heated samples, indicating that irradiation changes the temperature dependency, in turn
1898 pointing to the fact that different chemical pathways exist (Vigano et al., 2008).
1899 In dark experiments on plant material at different temperatures CH₄ emissions were still
1900 observed, while again higher temperatures revealed much higher emissions, emphasizing the
1901 strong temperature dependency also without UV irradiation (Vigano et al., 2008; Wang et al.,
1902 2008; Bruhn et al., 2009). The release of ethane along with methane from pectin was also
1903 stimulated under UV radiation (McLeod et al., 2008).

hat gelöscht: a

1905 Regarding our measurements, the sample vessel in the $\delta^{13}\text{C}$ -CH₄ device is encased by a UV
1906 blocker foil absorbing the shortwave (<600 nm) emissions from the heating bulbs when melting
1907 the ice sample, while in the δD -CH₄ device the sample vessel is completely shielded from light
1908 (Sect. 2.2 and 2.3). Two NGRIP ice core samples were measured with the $\delta^{13}\text{C}$ -CH₄ device in
1909 the dark (“dark extraction”) showing the same amount of excess alkanes as the regular
1910 measurements at day light. This indicates that light >600 nm has no influence on an *in extractu*
1911 reaction during our measurements.

1913 We stress that although we can exclude a direct UV effect during sample extraction, it is
1914 possible that UV irradiation during dust aerosol transport to Greenland and within the upper
1915 snow layer after deposition until the snow gets buried into deeper layers may precondition
1916 organic precursors attached to mineral dust to allow for alkane production to occur during
1917 extraction. In particular, the first step of the reaction (excitation of the homolytic bond of a
1918 precursor compound) may start already in the atmosphere or in the upper firn layer where
1919 energy from UV radiation is available. Within the ice sheet the reaction may be paused (“frozen
1920 reaction”) and the total reaction pathway is only completed during the melting process when
1921 liquid water is present.

hat formatiert: Schriftart: 12 Pt.

hat gelöscht:

hat formatiert: Schriftart: 12 Pt., Schriftfarbe: Text 1

hat formatiert: Schriftart: 12 Pt.

hat formatiert: Schriftart: 12 Pt., Schriftfarbe: Text 1

hat formatiert: Schriftart: 12 Pt.

hat formatiert: Schriftart: 12 Pt., Schriftfarbe: Text 1

hat formatiert: Schriftart: 12 Pt.

hat formatiert: Schriftart: 12 Pt.

hat gelöscht: becomes reactivated

hat gelöscht: ¶

hat formatiert: Schriftart: Schriftfarbe: Text 1, Rahmen: :
(Kein Rahmen)

1923 Finally, we consider the role of reactive oxygen species in an abiotic production pathway. ROS
1924 are widely produced in metabolic pathways during biological activity but also during

Formatiert: Kommentartext, Abstand zwischen asiatischem
und westlichem Text anpassen, Abstand zwischen asiatischem
Text und Zahlen anpassen

1929 photochemical reactions with mineral oxides (Apel and Hirt, 2004; Messenger et al., 2009;
1930 Georgiou et al., 2015). Through their high oxidative potential ROS are capable to cleave
1931 functional groups from precursor compounds. Several studies have demonstrated this
1932 mechanism for the production of abiotic CH₄ in soils and plant matter (McLeod et al., 2008;
1933 Messenger et al., 2009; Althoff et al., 2010, 2014; Jugold et al., 2012; Wang et al., 2011, 2013)
1934 and for other trace gases such as CO₂, ethane, and ethylene from plant pectins (McLeod et al.,
1935 2008). UV radiation or thermal energy has no direct influence on the degradation process by
1936 the reaction with ROS, however, it might also be a stimulating factor and evoke further indirect
1937 reactions. For instance, UV radiation can lead to changes in plants which in turn lead to ROS
1938 generation (Liu et al., 2015). It was demonstrated that UV radiation induces the formation of
1939 organic photosensitizers or photo-catalysts which increase CH₄ emissions from pectin
1940 (Messenger et al., 2009) and clay minerals. For example, the formation of OH from
1941 montmorillonite and other clay minerals upon UV (and visible light) irradiation shows that
1942 clays might play a significant role in the oxidation of organic compounds on their surface in
1943 different environments (Katagi, 1990; Wu et al., 2008; Kibanova et al., 2011).

1944
1945 It has been proven that the species type and the overall amount of ROS available for, or involved
1946 in a reaction, has a significant effect on the amount of emissions through such a process (Jugold
1947 et al., 2012; Wang et al., 2013, 2017). For the production of methane (and ethane), hydrogen
1948 peroxide (H₂O₂) and hydroxyl radicals (OH) have been proven to be the prominent species
1949 (Messenger et al., 2009; Althoff et al., 2010; Wang et al., 2011, 2013; Jugold et al., 2012,
1950 McLeod et al., 2008). Such ROS could be already present in the snow and ice or being produced
1951 in the meltwater. For example, H₂O₂ can be unambiguously detected in Greenland Holocene
1952 ice using CFA, however, H₂O₂ in dusty glacial ice is mostly below the detection limit, likely
1953 due to oxidation reactions in the ice sheet or during melt extraction.

1954
1955 In summary, we believe that in our case of excess alkane production/ release in the meltwater
1956 at low temperatures and without any UV irradiation, the ROS-induced mechanism appears
1957 possible. In experiments with plant pectin McLeod et al. (2008) observed not only CH₄ but also
1958 ethane and found a methane to ethane production ratio of around 5 which is similar to our value
1959 of around 7. Accordingly, we see that a ROS-induced production pathway has the potential to
1960 explain excess alkanes in our samples, however, little is known about ROS chemistry in ice
1961 cores in particular for reactions with organic precursors and more research is needed to
1962 understand the role of ROS in organic decomposition in ice. Another alternative to the two-

hat gelöscht: ; Wang et al., 2013

hat gelöscht: ,

hat gelöscht:

hat gelöscht:

Formatiert: Block, Zeilenabstand: 1,5 Zeilen

hat gelöscht:

hat formatiert: Schriftfarbe: Text 1

hat formatiert: Schriftfarbe: Text 1

hat gelöscht: analyses

hat formatiert: Schriftart: 12 Pt., Schriftfarbe: Text 1, Englisch (USA)

1969 stage reaction pathway with ROS would be a reaction catalyzed in the meltwater by dust-
1970 derived transition metals. This has been observed for example for the oxidation of SO₂ in water-
1971 activated aerosol particles (Harris et al., 2013), but to our knowledge it has not been described
1972 in the literature for alkane production via organic precursors so far. Accordingly, we can only
1973 speculate on this pathway at the moment. ▲

hat formatiert: Schriftart: 12 Pt., Schriftfarbe: Text 1, Englisch (USA), Tiefgestellt

hat formatiert: Schriftart: 12 Pt., Schriftfarbe: Text 1, Englisch (USA)

hat formatiert: Schriftart: 12 Pt., Schriftfarbe: Text 1, Englisch (USA)

hat formatiert: Schriftfarbe: Text 1, Englisch (USA)

1974
1975
1976 Another key parameter influencing all abiotic pathways might be the presence of liquid water
1977 or moisture. In experiments testing the hypothesis of non-microbial CH₄ formation in different
1978 soil samples, it was demonstrated that the addition of water/moisture led to an up to eight-fold
1979 increase in CH₄ emissions (Hurkuck et al., 2012; Jugold et al., 2012; Wang et al., 2013). It is
1980 hypothesized that the presence of liquid water or moisture stimulates (in addition to heating or
1981 UV radiation) the cleaving process of a functional group from the primary precursor compound
1982 and therefore increases the production of CH₄. However, it seems that the stimulating effect by
1983 water cannot be generalized, as Wang et al. (2013) emphasized that this process is highly
1984 dependent on “water of proper amount”. In their experiments, CH₄ emissions from peat and
1985 grassland soil samples treated with a varying amount of water in oxa–anoxia cycles at 70°C
1986 were measured. They observed that under both aerobic and anaerobic conditions water does not
1987 always stimulate non-microbial CH₄ release and that too much water can also suppress CH₄
1988 emissions. Wang et al. (2013) observed differences between different soil samples in response
1989 to a varying water content indicating that the water effect is different for different precursors.
1990 With respect to our observations on NGRIP and GRIP samples the presence of water seems to
1991 be a fundamental parameter influencing the second step of a “frozen reaction” in extractu
1992 process, where the duration of water presence plays an important role. ▼

hat gelöscht:

hat gelöscht: 8

hat gelöscht: As Hurkuck et al. (2012) and Jugold et al. (2012) only observed a positive effect of water on CH₄ emissions in oxic soils, it is hypothesized that the amount of water they added to their samples is by chance in the stimulating range (Wang et al., 2013). In addition,

hat gelöscht: t

hat gelöscht: an

hat gelöscht: in these reactions.

1994 A final puzzle piece for a possible abiotic methane production comes from our dual isotopic
1995 fingerprints of the excess CH₄. As illustrated in Fig. 11 (right panel) our δD-CH_{4(x)s} signature
1996 lies well within the distribution of the hydrogen isotopic composition of CH₄ produced from
1997 potential organic precursors. For δ¹³C our values lie outside and on the heavier side of the
1998 isotopic carbon signature spectrum. ▼

hat gelöscht: both δ¹³C and

hat formatiert: Tiefgestellt

hat gelöscht: of the CH₄ produced are

hat gelöscht: in overall agreement

hat gelöscht: with

hat gelöscht: carbon and

hat gelöscht: but still within the wide distribution of possible isotopic precursor signatures... F, for δD the signature lies F, for δD the signature lies well within the distribution.

hat gelöscht: F, for δD the signature lies well within the distribution....

Formatiert: Zeilenabstand: 1,5 Zeilen

2000 We conclude that despite our inability to pinpoint the exact organic precursors that lead to
2001 abiotic excess alkane production during the melt extraction of our ice samples at this point, both
2002 the ratio of the excess alkanes as well as the isotopic signature of excess CH₄ is generally in

line with this pathway. Thus, without further contradicting evidence from targeted studies on organic precursors in ice core samples and their chemical degradation, we believe that the ROS-induced production pathway is to date the most likely explanation for the observed excess alkanes during extraction. However, we cannot completely rule out an adsorption-desorption process of thermogenic gas on dust particles.

Table 1: Overview of the different hypotheses explaining the possible sources for excess alkanes, as illustrated in Figure 10) in relation to our experimental and analytical observations. A green checkmark indicates that the observation is in line with the respective mechanism, a black cross indicates that the observation is in not line with the respective mechanism. A grey shaded area means that this observation does not apply or does not affect the respective mechanism.

	(1) ADSORPTION- DESORPTION OF THERMOGENIC/ ATMOSPHERIC GAS _x		(2) MICROBIAL PRODUCTION			(3) ABIOTIC/ CHEMICAL PRODUCTION	
	A1	A2	M0	M1	M2	C1	C2
Correlation to Ca ²⁺ / mineral dust	✓	✓	✓	✓	✓	✓	✓
Alkane pattern	✓	✗	✗	✗	✗	✓	✓
CFA evidence			✗				
δ ¹³ C-CH _{4(x)s}	✗	✓	✗	✗	✗	✓	✓
δD-CH _{4(x)s}	✓	✗	✓	✓	✓	✓	✓
δD-CH _{4(x)s} estimated by Lee et al. (2020)	✓	✗	✓	✓	✓	✓	✓
Poisoning experiment by Lee et al. (2020)					✗		

5. Conclusions and Outlook

The comparison of methane records from ice cores samples measured with different extraction techniques requires careful consideration and interpretation. Non-atmospheric methane contributions to the total methane concentration were discovered in specific Greenland ice core sections pointing to a process occurring during the wet extraction. To better assess this finding, we measured new records of [methane], [ethane], [propane], δD-CH₄, and δ¹³C-CH₄ on discrete NGRIP and GRIP ice core samples using two different wet extraction systems. With our new

- hat gelöscht:
- hat formatiert: Schriftart: Nicht Kursiv, Schriftfarbe: Text 1, Englisch (USA)
- hat formatiert: Schriftart: Nicht Kursiv, Schriftfarbe: Text 1, Englisch (USA)
- hat gelöscht: Thus, without further contradicting evidence from targeted studies on organic precursors in ice core samples and their degradation by ROS, we believe that the ROS-induced production pathway is to date the most likely explanation for the observed excess alkane production during extraction. u
- hat formatiert: Schriftart: 10 Pt., Schriftfarbe: Text 1, Englisch (USA)
- hat gelöscht: ¶ ... [48]
- hat formatiert ... [49]
- hat formatiert ... [50]
- hat gelöscht: u
- hat formatiert ... [51]
- hat gelöscht: a
- hat formatiert ... [52]
- hat formatiert: Englisch (USA)
- hat formatiert ... [53]
- hat formatiert: Schriftart: Nicht Fett
- hat formatiert ... [55]
- hat formatiert: Schriftart: Nicht Fett
- Formatiert: Abstand Vor: 3 Pt.
- hat formatiert: Schriftart: Nicht Fett
- Formatiert: Abstand Vor: 3 Pt.
- hat formatiert: Schriftart: Nicht Fett
- Formatiert: Abstand Vor: 3 Pt.
- hat formatiert: Schriftart: Nicht Fett
- hat formatiert ... [56]
- hat formatiert ... [54]
- hat formatiert: Englisch (USA)
- hat formatiert ... [57]
- hat formatiert: Schriftfarbe: Text 1
- hat formatiert: Schriftart: Nicht Fett
- hat formatiert: Schriftfarbe: Text 1
- hat formatiert: Schriftart: Nicht Fett
- hat formatiert: Schriftfarbe: Text 1
- hat formatiert: Schriftfarbe: Text 1
- hat formatiert: Schriftart: Nicht Fett
- hat formatiert: Schriftfarbe: Text 1
- hat formatiert: Schriftart: Nicht Fett
- hat formatiert ... [58]
- hat formatiert: Schriftfarbe: Text 1
- hat formatiert: Schriftart: Nicht Fett
- hat formatiert ... [59]
- hat formatiert: Schriftfarbe: Text 1

2068 data we confirm the production of CH_{4(xS)} in the meltwater and quantify its dual isotopic
2069 signature. With the simultaneous detection of ethane and propane we discovered that these
2070 short-chain alkanes are co-produced in a fixed **molar** ratio pointing to a common production
2071 pathway. With our 2nd extraction we constrained the temporal dynamics of this process, which
2072 occurs on the timescale of **hours**.

hat gelöscht:

2073
2074 Based on our new experimental data we provide an improved assessment of several potential
2075 mechanisms that could be relevant for the observed variations in NGRIP and GRIP ice samples.
2076 A microbial CH₄ production represents **in principle** an obvious candidate but regardless of
2077 whether this CH₄ is produced in situ or *in extractu*, several lines of evidence gained from our
2078 measurements (low CH₄/(C₂H₆+C₃H₈) ratio, heavy δ¹³C-CH_{4(xS)} signature) demonstrate that the
2079 fingerprint of the produced excess alkanes is unlikely to have a microbial source. Also an
2080 adsorption-desorption process of atmospheric or thermogenic CH₄ on dust particles does not
2081 match many of our observations and is therefore unlikely. However, with the current knowledge
2082 we cannot definitely exclude such an **adsorption of thermogenic gas** to be responsible for the
2083 observed excess alkane levels in our samples.

hat gelöscht: an

hat gelöscht: (low CH₄/(C₂H₆+C₃H₈) ratio, light δD-CH_{4(xS)} signature) ...

hat gelöscht: b

hat gelöscht: process

2084
2085 At present we favor to explain the formation of excess alkanes by abiotic decomposition of
2086 organic precursors during prolonged wet extraction. Such an abiotic source for methane and
2087 other short-chain alkanes was discovered previously in other studies (Keppler et al., 2006;
2088 Vigano et al., 2008, 2009, 2010; Messenger et al., 2009; Hurkuck et al., 2012; Wang et al.,
2089 2013, and others listed above) using different organic samples, e.g. from plant or soil material,
2090 however, this process has not been connected to excess CH₄ production **during** ice core
2091 analyses. This process matches many of our observations and such a mechanism can be
2092 responsible for excess alkanes in Greenland ice core samples. To better assess a potential abiotic
2093 production process in ice analyses the most important questions to solve in the future are: What
2094 are the specific precursor substances? Which parameters control an abiotic production during
2095 wet extractions? How does the fixed molar ratio between methane, ethane, and propane come
2096 about in this process? And finally, in which way is this excess alkane production causally
2097 related to the amount of mineral dust within the ice sample?

hat gelöscht: in

2098
2099 Identifying a specific reaction pathway that leads to the short-chain alkanes with their observed
2100 ratios would certainly benefit from identifying targeted organic precursor substances in the ice.
2101 However, detecting these postulated organic precursors in the ice core is inherently difficult as

2109 these compounds must be very labile in water as our experiments demonstrated that after about
2110 30 min only a fraction of these compounds remains in the meltwater while the majority already
2111 reacted to excess alkanes. Future studies may also focus on further isotopic measurements
2112 ($\delta^{13}\text{C-CH}_4$ and $\delta\text{D-CH}_4$) including isotope labeling experiments providing an option to
2113 unambiguously detect methane produced during the measurement procedure in a commonly
2114 used wet extraction technique, and again, to uncover potential reaction mechanisms for $\text{CH}_{4(\text{xs})}$
2115 production.

2116
2117 To better assess the viability of the alternative hypothesis of a release of previously adsorbed
2118 alkanes from dust particles (scenario A1 and A2) during the extraction, dust particles from the
2119 Taklamakan or Gobi desert need to be tested whether they contain relevant amounts of adsorbed
2120 alkanes that are released when in contact with liquid water. A second step could be to expose
2121 such dust samples to high levels of alkanes to mimic the adsorption process of natural gas seeps.
2122 It also needs to be shown that the adsorbed alkanes stay adsorbed on the dust particles for a
2123 prolonged time (months, ideally years) after exposing the particles to ambient air and that
2124 droplet and ice nucleation during aerosol transport does not lead to a loss of the previously
2125 adsorbed CH_4 . To quantify any isotopic fractionation involved with the ad- and desorption step,
2126 $\delta^{13}\text{C-CH}_4$ and $\delta\text{D-CH}_4$ analyses will be most valuable.

2127
2128 Finally, our studies clearly show that the published Greenland ice core CH_4 record is biased
2129 high for selected (glacial, dust-rich) time intervals and needs to be corrected for the excess CH_4
2130 contribution. This is particularly important for studies of the IPD in CH_4 and stable isotope
2131 ratios of methane. Methodological ways to remedy excess methane (and ethane and propane)
2132 in future measurements of atmospheric $[\text{CH}_4]$ from air trapped in ice cores could be to use
2133 continuous online CH_4 measurements, which apparently avoid sizeable $\text{CH}_{4(\text{xs})}$ production. But
2134 also dry extraction methods and sublimation techniques for discrete samples, which are
2135 expected to avoid *in extractu* production by evading the melting phase, could be used. Finally,
2136 our own $\delta^{13}\text{C-CH}_4$ device, which allows to measure $\delta^{13}\text{C-CH}_4$ as well as methane, ethane, and
2137 propane concentrations from the same sample, can be used to correct the measured CH_4 values
2138 making use of the co-production of the other two alkanes.

2139
2140 It is clear that $\text{CH}_{4(\text{xs})}$ needs to be corrected for when interpreting the already existing discrete
2141 CH_4 records and its stable isotopes in dust-rich intervals in Greenland ice core samples. Impact
2142 of $\text{CH}_{4(\text{xs})}$ on interpreting past atmospheric $[\text{CH}_4]$ will only slightly affect radiative forcing

hat gelöscht:

hat gelöscht: y

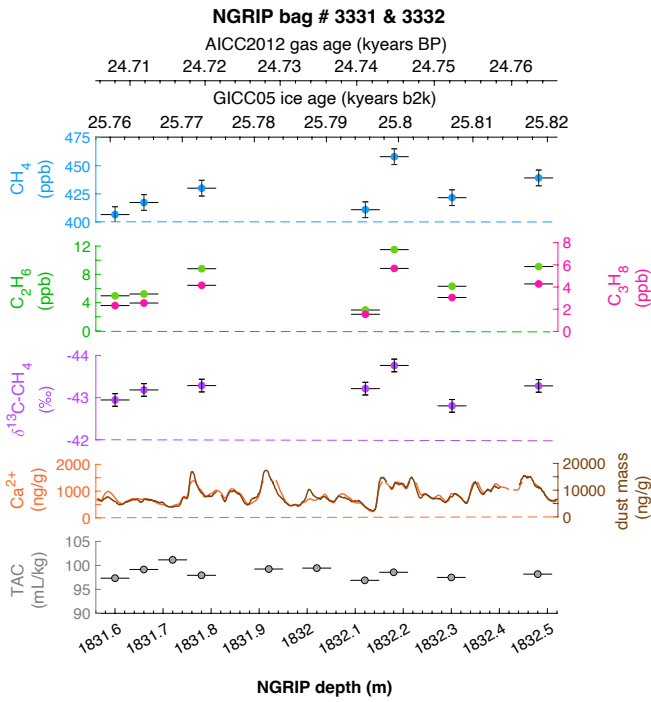
2145 reconstructions, however, it will have a significant effect on the assessment of the global CH₄
2146 cycle and in particular on the hemispheric CH₄ source distribution which is based on the IPD.
2147 We observe that in some intervals CH_{4(xss)} is in the same range as the previously reconstructed
2148 IPD implying that correcting for CH_{4(xss)} will lower the IPD considerably and hence lower also
2149 the relative contribution of northern hemispheric sources at those times. We see that there is the
2150 urgent need to reliably revisit Greenland ice core CH₄ records for the excess CH₄ contribution
2151 and in future work we aim to establish an applicable correction for excess methane (CH_{4(xss)},
2152 $\delta^{13}\text{C-CH}_{4(xss)}$, $\delta\text{D-CH}_{4(xss)}$) in existing records using the co-production ratios of methane, ethane,
2153 and propane, the isotopic mass balance of excess and atmospheric CH₄ in ice core samples as
2154 well as the overall correlation of excess CH₄ with the mineral dust content in the ice.

2155
2156
2157
2158
2159
2160
2161
2162
2163
2164
2165
2166
2167
2168
2169
2170
2171
2172
2173
2174
2175
2176
2177
2178

2179
2180

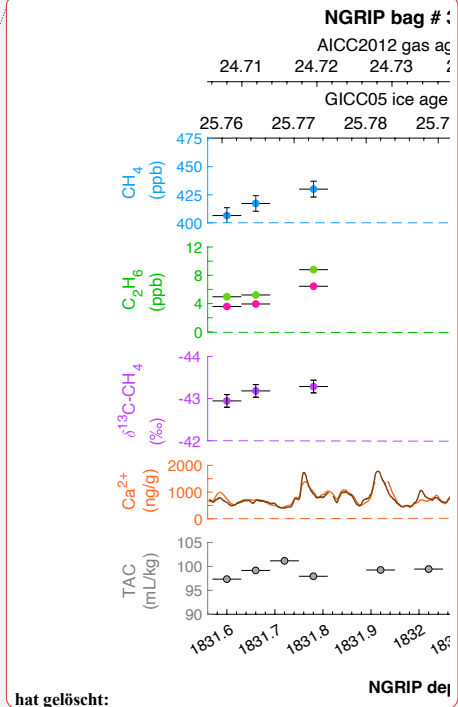
Appendix A

hat gelöscht: ¶

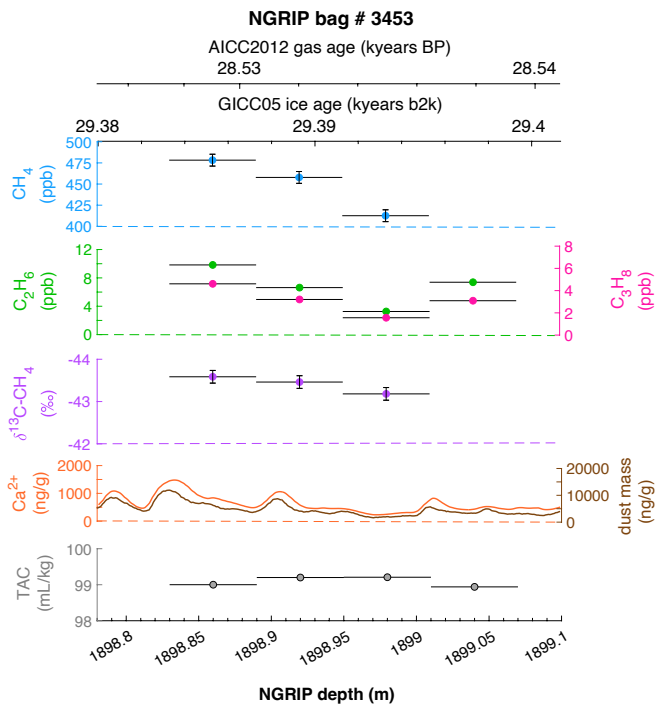


2181
2182
2183
2184
2185
2186
2187
2188

Figure A1: Detailed data overview for the neighbouring NGRIP bags 3331 & 3332. Bag-specific overview of several parameters measured for each sample in this bag: methane, ethane, propane, Ca²⁺, mineral dust mass, TAC (Total Air Content), $\delta^{13}\text{C}-\text{CH}_4$, indicated at the NGRIP depth (bottom axis) and the AICC2012 gas age (upper top axis) and the GICC05 ice age (lower top axis). The mineral dust record is taken from Ruth et al. (2003), the Ca²⁺ record from Erhardt et al. (2022).



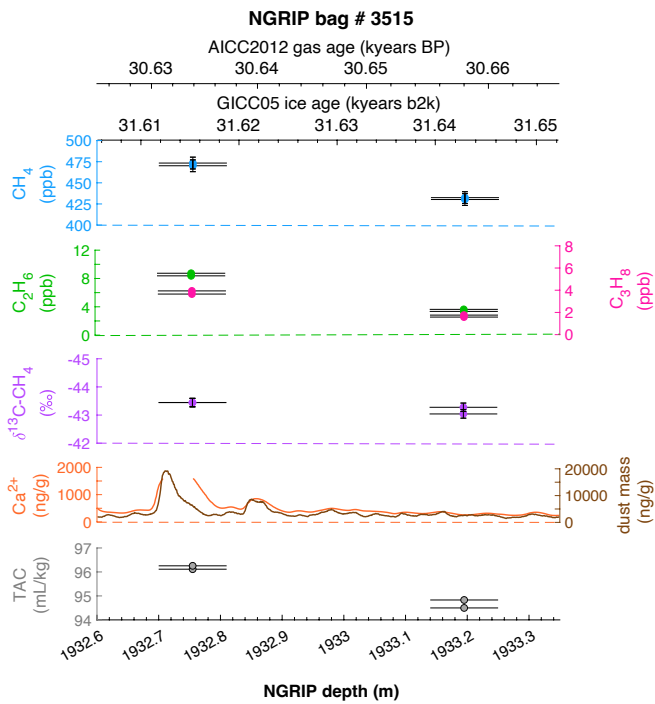
hat gelöscht:



2192
2193
2194
2195
2196
2197
2198
2199
2200
2201

Figure A2: Detailed data overview for NGRIP bag 3453. Bag-specific overview of parameters measured for each sample in this bag: methane, ethane, propane, Ca^{2+} , mineral dust mass, TAC (Total Air Content), $\delta^{13}\text{C-CH}_4$, indicated at the NGRIP depth (bottom axis) and the AICC2012 gas age (upper top axis) and the GICC05 ice age (lower top axis). The mineral dust record is taken from Ruth et al. (2003), the Ca^{2+} record from Erhardt et al. (2022).

hat formatiert: Schriftart: Nicht Fett



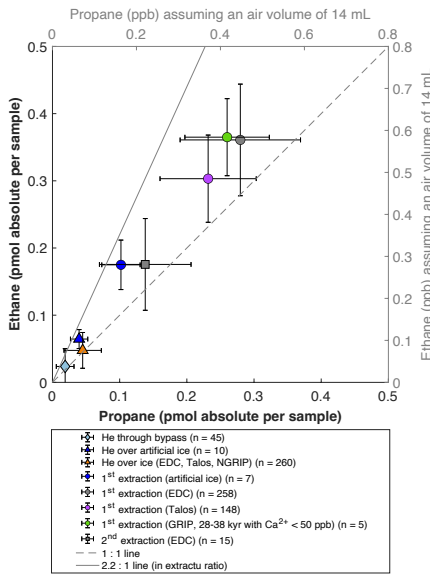
2202
 2203
 2204
 2205
 2206
 2207
 2208
 2209
 2210
 2211
 2212
 2213
 2214
 2215
 2216
 2217
 2218
 2219
 2220
 2221
 2222
 2223

Figure A3: Detailed data overview for NGRIP bag 3515. Bag-specific overview of parameters measured for each sample in this bag: methane, ethane, propane, Ca^{2+} , mineral dust mass, TAC (Total Air Content), $\delta^{13}\text{C-CH}_4$, indicated at the NGRIP depth (bottom axis) and the AICC2012 gas age (upper top axis) and the GICC05 ice age (lower top axis). The mineral dust record is taken from Ruth et al. (2003), the Ca^{2+} record from Erhardt et al. (2022). Note that there is a gap in the Ca^{2+} record which was corrected by a fill routine for the analysis of the two measured samples at this depth.

hat formatiert: Schriftart: Nicht Fett

2224 **Appendix B**

2225



2226

2227 **Figure B1: Collection of different measurement modes and ice core sample locations to estimate individual**
 2228 **blank contributions.** The mode “He through bypass” (diamond) refers to a measurement type where helium is
 2229 injected into our system but without flowing through our extraction vessel. “He over ice” (triangles) refers to
 2230 helium injections over the unmelted ice core sample. Results from the 1st extraction are shown for different ice
 2231 cores (artificial gas-free ice, Talos Dome, EDC, GRIP; colored circles). The 2nd extraction of the Antarctic EDC
 2232 ice core is marked as grey square. Lines with ethane/propane ratios are for orientation only.

2234 In this section we provide background information of how we determined the blank
 2235 contributions for our alkane measurements for the different measurement modes. Overall, our
 2236 strategy is similar to the measurements which were published earlier in 2014 (Schmitt et al.,
 2237 2014). Here we include more measurements performed since then with our $\delta^{13}\text{C}\text{-CH}_4$ device.
 2238 Following the classic usage, blank contributions are related to the measurement device itself
 2239 rather than to the sample, thus we report the measured values of the species as absolute amount
 2240 in pmol with respect to a measurement procedure (sample run). To compare these absolute
 2241 values with the classic units of species concentration in the air for an ice sample in ppb, Fig.
 2242 B1 has secondary axes (grey) for the species concentrations in ppb for an assumed sample size
 2243 of air of 14 mL STP (our typical ice core sample size).

2244 Since our extraction device is at vacuum conditions, a blank contribution from leaks that allow
 2245 ambient air with relatively high ethane and propane concentrations to be collected together with
 2246 our sample seems the most straightforward risk. To quantify this leak contribution, we routinely

hat formatiert: Schriftart: 10 Pt., Nicht Fett

hat formatiert: Schriftart: 10 Pt., Fett, Schriftfarbe: Text 1

Formatiert: Block, Zeilenabstand: einfach

hat formatiert: Schriftart: 10 Pt., Schriftfarbe: Text 1

hat formatiert: Schriftart: 10 Pt., Schriftfarbe: Text 1

hat formatiert: Schriftart: 10 Pt., Schriftfarbe: Text 1

hat formatiert: Schriftart: 10 Pt., Schriftfarbe: Text 1

hat formatiert: Schriftart: 10 Pt., Schriftfarbe: Text 1

hat formatiert: Schriftart: 10 Pt., Nicht Fett

hat formatiert: Schriftfarbe: Text 1

Formatiert: Block, Zeilenabstand: 1,5 Zeilen

hat formatiert: Schriftfarbe: Text 1

hat formatiert: Schriftfarbe: Text 1

hat formatiert: Schriftfarbe: Text 1

hat formatiert: Schriftfarbe: Text 1

hat formatiert: Schriftfarbe: Text 1

hat formatiert: Schriftfarbe: Text 1

Formatiert: Block

2247 perform so called “He over ice” runs where a helium flow is passed over the unmelted ice core
2248 sample and the species are trapped on the cold activated carbon trap (see details in Schmitt et
2249 al., 2014). The trapping duration is the same as for the 1st extraction, thus this “He over ice”
2250 run mimics the contribution for the 1st extraction. As can be seen in Fig. B1, for ethane this
2251 “leak contribution” is typically <0.1 ppb, thus small compared to concentrations we see for
2252 dust-rich Greenland ice samples with about 6 ppb (see Fig. 5). However, this “He over ice”
2253 does not capture the actual melting process of the ice sample and represents the lowest blank
2254 boundary for our ice core samples. To mimic the full procedure an ice core samples experiences,
2255 we run a limited number of artificial gas-free ice samples (blue circles in Fig. B1). The ethane
2256 values obtained for these artificial ice sample is around 0.3 ppb and thus considerably higher
2257 than for the procedure without melting. This indicates that the presence of liquid water may
2258 lead to a desorption or production of alkanes from the inner walls of our extraction vessel.
2259 Alternatively, our artificial ice still contains traces of alkanes. So far, we could not solve this
2260 issue and more experiments are needed. A much larger data set on the upper boundary of the
2261 extraction blank comes from routine measurements of Antarctic ice core samples with the
2262 primary target of stable isotope analyses of CH₄ and N₂O. These Antarctic samples cover glacial
2263 and interglacial time intervals and the measured ethane values are typically around 0.55 ppb.
2264 Since the reconstructed atmospheric background for ethane in Antarctic ice is lower with values
2265 in the range of 0.1 – 0.15 ppb for the late Holocene (Nicewonger et al., 2018), a realistic blank
2266 contribution for our 1st extraction is on the order of 0.4 to 0.5 ppb. An additional constraint
2267 comes from five stadial GRIP samples from the time interval 28-38 kyears (green circle in Fig.
2268 B1) that have very low Ca²⁺ content (< 50 ppb) and thus have likely a negligible contribution
2269 from a dust-related *in extractu* component. The measured ethane concentration from these
2270 GRIP samples is very similar to the Antarctic ice core samples. One possible explanation would
2271 be that the atmospheric ethane concentration during the glacial was similar and low for both
2272 hemispheres. Regardless of the individual contributions, for our considerations of dust-related
2273 *in extractu* production in Greenland ice cores the upper estimate for the sum of atmospheric
2274 background and blank contribution is about 0.55 ppb (about 0.35 pmol) for ethane. Since the
2275 ethane to propane ratio for these non-dust contributions is about 1.5, the corresponding propane
2276 values are lower by that value. Importantly, since the ethane to propane ratio for our dust-related
2277 production is with 2.2 rather similar, its impact on the calculated ethane to propane ratio (e.g.
2278 Fig. 4) is very minor and small within the error estimate. For that reason, we did not correct our
2279 Greenland measurements for any blank contribution and showed the values as measured along
2280 with measurements of Antarctic ice cores samples which serve as first-order blank estimates.

hat formatiert: Schriftfarbe: Text 1

hat formatiert: Schriftfarbe: Text 1

hat formatiert: Schriftfarbe: Text 1

hat gelöscht:

hat formatiert: Schriftfarbe: Text 1

hat gelöscht: either

hat gelöscht: s

hat formatiert: Schriftfarbe: Text 1

hat formatiert: Schriftfarbe: Text 1

hat formatiert: Schriftfarbe: Text 1, Tiefgestellt

hat formatiert: Schriftfarbe: Text 1

hat formatiert: Schriftfarbe: Text 1, Tiefgestellt

hat formatiert: Schriftfarbe: Text 1

hat formatiert: Schriftfarbe: Text 1

hat formatiert: Schriftfarbe: Text 1

hat formatiert: Schriftfarbe: Text 1

hat formatiert: Schriftfarbe: Text 1

hat formatiert: Schriftfarbe: Text 1

hat formatiert: Hochgestellt

hat formatiert: Schriftfarbe: Text 1

hat formatiert: Schriftart: Kursiv, Schriftfarbe: Text 1

hat formatiert: Schriftfarbe: Text 1

hat formatiert: Schriftart: Kursiv, Schriftfarbe: Text 1

hat formatiert: Schriftfarbe: Text 1

hat formatiert: Schriftfarbe: Text 1

hat formatiert: Schriftfarbe: Text 1

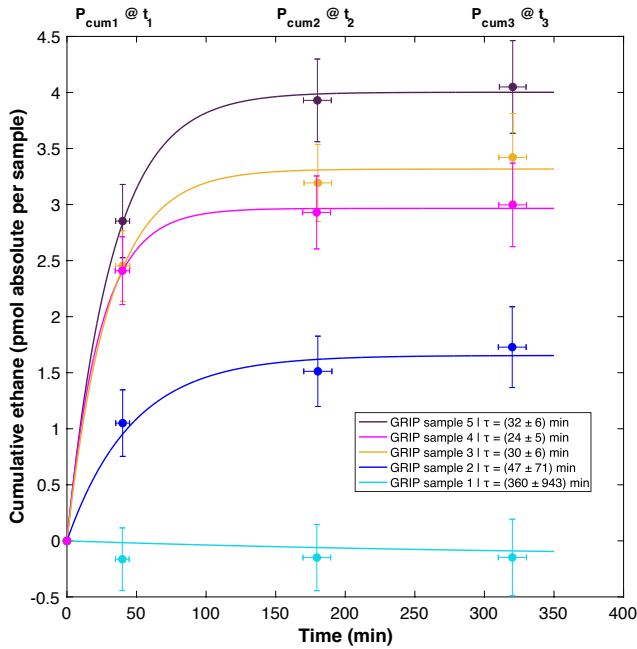
hat formatiert: Schriftfarbe: Text 1

hat formatiert: Schriftfarbe: Text 1

hat formatiert: Schriftart: Nicht Fett

2284 **Appendix C**

2285



2286

2287

2288 **Figure C1: Temporal dynamics of excess ethane production in GRIP ice core samples.** Cumulative ethane
 2289 amount from the 1st, 2nd, and 3rd extraction in relation to the time available for a potential reaction in the meltwater
 2290 during each extraction. We assume a first-order reaction kinetic as model for our observations where the mean
 2291 half-life time (τ) and standard deviations are calculated for each GRIP sample from the compilation of all 1000
 2292 iterations of our Monte Carlo approach. The numbered samples can also be found in Fig. 7a.

2293

2294 The general equation to describe a first-order chemical reaction or exponential decay process
 2295 (e.g. release of adsorbed gas from the adsorbent) is Eqn. (1).

2296

2297
$$N(t) = N_0 \cdot e^{(-t/\tau)} \quad (1)$$

2298

2299 With N_0 being the total amount of substance (reactant) at the start of the reaction, $N(t)$ equals
 2300 the remaining amount of the reactant at time t , and t being time of reaction and τ , the mean
 2301 lifetime of the reaction. In our case, we cannot determine $N(t)$ neither do we know N_0 but we
 2302 experimentally determined the cumulative amount of the product, $P_{cum(t)}$, at three different times
 2303 as our observable quantity. Thus, in Eqn. 2 we define $P_{cum(t)}$ as the difference between N_0 and
 2304 $N(t)$.

hat gelöscht:

hat formatiert: Schriftart: Nicht Fett

hat gelöscht: B

hat gelöscht:

hat gelöscht: assuming an uncertainty in x of ± 5 min and an uncertainty in y of $\pm 5\%$ of the measured value in the 1st extraction and $\pm 10\%$ in both the 2nd and 3rd extraction.

hat gelöscht: ¶

hat formatiert: Schriftart: (Standard) Times New Roman, Nicht Kursiv, Schriftfarbe: Text 1, Englisch (USA)

Formatiert: Zeilenabstand: 1,5 Zeilen

hat formatiert: Schriftart: (Standard) Times New Roman, Nicht Kursiv, Schriftfarbe: Text 1, Englisch (USA)

hat formatiert: Schriftart: Nicht Kursiv, Englisch (USA)

hat formatiert: Schriftart: (Standard) Times New Roman, Nicht Kursiv, Schriftfarbe: Text 1, Englisch (USA)

hat formatiert: Schriftart: Nicht Kursiv

hat formatiert: Schriftart: (Standard) Times New Roman, Nicht Kursiv, Schriftfarbe: Text 1, Englisch (USA)

hat formatiert: Schriftart: Nicht Kursiv, Englisch (USA)

hat formatiert: Schriftart: (Standard) Times New Roman, Nicht Kursiv, Schriftfarbe: Text 1, Englisch (USA)

2B13
2B14
2B15
2B16
2B17
2B18
2B19
2B20
2B21
2B22
2B23
2B24
2B25
2B26
2B27
2B28
2B29
2B30
2B31
2B32
2B33
2B34
2B35
2B36
2B37
2B38
2B39
2B40
2B41
2B42
2B43
2B44
2B45
2B46

$$P_{cum(t)} = N_0 - N(t) \quad (2)$$

Replacing $N(t)$ in Eqn. 1 with our definition in Eqn. 2 we obtain Eqn. 3, which contains two fit parameters, N_0 and τ , as well as our observable parameter $P_{cum(t)}$, i.e. the cumulative amount of alkane for a certain time step.

$$P_{cum(t)} = N_0 - N_0 * e^{-t/\tau} \quad (3)$$

For the five GRIP samples we have three consecutive measurements each, the 1st, 2nd, and 3rd extraction. The time dependent $P_{cum(t)}$ values are as follows: P_{cum0} is defined as 0, representing the state of the unmelted ice sample before liquid water is present. P_{cum1} is the measured amount from the 1st extraction (ice extraction) minus the estimated contribution from the atmosphere and minus the blank contribution for the 1st extraction. P_{cum2} is the sum of P_{cum1} and the value from the 2nd extraction minus the blank contribution of the 2nd extraction. Similarly, P_{cum3} is the sum of P_{cum2} and the value from the 3rd extraction minus the blank for the 3rd extraction.

To account for the uncertainties of the involved measurements and corrections, we added normally distributed errors to the following parameters (measured value $\pm 5\%$; blank $\pm 20\%$; atmospheric contribution $\pm 50\%$), and we also assigned an uncertainty of 5 min to the time to account for variations of the melting speed of the ice and delays between the individual measurements (1st, 2nd, 3rd).

For the fitting procedure we used the Matlab built in nonlinear least-squares solver called 'lsqcurvefit' and performed 1000 runs where we varied the above-mentioned input parameters. The output of the function are the two fit parameters, i.e., N_0 and τ . From the 1000 runs we calculated the mean and the 1 sigma standard deviation of the lifetime.

Note, this approach can only be suitably applied to ethane and propane as the past atmospheric contribution for these gases in the 1st extraction is typically small against the excess contribution for dust-rich samples. For our five GRIP samples, where we have three consecutive extractions, four samples are considered "dust-rich" and are suitable to provide robust estimates for τ . In contrast, one sample is from an interstadial period with very low dust content and thus shows negligible production of alkanes in all three extractions. While this sample is not suited to provide robust estimates for τ , this sample allows to assess the first-order plausibility of the blank correction and the assumed atmospheric background for ethane for the 1st extraction

- hat formatiert: Schriftart: Nicht Kursiv, Englisch (USA)
- hat formatiert: Schriftart: (Standard) Times New Roman, Nicht Kursiv, Schriftfarbe: Text 1, Englisch (USA)
- hat formatiert: Schriftart: Nicht Kursiv, Englisch (USA)
- hat formatiert: Schriftart: (Standard) Times New Roman, Nicht Kursiv, Schriftfarbe: Text 1, Englisch (USA)
- hat formatiert: Schriftart: Nicht Kursiv
- hat formatiert: Schriftart: (Standard) Times New Roman, Nicht Kursiv, Schriftfarbe: Text 1, Englisch (USA)
- hat formatiert: Schriftart: Nicht Kursiv
- hat formatiert: Schriftart: (Standard) Times New Roman, Nicht Kursiv, Schriftfarbe: Text 1, Englisch (USA)
- hat formatiert: Schriftart: Nicht Kursiv
- hat formatiert: Schriftart: (Standard) Times New Roman, Nicht Kursiv, Schriftfarbe: Text 1, Englisch (USA)
- hat formatiert: Schriftart: Nicht Kursiv
- hat formatiert: Schriftart: Nicht Kursiv, Schriftfarbe: Text 1, Englisch (USA)
- hat formatiert: Schriftart: Nicht Kursiv, Englisch (USA)
- hat formatiert: Schriftart: Nicht Kursiv
- hat formatiert: Schriftart: Nicht Kursiv, Englisch (USA)
- hat formatiert: Schriftart: (Standard) Times New Roman, Nicht Kursiv, Schriftfarbe: Text 1, Englisch (USA)
- hat formatiert: Englisch (USA)
- hat formatiert: Schriftart: (Standard) Times New Roman, Nicht Kursiv, Schriftfarbe: Text 1, Englisch (USA)
- hat formatiert: Schriftart: Nicht Kursiv
- hat formatiert: Schriftart: (Standard) Times New Roman, Nicht Kursiv, Schriftfarbe: Text 1, Englisch (USA)
- hat formatiert: Schriftart: (Standard) Times New Roman, Nicht Kursiv, Schriftfarbe: Text 1, Englisch (USA)
- hat formatiert: Schriftart: (Standard) Times New Roman, Nicht Kursiv, Schriftfarbe: Text 1, Englisch (USA)
- Formatiert: Zeilenabstand: 1,5 Zeilen
- hat formatiert: Schriftart: Nicht Kursiv, Englisch (USA)
- hat formatiert: Schriftart: (Standard) Times New Roman, Nicht Kursiv, Schriftfarbe: Text 1, Englisch (USA)
- hat formatiert: Schriftart: Nicht Kursiv, Englisch (USA)
- hat formatiert: Schriftart: (Standard) Times New Roman, Nicht Kursiv, Schriftfarbe: Text 1, Englisch (USA)
- hat formatiert: Schriftart: Nicht Kursiv
- hat formatiert: Schriftart: Times New Roman, Nicht Kursiv, Schriftfarbe: Text 1, Englisch (USA)
- hat formatiert: Schriftart: Nicht Kursiv
- hat formatiert: Schriftart: (Standard) Times New Roman, Nicht Kursiv, Schriftfarbe: Text 1, Englisch (USA)

2347 (sample number 1, bottom-most sample). For a sample without any *in extractu* production, the
2348 cumulative curve should be flat at around 0 which is the case within our error estimates.

hat formatiert: Schriftart: Nicht Kursiv, Englisch (USA)

hat formatiert: Schriftart: (Standard) Times New Roman, Nicht Kursiv, Schriftfarbe: Text 1, Englisch (USA)

2349
2350
2351
2352
2353
2354
2355
2356
2357
2358
2359
2360
2361
2362
2363
2364
2365
2366
2367
2368
2369
2370
2371
2372
2373
2374
2375
2376
2377
2378
2379
2380

2381 **Code availability**

2382 No special code related to the manuscript.

2383 ▲

2384 **Data availability**

2385 Data is provided on request to the authors.

2386 ▼

2387 **Author contribution**

2388 The experimental approach was defined by JS, HF and MM. MM and BS performed the

2389 measurements; MM and JS analyzed the data; MM wrote the manuscript draft; MM prepared

2390 the manuscript with contributions from all co-authors.

2391 ▼

2392 **Competing interests**

2393 The authors declare that they have no conflict of interest.

2394 ▲

2395 **Disclaimer**

2396 None.

2397 ▲

2398 **Special issue statement**

2399 Ice core science at the three poles (CP/TC inter-journal SI)

2400 ▼

2401 **Acknowledgments**

2402 We thank Murat Aydin for very helpful review comments. The research leading to these results

2403 has received funding from the Swiss National Science Foundation (no. 200020_172506 &

2404 200020B_200328). This work is a contribution to the NorthGRIP ice core project, which is

2405 directed and organized by the Department of Geophysics at the Niels Bohr Institute for

2406 Astronomy, Physics and Geophysics, University of Copenhagen. It is supported by funding

2407 agencies in Denmark (SNF), Belgium (FNRS-CFB), France (IFRTP and NSU/CNRS),

2408 Germany (AWI), Iceland (RannIs), Japan (MEXT), Sweden (SPRS), Switzerland (SNF), and

2409 the United States (NSF).

2410 ▼

2411 **References**

2412

2413 Althoff, F., Jugold, A. and Keppler, F.: Methane formation by oxidation of ascorbic acid

2414 using iron minerals and hydrogen peroxide. Chemosphere 80, 286–292,

2415 <https://doi.org/10.1016/j.chemosphere.2010.04.004>, 2010

2416

- hat formatiert: Schriftart: (Standard) Times New Roman, 12 Pt., Schriftfarbe: Text 1
- hat formatiert: Schriftfarbe: Text 1
- hat formatiert: Schriftart: (Standard) Times New Roman, 12 Pt., Schriftfarbe: Text 1
- Formatiert: Zeilenabstand: 1,5 Zeilen
- hat formatiert: Schriftart: (Standard) Times New Roman, 12 Pt., Schriftfarbe: Text 1, Englisch (USA)
- hat formatiert: Schriftart: (Standard) Times New Roman, 12 Pt., Schriftfarbe: Text 1
- hat formatiert: Schriftfarbe: Text 1, Englisch (USA)
- hat formatiert: Schriftart: (Standard) Times New Roman, 12 Pt., Schriftfarbe: Text 1, Englisch (USA)
- Formatiert: Abstand Vor: 0 Pt., Nach: 0 Pt., Zeilenabstand: 1,5 Zeilen, Keine Aufzählungen oder Nummerierungen
- hat formatiert: Schriftart: (Standard) Times New Roman, 12 Pt., Schriftfarbe: Text 1
- hat formatiert: Schriftfarbe: Text 1
- hat gelöscht: ¶
- hat formatiert: Schriftart: (Standard) Times New Roman, 12 Pt., Schriftfarbe: Text 1
- Formatiert: Links
- hat formatiert: Schriftart: (Standard) Times New Roman, 12 Pt., Schriftfarbe: Text 1, Englisch (USA)
- hat formatiert: Schriftart: (Standard) Times New Roman, 12 Pt., Schriftfarbe: Text 1
- hat formatiert: Schriftart: Nicht Fett
- hat gelöscht: ¶
- ¶
- ¶
- ¶
- hat gelöscht: ¶
- hat formatiert: Schriftfarbe: Text 1
- hat formatiert: Schriftart: Fett, Schriftfarbe: Text 1
- hat formatiert: Schriftfarbe: Text 1
- hat formatiert: Schriftfarbe: Text 1
- hat formatiert: Schriftart: (Standard) Times New Roman, 12 Pt., Schriftfarbe: Text 1
- Formatiert: Zeilenabstand: 1,5 Zeilen
- hat formatiert: Schriftfarbe: Text 1
- hat formatiert: Schriftart: (Standard) Times New Roman, 12 Pt., Schriftfarbe: Text 1, Englisch (USA)
- hat formatiert: Schriftfarbe: Text 1, Englisch (USA)
- hat gelöscht: ¶
- Formatiert: Links
- hat formatiert: Schriftfarbe: Text 1
- hat gelöscht: ¶
- hat formatiert: Schriftfarbe: Text 1
- hat gelöscht: ¶
- ¶

2445 Althoff, F., Benzing, K., Comba, P., McRoberts, C., Boyd, D. R., Greiner, S. and Keppler, F.:
 2446 Abiotic methanogenesis from organosulphur compounds under ambient conditions, *Nat*
 2447 *Commun*, 5, 4205, <https://doi.org/10.1038/ncomms5205>, 2014
 2448
 2449 Anklin, M., Barnola, J.-M., Schwander, J., Stauffer, B., and Raynaud, D.: Processes affecting
 2450 the CO₂ concentrations measured in Greenland ice, *Tellus*, 47, 461-470,
 2451 <https://doi.org/10.1034/j.1600-0889.47.issue4.6.x>, 1995
 2452
 2453 Apel, K. and Hirt, H.: Reactive Oxygen Species: Metabolism, Oxidative Stress, and Signal
 2454 Transduction, *Annual Review of Plant Biology* 2004, 55:1, 373-399,
 2455 <https://doi.org/10.1146/annurev.arplant.55.031903.141701>, 2004
 2456
 2457 Austin, A. T., Méndez, M. S., and Ballaré, C. L.: Photodegradation alleviates the lignin
 2458 bottleneck for carbon turnover in terrestrial ecosystems, *PNAS*, 13 (16), 4392-4397,
 2459 <https://doi.org/10.1073/pnas.1516157113>, 2016
 2460
 2461 Baumgartner, M., Schilt, A., Eicher, O., Schmitt, J., Schwander, J., Spahni, R., Fischer, H.,
 2462 and Stocker, T. F.: High-resolution inter-polar difference of atmospheric methane around the
 2463 Last Glacial Maximum, *Biogeosciences*, 9, 3961–3977, [https://doi.org/10.5194/bg-9-3961-](https://doi.org/10.5194/bg-9-3961-2012)
 2464 [2012](https://doi.org/10.5194/bg-9-3961-2012), 2012
 2465
 2466 Baumgartner, M., Kindler, P., Eicher, O., Floch, G., Schilt, A., Schwander, J., Spahni, R.,
 2467 Capron, E., Chappellaz, J., Leuenberger, M., Fischer, H., and Stocker, T. F.: NGRIP
 2468 CH₄ concentration from 120 to 10 kyr before present and its relation to a δ¹⁵N temperature
 2469 reconstruction from the same ice core, *Clim. Past*, 10, 903–920, [https://doi.org/10.5194/cp-](https://doi.org/10.5194/cp-10-903-2014)
 2470 [10-903-2014](https://doi.org/10.5194/cp-10-903-2014), 2014
 2471
 2472 Beck, J., Bock, M., Schmitt, J., Seth, B., Blunier, T., and Fischer, H.: Bipolar carbon and
 2473 hydrogen isotope constraints on the Holocene methane budget, *Biogeosciences*, 15, 7155–
 2474 7175, <https://doi.org/10.5194/bg-15-7155-2018>, 2018
 2475
 2476 Bernard, B., Brooks, J.M. and Sackett, W.M.: A geochemical model for characterization of
 2477 hydrocarbon gas sources in marine sediments. In: 9th Annual Offshore Technology
 2478 Conference, Houston, Texas, May 1977, 435–438 (OTC 2934), [https://doi.org/10.4043/2934-](https://doi.org/10.4043/2934-MS)
 2479 [MS](https://doi.org/10.4043/2934-MS), 1977
 2480
 2481 Biscaye, P. E., Grousset, F. E., Revel, M., Van der Gaast, S., Zielinski, G. A., Vaars, A.
 2482 and G. Kukla: Asian provenance of Glacial dust (stage 2) in the Greenland Ice Sheet Project 2
 2483 Ice Core, Summit, Greenland, *J. Geophys. Res.*, 102, 26,765–26,781, 1997
 2484
 2485 Bock, M., Schmitt, J., Behrens, M., Möller, L., Schneider, R., Sapart, C. and Fischer, H.: A
 2486 gas chromatography/pyrolysis/isotope ratio mass spectrometry system for high- precision dD
 2487 measurements of atmospheric methane extracted from ice cores, *Rapid Commun. Mass*
 2488 *Spectrom*, 24, 621–633, <https://doi.org/10.1002/rcm.4429>, 2010a
 2489
 2490 Bock, M., Schmitt, J., Blunier, T., Fischer, H., Möller, L. and Spahni, R.: Hydrogen
 2491 Isotopes Preclude Marine Hydrate CH₄ Emissions at the Onset of Dansgaard- Oeschger
 2492 Events, *Science*, 328, 1686-1689, <https://doi.org/10.1126/science.1187651>, 2010b
 2493
 2494 Bock, M., Schmitt, J., Beck, J., Schneider, R., and Fischer, H.: Improving accuracy and
 2495 precision of ice core δD(CH₄) analyses using methane pre-pyrolysis and hydrogen post-

Feldfunktion geändert

hat formatiert: Schriftart: (Standard) Times New Roman, 12 Pt., Schriftfarbe: Text 1, Englisch (USA)

hat formatiert: Schriftart: (Standard) Times New Roman, 12 Pt., Schriftfarbe: Text 1, Englisch (USA)

hat formatiert: Schriftart: (Standard) Times New Roman, 12 Pt., Schriftfarbe: Text 1, Englisch (USA)

hat formatiert: Schriftart: (Standard) Times New Roman, 12 Pt., Schriftfarbe: Text 1, Englisch (USA)

Formatiert: Zeichenausrichtung: Automatisch

hat formatiert: Schriftart: (Standard) Times New Roman, 12 Pt., Schriftfarbe: Text 1, Englisch (USA)

hat formatiert: Schriftart: (Standard) Times New Roman, 12 Pt., Schriftfarbe: Text 1, Englisch (USA)

hat formatiert: Schriftart: (Standard) Times New Roman, 12 Pt., Schriftfarbe: Text 1, Englisch (USA)

2496 pyrolysis trapping and subsequent chromatographic separation, *Atmos. Meas. Tech.*, 7, 1999–
 2497 2012, <https://doi.org/10.5194/amt-7-1999-2014>, 2014
 2498
 2499 Bock, M., Schmitt, J., Beck, J., Seth, B., Chappellaz, J. and Fischer, H.: Glacial/ interglacial
 2500 wetland, biomass burning, and geologic methane emissions constrained by dual stable
 2501 isotopic CH₄ ice core records, *PNAS*, 114 (29), E5778-E5786,
 2502 <https://doi.org/10.1073/pnas.1613883114>, 2017
 2503
 2504 Bruhn, D., Mikkelsen, T. N., Øbro, J., Willats, W. G. T. and Ambus, P.: Effects of
 2505 temperature, ultraviolet radiation and pectin methyl esterase on aerobic methane release from
 2506 plant material, *Plant Biology*, 11, 43-48, <https://doi.org/10.1111/j.1438-8677.2009.00202.x>,
 2507 2009
 2508
 2509 Campen, R. K., Sowers, T., and Alley, R. B.: Evidence of microbial consortia metabolizing
 2510 within a low-latitude mountain glacier, *Geology*, 31, 231–234, [https://doi.org/10.1130/0091-7613\(2003\)031<0231:EOMCMW>2.0.CO;2](https://doi.org/10.1130/0091-7613(2003)031<0231:EOMCMW>2.0.CO;2), 2003
 2511
 2512
 2513 Chappellaz, J., Blunier, T., Kints, S., Dällenbach, A., Barnola, J. M., Schwander, J., Raynaud,
 2514 D. and Stauffer B.: Changes in the atmospheric CH₄ gradient between Greenland and
 2515 Antarctica during the Holocene, *Geophys. Res. Lett.*, Volume 102, 15987-15997,
 2516 <https://doi.org/10.1029/97JD01017>, 1997
 2517
 2518 Cheng, A. L. and Huang, W. L.: Selective adsorption of hydrocarbon gases on clays and
 2519 organic matter, *Org. Geochem.*, 35, 413-423,
 2520 <https://doi.org/10.1016/j.orggeochem.2004.01.007>, 2004
 2521
 2522 Dan, J., Kumai, T., Sugimoto, A. and Murase, J.: Biotic and abiotic methane releases from
 2523 Lake Biwa sediment slurry, *Limnology* 5, 149–154, <https://doi.org/10.1007/s10201-004-0124-7>, 2004
 2524
 2525
 2526 Derendorp, L., Holzinger, R., Wishkerman, A., Keppler, F., and Röckmann, T.: VOC
 2527 emissions from dry leaf litter and their dependence on temperature, *Biogeosciences Discuss.*,
 2528 7, 823–854, <https://doi.org/10.5194/bgd-7-823-2010>, 2010
 2529
 2530 Derendorp, L., Holzinger, R., Wishkerman, A., Keppler, F., and Röckmann, T.: Methyl
 2531 chloride and C₂-C₅ hydrocarbon emissions from dry leaf litter and their dependence on
 2532 temperature, *Atmospheric Environment*, 45, 3112-3119,
 2533 <https://doi.org/10.1016/j.atmosenv.2011.03.016>, 2011
 2534
 2535 Dumelin, E.E. and Tappel, A.L.: Hydrocarbon gases produced during in vitro peroxidation of
 2536 polyunsaturated fatty acids and decomposition of preformed hydroperoxides, *Lipids*, 12, 894,
 2537 <https://doi.org/10.1007/BF02533308>, 1977
 2538
 2539 Dyonisius, M. N., Petrenko, V. V., Smith, A.M., Hua, Q., Yang, B., Schmitt, J., Beck, J.,
 2540 Seth, B., Bock, M., Hmiel, B., Vimont, I., Menking, J. A., Shackleton, S. A., Baggenstos, D.,
 2541 Bauska, T. K., Rhodes, R., Sperlich, P., Beaudette, R., Harth, C., Kalk, M., Brook, E. J.,
 2542 Fischer, H., Severinghaus, J. P. and Weiss, R. F.: Old carbon reservoirs were not important in
 2543 the deglacial methane budget, *Science*, 367(6480), 907-910,
 2544 <https://doi.org/10.1126/science.aax0504>, 2020
 2545

hat gelöscht: ¶

Bory, A. J. M., Biscaye, P. E. and Grousset, F. E.: Two distinct seasonal Asian source regions for mineral dust deposited in Greenland (NorthGRIP), *Geophys. Res. Lett.* 30, 1167, <https://doi.org/10.1029/2002GL016446>, 2003 ¶

¶ Biscaye P., Grousset F., Revel M., Van der Gaast S., Zielinski G., Vaars A. and Kukla, G.: Asian provenance of glacial dust (Stage 2) in the Greenland Ice Sheet Project 2 ice core, Summit, Greenland. *J. Geophys. Res.-Oceans* 102, 26765–26781, <https://doi.org/10.1029/97JC01249>, 1997 ¶

Feldfunktion geändert

2557 Erhardt, T., Bigler, M., Federer, U., Gfeller, G., Leuenberger, D., Stowasser, O.,
2558 Röthlisberger, R., Schüpbach, S., Ruth, U., Twarloh, B., Wegner, A., Goto-Azuma, K.,
2559 Kuramoto, T., Kjør, H. A., Vallelonga, P. T., Siggaard-Andersen, M.-L., Hansson, M. E.,
2560 Benton, A. K., Fleet, L. G., Mulvaney, R., Thomas, E. R., Abram, N., Stocker, T. F., and
2561 Fischer, H.: High resolution aerosol concentration data from the Greenland NorthGRIP and
2562 NEEM deep ice cores, *Earth Syst. Sci. Data Discuss.*, **14**, 1215–1231,
2563 <https://doi.org/10.5194/essd-14-1215, 2022>,
2564
2565 Etiope, G. and Klusman, R. W.: Geologic emissions of methane to the atmosphere,
2566 *Chemosphere*, **49**, 8, 777-789, [https://doi.org/10.1016/S0045-6535\(02\)00380-6, 2002](https://doi.org/10.1016/S0045-6535(02)00380-6, 2002)
2567
2568 Etiope G., Martinelli G., Caracausi, A. and Italiano, F.: Methane seeps and mud volcanoes in
2569 Italy: gas origin, fractionation and emission to the atmosphere, *Geophys. Res. Lett.*, **34**,
2570 <https://doi.org/10.1029/2007GL030341, 2007>
2571
2572 Etiope G., Lassey K. R., Klusman R. W. and Boschi, E.: Reappraisal of the fossil methane
2573 budget and related emission from geologic sources, *Geophys. Res. Lett.*, **35**,
2574 <https://doi.org/10.1029/2008GL033623, 2008>
2575
2576 Frahy, G. and Schopfer, P.: Hydrogen peroxide production by roots and its stimulation by
2577 exogenous NADH, *Physiologia Plantarum*, **103**, 395-404, <https://doi.org/10.1034/j.1399-3054.1998.1030313.x, 1998>
2578
2579
2580 Flückiger J., Blunier T., Stauffer B., Chappellaz M., Spahni R., Kawamura K., Schwander J.,
2581 Stocker T. F. and Dahl-Jensen D.: N₂O and CH₄ variations during the last glacial epoch:
2582 Insight into global processes, *Global Biogeochem. Cy* **18**, 1020,
2583 <https://doi.org/10.1029/2003GB002122, 2004>
2584
2585 Fuhrer, K. and Legrand, M.: Continental biogenic species in the Greenland Ice Core Project
2586 ice core: Tracing back the biomass history of the North American continent, *J. Geophys. Res.*,
2587 **102**(C12), 26735–26745, <https://doi.org/10.1029/97JC01299, 1997>
2588
2589 Georgiou, C. D., Sun, H. J., McKay, C. P., Grintzalis, K., Papapostolou, I., Zisimopoulos, D.,
2590 Panagiotidis, K., Zhang, G., Koutsopoulou, E., Christidis, G. E. and Margiolaki, I.: Evidence
2591 for photochemical production of reactive oxygen species in desert soils, *Nat.*
2592 *Commun.*, **6**, 7100, <https://doi.org/10.1038/ncomms8100, 2015>
2593
2594 Giorio, C., Kehrwald, N., Barbante, C., Kalberer, M., King, A. C. F., Thomas, E. R., Wolff,
2595 E. W. and Zennaro, P.: Prospects for reconstructing paleoenvironmental conditions from
2596 organic compounds in polar snow and ice, *Quaternary Science Reviews*, **183**, 1-22,
2597 <https://doi.org/10.1016/j.quascirev.2018.01.007, 2018>
2598
2599 Gu, Q., Chang, S. X., Wang, Z. P., Feng, J. C., Chen, Q. S. and Han, X. G.: Microbial versus
2600 non-microbial methane releases from fresh soils at different temperatures, *Geoderma*, **284**,
2601 178-184, <https://doi.org/10.1016/j.geoderma.2016.08.027, 2016>
2602
2603 Han, C., Do Hur, S., Han, Y., Lee, K., Hong, S., Erhard, T., Fischer, H., Svensson, A. M.,
2604 Steffensen, J. P. and Vallelonga, P.: High-resolution isotopic evidence for a potential Saharan
2605 provenance of Greenland glacial dust. *Sci Rep* **8**, 15582, <https://doi.org/10.1038/s41598-018-33859-0, 2018>
2606
2607

hat formatiert: Englisch (USA)

hat formatiert: Englisch (USA)

2608 [Harris, E., Sinha, B., van Pinxteren, D., Tilgner, A., Wadinga Fomba, K., Schneider, J., Roth,](#)
2609 [A., Gnauk, T., Fahlbusch, B., Mertes, S., Lee, T., Collett, J., Foley, S., Borrmann, S., Hoppe,](#)
2610 [P., and Herrmann, H.; Enhanced Role of Transition Metal Ion Catalysis During In-Cloud](#)
2611 [Oxidation of SO₂. *Science*, 340, 727-730, <https://doi.org/doi:10.1126/science.1230911>, 2013.](#)
2612
2613 Helmig, D., Petrenko, V., Martinerie, P., Witrant, E., Röckmann, T., Zunderweg, A.,
2614 Holzinger, R., Hueber, J., Thompson, C., White, J. W. C., Sturges, W., Baker, A., Blunier, T.,
2615 Etheridge, D., Rubino, M., and Tans, P.: Reconstruction of Northern Hemisphere 1950–2010
2616 atmospheric non-methane hydrocarbons, *Atmos. Chem. Phys.*, 14, 1463-1483,
2617 <https://doi.org/10.5194/acp-14-1463>, 2014
2618
2619 [Hoheisel, A., Yeman, C., Dinger, F., Eckhardt, H., and Schmidt, M.: An improved method for](#)
2620 [mobile characterisation of \$\delta^{13}\text{C}_{\text{CH}_4}\$ source signatures and its application in Germany, *Atmos.*
2621 \[Meas. Tech.\]\(#\), 12, 1123–1139, <https://doi.org/10.5194/amt-12-1123-2019>, 2019.](#)
2622
2623 Hurkuck, M., Althoff, F., Jungkunst, H. F., Jugold, A. and Keppler, F.: Release of methane
2624 from aerobic soil: An indication of a novel chemical natural process?, *Chemosphere*, 86, 684-
2625 689, <https://doi.org/10.1016/j.chemosphere.2011.11.024>, 2012
2626
2627 Ji L., Zhang T., Milliken K. L., Qu J. and Zhang X.: Experimental investigation of main
2628 controls to methane adsorption in clay-rich rocks, *Appl. Geochem.* 27, 2533–2545,
2629 <https://doi.org/10.1016/j.apgeochem.2012.08.027>, 2012
2630
2631 John, W. W. and Curtis, R. W.: Isolation and Identification of the Precursor of Ethane
2632 in *Phaseolus vulgaris* L., *Plant Physiology*, 59, 521–522, <https://doi.org/10.1104/pp.59.3.521>,
2633 1977
2634
2635 Jugold, A., Althoff, F., Hurkuck, M., Greule, M., Lenhart, K., Lelieveld, J., and Keppler, F.:
2636 Non-microbial methane formation in oxic soils, *Biogeosciences*, 9, 5291–5301,
2637 <https://doi.org/10.5194/bg-9-5291-2012>, 2012
2638
2639 Katagi, T.: Photoinduced Oxidation of the organophosphorus Fungicide Tolclofs-methyl on
2640 Clay Minerals, *J. Agric. Food Cham.*, 38, 1595-1600, 1990
2641
2642 Kaufmann, P. R., Federer, U., Hutterli, M. A., Bigler, M., Schüpbach, S., Ruth, U., Schmitt, J.
2643 and Stocker, T. F.: An Improved Continuous Flow Analysis System for High-Resolution
2644 Field Measurements on Ice Cores, *Environmental Science & Technology*, 42 (21), 8044-
2645 8050, <https://doi.org/10.1021/es8007722>, 2008
2646
2647 Keeling, C. D.: The concentration and isotopic abundance of carbon dioxide in rural areas,
2648 *Geochim. Cosmochim. Acta*, 13, 322–334 [https://doi.org/10.1016/0016-7037\(58\)90033-](https://doi.org/10.1016/0016-7037(58)90033-4)
2649 [4.1958](https://doi.org/10.1016/0016-7037(58)90033-4), 1958
2650
2651 Keeling, C. D.: The concentration and isotopic abundance of carbon dioxide in rural and
2652 marine air, *Geochim. Cosmochim. Acta*, 24, 277–298, [https://doi.org/10.1016/0016-](https://doi.org/10.1016/0016-7037(61)90023-0)
2653 [7037\(61\)90023-0](https://doi.org/10.1016/0016-7037(61)90023-0), 1961
2654
2655 Keppler, F., Hamilton, J. T. G., Braß, M. and Röckmann, T.: Methane emissions from
2656 terrestrial plants under aerobic conditions, *Nature* 439, 187–191,
2657 <https://doi.org/10.1038/nature04420>, 2006
2658

hat formatiert: Schriftart: (Standard) Times New Roman, Nicht unterstrichen, Schriftfarbe: Automatisch, Englisch (USA)

hat formatiert: Schriftart: (Standard) Times New Roman, Englisch (USA)

hat formatiert: Schriftart: (Standard) Times New Roman

hat formatiert: Schriftart: (Standard) Times New Roman, Englisch (USA)

hat formatiert: Schriftart: (Standard) Times New Roman

hat formatiert: Schriftart: (Standard) Times New Roman, Englisch (USA)

hat formatiert: Schriftart: (Standard) Times New Roman

hat formatiert: Schriftart: 12 Pt., Englisch (USA)

hat gelöscht: ¶

hat formatiert: Schriftart: 12 Pt., Tiefgestellt

hat formatiert: Schriftart: 12 Pt., Englisch (USA)

hat formatiert: Schriftart: 12 Pt., Englisch (USA)

hat formatiert: Schriftart: 12 Pt., Nicht Fett, Englisch (USA)

hat formatiert: Schriftart: 12 Pt., Englisch (USA)

hat formatiert: Englisch (USA)

hat formatiert: Schriftart: 12 Pt., Englisch (USA)

hat formatiert: Absatz-Standardschriftart, Schriftart: 12 Pt., Englisch (USA)

hat formatiert: Englisch (USA)

hat formatiert: Schriftart: (Standard) Times New Roman, 12 Pt., Schriftfarbe: Text 1, Englisch (USA)

hat formatiert: Schriftart: (Standard) Times New Roman, 12 Pt., Schriftfarbe: Text 1

hat formatiert: Schriftart: (Standard) Times New Roman, 12 Pt., Schriftfarbe: Text 1, Englisch (USA)

hat formatiert: Schriftart: (Standard) Times New Roman, 12 Pt., Schriftfarbe: Text 1

hat formatiert: Deutsch

hat gelöscht: ¶

Iseli, R.: Stable Isotope Analysis of Hydrogen in Methane using Antarctic Ice Cores. M.S. thesis, Climate and Environmental Physics, University of Bern, Switzerland, 2019¶

2665 Keppler, F., Hamilton, J. T. G., McRoberts, W. C., Vigano, I., Braß, M. and Röckmann, T.:
2666 Methoxyl groups of plant pectin as a precursor of atmospheric methane: evidence from
2667 deuterium labelling studies, *New Phytologist*, 178, 808-814, <https://doi.org/10.1111/j.1469-8137.2008.02411.x>, 2008
2669
2670 Kibanova, D., Trejo, M., Destailats, H. and Cervini-Silva, J.: Photocatalytic activity of
2671 kaolinite, *Catalysis Communications*, 12, 698-702,
2672 <https://doi.org/10.1016/j.catcom.2010.10.029>, 2011
2673
2674 Köhler, P., Fischer, H., Schmitt, J., and Munhoven, G.: On the application and interpretation
2675 of Keeling plots in paleo climate research – deciphering $\delta^{13}\text{C}$ of atmospheric CO_2 measured in
2676 ice cores, *Biogeosciences*, 3, 539–556, <https://doi.org/10.5194/bg-3-539-2006>, 2006
2677
2678 Lee, L. E., Edwards, J. S., Schmitt, J., Fischer, H., Bock, M. and Brook, E. J.: Excess methane
2679 in Greenland ice cores associated with high dust concentrations, *Geochim. Cosmochim. Acta*,
2680 270, 409-430, <https://doi.org/10.1016/j.gca.2019.11.020>, 2020
2681
2682 Legrand, M., and Delmas, R.: Soluble Impurities in Four Antarctic Ice Cores Over the Last
2683 30000 Years, *Annals of Glaciology*, 10, 116-120,
2684 <https://doi.org/10.3189/S0260305500004274>, 1988
2685
2686 Liu, J., Chen, H., Zhu, Q., Shen, Y., Wang, X., Wang, M., Peng, C.: A novel pathway of
2687 direct methane production and emission by eukaryotes including plants, animals and fungi:
2688 An overview, *Atmospheric Environment*, 115, 26,
2689 <https://doi.org/10.1016/j.atmosenv.2015.05.019>, 2015
2690
2691 Liu, D., Yuan, P., Liu, H., Li, T., Tan, D., Yuan, W., He, H.: High-pressure adsorption of
2692 methane on montmorillonite, kaolinite and illite, *Applied Clay Science*, 85, 25-30,
2693 <https://doi.org/10.1016/j.clay.2013.09.009>, 2013
2694
2695 Lupker, M., Aciego, S. M., Bourdon, B., Schwander, J., and Stocker, T. F.: Isotopic tracing
2696 (Sr, Nd, U and Hf) of continental and marine aerosols in an 18th century section of the Dye-3
2697 ice core (Greenland), *Earth Pla Sci Let*, 295, 277-286,
2698 <https://doi.org/10.1016/j.epsl.2010.04.010>, 2010
2699
2700 McLeod, A. R., Newsham, K. K. and Fry, S.C.: Elevated UV-B radiation modifies the
2701 extractability of carbohydrates from leaf litter of *Quercus robur*, *Soil Biology and*
2702 *Biochemistry*, 39, Issue 1, 116-126, <https://doi.org/10.1016/j.soilbio.2006.06.019>, 2007
2703
2704 McLeod, A.R., Fry, S.C., Loake, G.J., Messenger, D.J., Reay, D.S., Smith, K.A. and Yun, B.-
2705 W.: Ultraviolet radiation drives methane emissions from terrestrial plant pectins, *New*
2706 *Phytologist*, 180, 124-132, <https://doi.org/10.1111/j.1469-8137.2008.02571.x>, 2008
2707
2708 Messenger, D.J., McLeod, A. R. and Fry, S.C.: The role of ultraviolet radiation,
2709 photosensitizers, reactive oxygen species and ester groups in mechanisms of methane
2710 formation from pectin, *Plant, Cell & Environment*, 32: 1-9, <https://doi.org/10.1111/j.1365-3040.2008.01892.x>, 2009
2711
2712
2713 Milkov, A. V. and Etiope, G.: Revised genetic diagrams for natural gases based on a global
2714 dataset of >20,000 samples, *Organic Geochemistry*, 125, 109-120,
2715 <https://doi.org/10.1016/j.orggeochem.2018.09.002>, 2018

2716
2717 Mitchell, L., Brook, E., Lee, J. E., Buizert, C., and Sowers, T.: Constraints on the Late
2718 Holocene anthropogenic contribution to the atmospheric methane budget, *Science* 342, 964–
2719 966, <https://doi.org/10.1126/science.1238920>, 2013
2720
2721 Miteva V., Teacher C., Sowers T. and Brenchley, J.: Comparison of the microbial diversity at
2722 different depths of the GISP2 Greenland ice core in relationship to deposition climates,
2723 *Environ. Microbiol.*, 11, 640–656, <https://doi.org/10.1111/j.1462-2920.2008.01835.x>, 2009
2724
2725 Möller, L., Sowers, T., Bock, M., Spahni, R., Behrens, M., Schmitt, J., Miller, H. and Fischer,
2726 H.: Independent variations of CH₄ emissions and isotopic composition over the past 160,000
2727 years, *Nature Geosci.*, 6, 885–890, <https://doi.org/10.1038/ngeo1922>, 2013
2728
2729 Mohnen, D.: Pectin structure and biosynthesis, *Current Opinion in Plant Biology*, 11, 266–
2730 277, <https://doi.org/10.1016/j.pbi.2008.03.006>, 2008
2731
2732 NEEM community members: Eemian interglacial reconstructed from a Greenland folded ice
2733 core, *Nature*, 493, 489–494, <https://doi.org/10.1038/nature11789>, 2013
2734
2735 Nicewonger, M. R., Verhulst, K. R., Aydin, M. and Saltzman, E. S.: Preindustrial
2736 atmospheric ethane levels inferred from polar ice cores: A constraint on the geologic sources
2737 of atmospheric ethane and methane, *Geophys. Res. Lett.*, 43,
2738 <https://doi.org/10.1002/2015GL066854>, 2016
2739
2740 Nicewonger, M. R., Aydin, M., Prather, M. J., and Saltzman, E.S.: Large changes in biomass
2741 burning over the last millennium inferred from paleoatmospheric ethane in polar ice cores.
2742 *Proc. Natl. Acad. Sci. USA*, 115 (49), 12413-12418.
2743 <https://doi.org/10.1073/pnas.1807172115>, 2018.
2744
2745 North Greenland Ice Core Project members, High-resolution record of Northern Hemisphere
2746 climate extending into the last interglacial period, *Nature* 431, 147–151,
2747 <https://doi.org/10.1038/nature02805>, 2004
2748
2749 Pires, J., Bestilleiro, M., Pinto, M. and Gil, A.: Selective adsorption of carbon dioxide,
2750 methane and ethane by porous clays heterostructures, *Separation and Purification*
2751 *Technology*, 61, 161-167, <https://doi.org/10.1016/j.seppur.2007.10.007>, 2008
2752
2753 Price, P. B. and Sowers, T.: Temperature dependence of metabolic rates for microbial growth,
2754 maintenance, and survival, *P. Natl. Acad. Sci. USA* 101, 4631–4636,
2755 <https://doi.org/10.1073/pnas.0400522101>, 2004
2756
2757 Rohde, R. A., Price, P. B., Bay, R. C. and Bramall, N. E.: In situ microbial metabolism as a
2758 cause of gas anomalies in ice, *P. Natl. Acad. Sci. USA*, 105, 8667–8672,
2759 <https://doi.org/10.1073/pnas.0803763105>, 2008
2760
2761 Rhodes, R. H., Faiñ, X., Stowasser, C., Blunier, T., Chappellaz, C., McConnell, J. R.,
2762 Romanini, D., Mitchell, L. E. and Brook, E. J.: Continuous methane measurements from a
2763 late Holocene Greenland ice core: Atmospheric and in situ signals, *Earth and Planetary*
2764 *Science Letters*, 368, 9-19, <https://doi.org/10.1016/j.epsl.2013.02.034>, 2013
2765

- hat formatiert: Schriftart: (Standard) Times New Roman, Schriftfarbe: Text 1, Englisch (USA)
- hat formatiert: Schriftart: (Standard) Times New Roman, Schriftfarbe: Text 1
- hat formatiert: Schriftart: (Standard) Times New Roman, Schriftfarbe: Text 1, Englisch (USA)
- hat formatiert: Schriftart: (Standard) Times New Roman, Schriftfarbe: Text 1
- hat formatiert: Schriftart: (Standard) Times New Roman, Schriftfarbe: Text 1, Englisch (USA)
- hat formatiert: Schriftart: (Standard) Times New Roman, Schriftfarbe: Text 1
- hat formatiert: Schriftart: (Standard) Times New Roman, Schriftfarbe: Text 1, Englisch (USA)
- hat formatiert: Schriftart: (Standard) Times New Roman, Schriftfarbe: Text 1
- hat formatiert: Schriftart: Times New Roman, 12 Pt., Schriftfarbe: Text 1, Englisch (USA)
- hat formatiert: Schriftart: (Standard) Times New Roman, Schriftfarbe: Text 1
- hat formatiert: Schriftart: (Standard) Times New Roman, Schriftfarbe: Text 1, Englisch (USA)
- hat formatiert: Schriftart: (Standard) Times New Roman, Schriftfarbe: Text 1
- hat formatiert: Absatz-Standardschriftart, Schriftart: (Standard) Times New Roman, 12 Pt., Schriftfarbe: Text 1, Englisch (USA)
- hat formatiert: Schriftfarbe: Text 1, Englisch (USA)
- hat formatiert: Schriftart: (Standard) Times New Roman, Schriftfarbe: Text 1
- hat formatiert: Schriftart: (Standard) Times New Roman, Schriftfarbe: Text 1, Englisch (USA)
- hat gelöscht: ¶
- hat gelöscht: ¶

2770 Rhodes, R. H., Faïn, X., Brook, E. J., McConnell, J. R., Maselli, O. J., Sigl, M., Edwards, J.,
 2771 Buizert, C., Blunier, T., Chappellaz, J., and Freitag, J.: Local artifacts in ice core methane
 2772 records caused by layered bubble trapping and in situ production: a multi-site investigation,
 2773 *Clim. Past*, 12, 1061–1077, <https://doi.org/10.5194/cp-12-1061-2016>, 2016
 2774
 2775 Ross, D. J. K. and Bustin, R. M.: The importance of shale composition and pore structure
 2776 upon gas storage potential of shale gas reservoirs, *Mar. Petrol. Geol.*, 26, 916-927,
 2777 <https://doi.org/10.1016/j.marpetgeo.2008.06.004>, 2009
 2778
 2779 Ruth, U., Wagenbach, D., Steffensen, J. P. and Bigler, M.: Continuous record of microparticle
 2780 concentration and size distribution in the central Greenland NGRIP ice core during the last
 2781 glacial period, *J. Geophys. Res.*, 108 (D3), 4098, <https://doi.org/10.1029/2002JD002376>,
 2782 2003
 2783
 2784 [Ruth, U., Bigler, M., Röthlisberger, R., Siggaard-Andersen, M.-L., Kipfstuhl, S., Goto-](#)
 2785 [Azuma, K., Hansson, M. E., Johnsen, S. J., Lu, H., and Steffensen, J. P.: Ice core evidence](#)
 2786 [for a very tight link between North Atlantic and east Asian glacial climate, *Geophys. Res.*](#)
 2787 [Lett.](#), 34, L03706, [doi:10.1029/2006GL027876](https://doi.org/10.1029/2006GL027876), 2007
 2788
 2789 Schade, G. W., Hofmann, R.-M. and Crutzen, P. J.: CO emissions from degrading plant
 2790 matter, *Tellus B: Chemical and Physical Meteorology*, 51:5, 889-908,
 2791 <https://doi.org/10.3402/tellusb.v51i5.16501>, 1999
 2792
 2793 Schilt, A., Baumgartner, M., Blunier, T., Schwander, J., Spahni, R., Fischer, H., and Stocker,
 2794 T. F.: Glacial–interglacial and millennial-scale variations in the atmospheric nitrous oxide
 2795 concentration during the last 800,000 years, *Quat Sci Rev*, 29, 182-192,
 2796 <https://doi.org/10.1016/j.quascirev.2009.03.011>, 2010
 2797
 2798 Schmitt, J., Seth, B., Bock, M. and Fischer, H.: Online technique for isotope and mixing ratios
 2799 of CH₄, N₂O, Xe and mixing ratios of organic trace gases on a single ice core sample, *Atmos.*
 2800 *Meas. Tech.*, 7, 2645–2665, <https://doi.org/10.5194/amt-7-2645-2014>, 2014
 2801
 2802 Smith, H. J., Wahlen, M., Mastoianni, D., and Taylor, K. C.: The CO₂ concentration of air
 2803 trapped in GISP2 ice from the Last Glacial Maximum-Holocene transition, *Geophys Res Lett*,
 2804 24, 1-4, <https://doi.org/10.1029/96GL03700>, 1997
 2805
 2806 Sugimoto, A., Dan, J., Kumai, T. and Murase J.: Adsorption as a methane storage process in
 2807 natural lake sediment, *Geophys. Res. Lett.* 30, 2080, <https://doi.org/10.1029/2003GL018162>,
 2808 2003
 2809
 2810 Svensson, A., Biscaye, P. E. and Grousset, F. E.: Characterization of late glacial continental
 2811 dust in the Greenland Ice Core Project ice core, *J. Geophys. Res.-Atmos.*, 105, 4637–4656,
 2812 <https://doi.org/10.1029/1999JD901093>, 2000
 2813
 2814 Tian, Y., Yan, C. and Jin, Z.: Characterization of Methane Excess and Absolute Adsorption in
 2815 Various Clay Nanopores from Molecular Simulation, *Sci Rep* 7, 12040,
 2816 <https://doi.org/10.1038/s41598-017-12123>, 2017
 2817
 2818 Tung, H. C., Bramall, N. E. and Price, P. B.: Microbial origin of excess methane in glacial ice
 2819 and implications for life on Mars, *P. Natl. Acad. Sci. USA* 102, 18292–18296,
 2820 <https://doi.org/10.1073/pnas.0507601102>, 2005

Formatiert: Block

hat formatiert: Schriftart: (Standard) Times New Roman, 12 Pt., Schriftfarbe: Text 1, Englisch (USA)

Formatiert: Abstand zwischen asiatischem und westlichem Text anpassen, Abstand zwischen asiatischem Text und Zahlen anpassen

hat formatiert: Schriftart: (Standard) Times New Roman, 12 Pt., Schriftfarbe: Text 1

2821 Tung, H., Price, P., Bramall, N. and Vrdoljak G.: Microorganisms metabolizing on clay
 2822 grains in 3-km-deep Greenland basal ice, *Astrobiology* 6, 69–86.
 2823 <https://doi.org/10.1089/ast.2006.6.69>, 2006
 2824
 2825 Vigano, I., van Weelden, H., Holzinger, R., Keppler, F., McLeod, A., and Röckmann, T.:
 2826 Effect of UV radiation and temperature on the emission of methane from plant biomass and
 2827 structural components, *Biogeosciences*, 5, 937–947, <https://doi.org/10.5194/bg-5-937-2008>,
 2828 2008
 2829
 2830 Vigano, I., Röckmann, T., Holzinger, R., van Dijk, A., Keppler, F., Greule, M., Brand, W. A.,
 2831 Geilmann, H. and van Weelden, H.: The stable isotope signature of methane emitted from
 2832 plant material under UV irradiation, *Atmospheric Environment*, 43, 5637-5646,
 2833 <https://doi.org/10.1016/j.atmosenv.2009.07.046>, 2009
 2834
 2835 Vigano, I., Holzinger, R., Keppler, F., Greule, M., Brand, W. A., Geilmann, H., van Weelden,
 2836 H. and Röckmann, T.: Water drives the deuterium content of the methane emitted from plants,
 2837 *Geochimica et Cosmochimica Acta*, 74, 3865-3873, <https://doi.org/10.1016/j.gca.2010.03.030>,
 2838 2010
 2839 Wang, Z.P., Han, X.G., Wang, G.G., Song, Y. and Gulledge, J.: Aerobic methane emission
 2840 from plants in the Inner Mongolia steppe, *Environmental Science & Technology* 42, 62– 68
 2841 <https://doi.org/10.1021/es071224l>, 2008
 2842
 2843 Wang, Z.P., Xie, Z.Q., Zhang, B.C., Hou, L.Y., Zhou, Y.H., Li, L.H. and Han, X.G.: Aerobic
 2844 and Anaerobic Nonmicrobial Methane Emissions from Plant Material, *Environmental Science*
 2845 *& Technology* 2011 45 (22), 9531-9537, <https://doi.org/10.1021/es2020132>, 2011
 2846
 2847 Wang, B., Hou, L., Liu, W. and Wang, Z.: Non-microbial methane emissions from soils,
 2848 *Atmospheric Environment*, 80, 290–298, <https://doi.org/10.1016/j.atmosenv.2013.08.010>,
 2849 2013
 2850
 2851 Wang, B., Lerdau, M. and He, Y.: Widespread production of nonmicrobial greenhouse gases
 2852 in soils, *Glob Change Biol.*, 23:4472–4482, <https://doi.org/10.1111/gcb.13753>, 2017
 2853
 2854 Watanabe, M., Watanabe, Y., Kim, Y. S., Koike, T.: Dark aerobic methane emission
 2855 associated to leaf factors of two Acacia and five Eucalyptus species, *Atmospheric*
 2856 *Environment*, 54, 277-281, <https://doi.org/10.1016/j.atmosenv.2012.02.012>, 2012
 2857
 2858 Wehr, R. and Saleska, S. R.: The long-solved problem of the best-fit straight line; application
 2859 to isotopic mixing lines, *Biogeosciences*, 14, 17–29, <https://doi.org/10.5194/bg-14-17-2017>,
 2860 2017.
 2861
 2862 Whiticar, M. J.: Carbon and hydrogen isotope systematics of bacterial formation and
 2863 oxidation of methane, *Chemical Geology*, 161, 291-314, [https://doi.org/10.1016/S0009-](https://doi.org/10.1016/S0009-2541(99)00092-3)
 2864 [2541\(99\)00092-3](https://doi.org/10.1016/S0009-2541(99)00092-3), 1999
 2865
 2866 Wu, F., Li, J., Peng, Z., Deng, N.: Photochemical formation of hydroxyl radicals catalyzed by
 2867 montmorillonite, *Chemosphere*, 72, 407-413,
 2868 <https://doi.org/10.1016/j.chemosphere.2008.02.034>, 2008
 2869
 2870 York, D.: Least squares fitting of a straight line with correlated errors, *Earth and Planetary*
 2871 *Science Letters*, 5, 320-324, [https://doi.org/10.1016/S0012-821X\(68\)80059-7](https://doi.org/10.1016/S0012-821X(68)80059-7), 1968

hat formatiert: Schriftart: (Standard) Times New Roman, 12 Pt., Schriftfarbe: Text 1, Englisch (USA)

hat formatiert: Schriftart: (Standard) Times New Roman, 12 Pt., Schriftfarbe: Text 1

hat formatiert: Schriftart: (Standard) Times New Roman, 12 Pt., Schriftfarbe: Text 1, Englisch (USA)

hat formatiert: Schriftfarbe: Text 1, Englisch (USA)

2872
2873 York, D., Evensen, N. M., Martinez, M. L., and De Basabe Delgado, J.: Unified equations for
2874 the slope, intercept, and standard errors of the best straight line, *Am. J. Phys.* 72, 367–375,
2875 <https://doi.org/10.1119/1.1632486>, 2004

Seite 7: [1] hat gelöscht Michaela Mühl 15.02.23 07:24:00

Seite 8: [2] hat gelöscht Michaela Mühl 04.01.23 07:47:00

Seite 10: [3] hat formatiert Michaela Mühl 23.02.23 08:59:00

Schriftart: Nicht Kursiv, Schriftfarbe: Text 1, Englisch (USA)

Seite 10: [4] hat formatiert Michaela Mühl 23.02.23 08:59:00

Schriftart: Nicht Kursiv, Schriftfarbe: Text 1, Englisch (USA)

Seite 10: [5] hat formatiert Michaela Mühl 23.02.23 08:59:00

Schriftart: Nicht Kursiv, Schriftfarbe: Text 1, Englisch (USA)

Seite 10: [6] hat gelöscht Michaela Mühl 23.02.23 08:59:00

Seite 10: [7] Formatiert Fischer, Hubertus (CLIMATE) 03.02.23 13:59:00

Leerraum zwischen asiatischem und westlichem Text nicht anpassen, Leerraum zwischen asiatischem Text und Zahlen nicht anpassen

Seite 10: [8] hat formatiert Michaela Mühl 08.03.23 11:21:00

Schriftart: 10 Pt., Nicht Kursiv, Schriftfarbe: Text 1

Seite 10: [9] Formatiert Michaela Mühl 06.03.23 14:54:00

Beschriftung, Vom nächsten Absatz trennen, Abstand zwischen asiatischem und westlichem Text anpassen, Abstand zwischen asiatischem Text und Zahlen anpassen

Seite 10: [10] hat gelöscht Michaela Mühl 06.03.23 14:54:00

Seite 10: [11] hat gelöscht Michaela Mühl 11.01.23 11:53:00

Seite 16: [12] hat gelöscht Michaela Mühl 03.01.23 10:01:00

Seite 16: [13] hat gelöscht Fischer, Hubertus (CLIMATE) 03.02.23 15:46:00

Seite 22: [14] hat gelöscht Michaela Mühl 19.02.23 20:01:00

Seite 22: [15] hat gelöscht Michaela Mühl 04.01.23 08:13:00

Seite 25: [16] hat gelöscht Michaela Mühl 06.03.23 17:06:00

Seite 25: [17] hat gelöscht Fischer, Hubertus (CLIMATE) 03.02.23 16:47:00

Seite 28: [18] Formatiert Michaela Mühl 06.03.23 17:18:00

Abstand zwischen asiatischem und westlichem Text anpassen, Abstand zwischen asiatischem Text und Zahlen anpassen

Seite 28: [19] hat gelöscht Michaela Mühl 07.02.23 08:21:00

Seite 28: [20] hat gelöscht Michaela Mühl 06.03.23 17:18:00

Seite 28: [21] hat formatiert Michaela Mühl 02.02.23 09:25:00

Schriftfarbe: Text 1

▲ Seite 28: [22] hat formatiert Michaela Mühl 02.02.23 09:25:00

Schriftfarbe: Text 1

▲ Seite 28: [23] hat formatiert Michaela Mühl 02.02.23 09:25:00

Schriftfarbe: Text 1

▲ Seite 28: [24] hat formatiert Michaela Mühl 02.02.23 09:25:00

Schriftfarbe: Text 1

▲ Seite 28: [25] hat formatiert Michaela Mühl 02.02.23 09:25:00

Schriftfarbe: Text 1

▲ Seite 28: [26] hat formatiert Michaela Mühl 02.02.23 09:25:00

Schriftfarbe: Text 1

▲ Seite 28: [27] hat formatiert Michaela Mühl 02.02.23 09:25:00

Schriftfarbe: Text 1

▲ Seite 28: [28] hat formatiert Michaela Mühl 02.02.23 09:25:00

Schriftfarbe: Text 1

▲ Seite 28: [29] hat formatiert Michaela Mühl 02.02.23 09:25:00

Schriftfarbe: Text 1

▲ Seite 28: [30] hat gelöscht Fischer, Hubertus (CLIMATE) 03.02.23 17:26:00

x.....
▲ Seite 28: [31] Formatiert Michaela Mühl 02.02.23 09:24:00

Standard, Zeilenabstand: 1,5 Zeilen, Leerraum zwischen asiatischem und westlichem Text nicht anpassen, Leerraum zwischen asiatischem Text und Zahlen nicht anpassen

▲ Seite 28: [32] hat gelöscht Fischer, Hubertus (CLIMATE) 03.02.23 17:26:00

x.....
▲ Seite 28: [33] hat gelöscht Fischer, Hubertus (CLIMATE) 03.02.23 17:26:00

x.....
▲ Seite 28: [34] hat formatiert Michaela Mühl 02.02.23 09:25:00

Schriftart: (Standard) Times New Roman, Nicht Fett, Schriftfarbe: Text 1

▲ Seite 28: [35] hat formatiert Michaela Mühl 02.02.23 09:25:00

Schriftart: (Standard) Times New Roman, Nicht Fett, Schriftfarbe: Text 1

▲ Seite 28: [36] hat gelöscht Fischer, Hubertus (CLIMATE) 03.02.23 17:28:00

x.....
▲ Seite 28: [37] hat formatiert Michaela Mühl 06.03.23 17:20:00

Schriftart: Nicht Fett

▲ Seite 28: [38] hat formatiert Michaela Mühl 06.03.23 17:20:00

Nicht Hervorheben

▲ Seite 28: [39] hat formatiert Michaela Mühl 06.03.23 17:20:00

Nicht Hervorheben

▲ Seite 28: [40] hat formatiert Michaela Mühl 06.03.23 17:20:00

Hochgestellt, Nicht Hervorheben

▲.....

Seite 28: [41] hat formatiert Michaela Mühl 06.03.23 17:20:00

Nicht Hervorheben

Seite 28: [42] hat formatiert Michaela Mühl 06.03.23 17:20:00

Hochgestellt, Nicht Hervorheben

Seite 28: [43] hat formatiert Michaela Mühl 06.03.23 17:20:00

Nicht Hervorheben

Seite 28: [44] hat formatiert Fischer, Hubertus (CLIMATE) 21.02.23 13:51:00

Schriftart: Nicht Fett

Seite 30: [45] hat gelöscht Michaela Mühl 10.01.23 14:56:00

Seite 30: [46] hat gelöscht Fischer, Hubertus (CLIMATE) 03.02.23 17:37:00

Seite 30: [47] hat gelöscht Fischer, Hubertus (CLIMATE) 03.02.23 17:40:00

Seite 38: [48] hat gelöscht Michaela Mühl 07.03.23 09:48:00

Seite 38: [49] hat formatiert Michaela Mühl 16.02.23 13:57:00

Schriftart: 12 Pt., Kursiv, Schriftfarbe: Automatisch

Seite 38: [50] hat formatiert Michaela Mühl 07.03.23 09:48:00

Schriftart: 10 Pt., Nicht Kursiv, Schriftfarbe: Text 1, Englisch (USA)

Seite 38: [50] hat formatiert Michaela Mühl 07.03.23 09:48:00

Schriftart: 10 Pt., Nicht Kursiv, Schriftfarbe: Text 1, Englisch (USA)

Seite 38: [50] hat formatiert Michaela Mühl 07.03.23 09:48:00

Schriftart: 10 Pt., Nicht Kursiv, Schriftfarbe: Text 1, Englisch (USA)

Seite 38: [50] hat formatiert Michaela Mühl 07.03.23 09:48:00

Schriftart: 10 Pt., Nicht Kursiv, Schriftfarbe: Text 1, Englisch (USA)

Seite 38: [50] hat formatiert Michaela Mühl 07.03.23 09:48:00

Schriftart: 10 Pt., Nicht Kursiv, Schriftfarbe: Text 1, Englisch (USA)

Seite 38: [50] hat formatiert Michaela Mühl 07.03.23 09:48:00

Schriftart: 10 Pt., Nicht Kursiv, Schriftfarbe: Text 1, Englisch (USA)

Seite 38: [50] hat formatiert Michaela Mühl 07.03.23 09:48:00

Schriftart: 10 Pt., Nicht Kursiv, Schriftfarbe: Text 1, Englisch (USA)

Seite 38: [50] hat formatiert Michaela Mühl 07.03.23 09:48:00

Schriftart: 10 Pt., Nicht Kursiv, Schriftfarbe: Text 1, Englisch (USA)

Seite 38: [50] hat formatiert Michaela Mühl 07.03.23 09:48:00

Schriftart: 10 Pt., Nicht Kursiv, Schriftfarbe: Text 1, Englisch (USA)

Seite 38: [50] hat formatiert Michaela Mühl 07.03.23 09:48:00

Schriftart: 10 Pt., Nicht Kursiv, Schriftfarbe: Text 1, Englisch (USA)

Seite 38: [50] hat formatiert Michaela Mühl 07.03.23 09:48:00

Schriftart: 10 Pt., Nicht Kursiv, Schriftfarbe: Text 1, Englisch (USA)

Seite 38: [50] hat formatiert Michaela Mühl 07.03.23 09:48:00

Schriftart: 10 Pt., Nicht Kursiv, Schriftfarbe: Text 1, Englisch (USA)

Seite 38: [50] hat formatiert Michaela Mühl 07.03.23 09:48:00

Schriftart: 10 Pt., Nicht Kursiv, Schriftfarbe: Text 1, Englisch (USA)

Seite 38: [50] hat formatiert	Michaela Mühl	07.03.23 09:48:00
Schriftart: 10 Pt., Nicht Kursiv, Schriftfarbe: Text 1, Englisch (USA)		
Seite 38: [51] hat formatiert	Michaela Mühl	12.01.23 10:17:00
Schriftart: 10 Pt., Nicht Kursiv, Schriftfarbe: Text 1		
Seite 38: [51] hat formatiert	Michaela Mühl	12.01.23 10:17:00
Schriftart: 10 Pt., Nicht Kursiv, Schriftfarbe: Text 1		
Seite 38: [51] hat formatiert	Michaela Mühl	12.01.23 10:17:00
Schriftart: 10 Pt., Nicht Kursiv, Schriftfarbe: Text 1		
Seite 38: [51] hat formatiert	Michaela Mühl	12.01.23 10:17:00
Schriftart: 10 Pt., Nicht Kursiv, Schriftfarbe: Text 1		
Seite 38: [52] hat formatiert	Michaela Mühl	12.01.23 10:17:00
Schriftart: 10 Pt., Nicht Kursiv, Schriftfarbe: Text 1		
Seite 38: [53] hat formatiert	Michaela Mühl	08.03.23 11:24:00
Schriftart: Nicht Fett, Englisch (USA)		
Seite 38: [53] hat formatiert	Michaela Mühl	08.03.23 11:24:00
Schriftart: Nicht Fett, Englisch (USA)		
Seite 38: [54] hat formatiert	Michaela Mühl	08.03.23 11:24:00
Schriftart: Nicht Fett, Englisch (USA)		
Seite 38: [54] hat formatiert	Michaela Mühl	08.03.23 11:24:00
Schriftart: Nicht Fett, Englisch (USA)		
Seite 38: [55] hat formatiert	Michaela Mühl	08.03.23 11:24:00
Schriftart: Nicht Fett, Englisch (USA)		
Seite 38: [55] hat formatiert	Michaela Mühl	08.03.23 11:24:00
Schriftart: Nicht Fett, Englisch (USA)		
Seite 38: [56] hat formatiert	Michaela Mühl	08.03.23 11:24:00
Schriftart: Nicht Fett		
Seite 38: [56] hat formatiert	Michaela Mühl	08.03.23 11:24:00
Schriftart: Nicht Fett		
Seite 38: [57] hat formatiert	Michaela Mühl	08.03.23 11:24:00
Schriftart: Nicht Fett, Englisch (USA)		
Seite 38: [57] hat formatiert	Michaela Mühl	08.03.23 11:24:00
Schriftart: Nicht Fett, Englisch (USA)		
Seite 38: [58] hat formatiert	Michaela Mühl	08.03.23 11:24:00
Schriftart: Nicht Fett		
Seite 38: [58] hat formatiert	Michaela Mühl	08.03.23 11:24:00
Schriftart: Nicht Fett		
Seite 38: [58] hat formatiert	Michaela Mühl	08.03.23 11:24:00
Schriftart: Nicht Fett		
Seite 38: [58] hat formatiert	Michaela Mühl	08.03.23 11:24:00
Schriftart: Nicht Fett		
Seite 38: [59] hat formatiert	Michaela Mühl	08.03.23 11:24:00

Schriftart: Nicht Fett, Englisch (USA)

Seite 38: [59] hat formatiert Michaela Mühl 08.03.23 11:24:00

Schriftart: Nicht Fett, Englisch (USA)

Seite 50: [60] hat gelöscht Michaela Mühl 08.03.23 11:03:00